Distinct roles of p75NTR and TrkB signaling in neural circuit remodeling in the developing visual system

Elena Ivanova Kutsarova

Integrated Program in Neuroscience,

McGill University

August 2018

A thesis submitted to the Faculty of Graduate Studies and Research, McGill University,

in partial fulfillment of the requirements for the degree of Doctor of Philosophy.

Table of Contents

1. Abstract

Building a brain which contains properly connected neurons is crucial for the survival of an animal in the surrounding world. Genetic and experience-dependent mechanisms both contribute to the establishment and refinement of neural connections (synapses) during development. Sensory experience translated into patterned neuronal activity instructs various aspects of topographic map refinement, crucial for orderly representation in the brain of the outside world. Forming and refining proper brain connectivity relies on the communication between a projecting neuron and its future postsynaptic partners. In this thesis, we asked how is patterned activity translated to into a molecular code that instructs circuit refinement. Brain-derived neurotrophic factor (BDNF) was identified as one of the prominent molecular candidates that underlies activity-dependent neural circuit refinement. BDNF is synthesized as a precursor protein proBDNF which has been shown to play a role in facilitating synaptic weakening through p75 neurotrophin receptor (p75NTR) signaling, whereas the post-cleavage mature form (mBDNF) signals through p75NTR and tropomyosin-related kinase B (TrkB) and is crucial for synaptic strengthening. Overall, BDNF signaling is essential for structural remodeling of dendrites and axons during development, but the pathways by which neural activity is translated to BDNF expression and in turn to structural and functional circuit plasticity are poorly understood.

We used multiphoton imaging of retinal ganglion cells (RGCs) projecting into the optic tectum (OT) in the albino *Xenopus laevis* tadpole to observe their structural remodeling *in vivo.* A single ectopic ipsilaterally projecting RGC axon was visually stimulated either synchronously or asynchronously with its neighboring inputs, while blocking BDNF signaling with TrkB-Fc, or knocking down its receptors TrkB or p75NTR in RGCs. We showed that acute BDNF signaling is required for suppression of axonal branch addition in response to correlated firing. p75NTR in RGCs is required for asynchrony-induced branch addition, while TrkB signaling in RGCs acts as an activity-dependent suppressor of branch elimination. p75NTR in RGCs is crucial for exploratory growth over days. p75NTR and TrkB appear to have distinct signaling in darkness compared to during visually evoked activity. These results provide cellular structural

details for BDNF, TrkB and p75NTR signaling as mechanisms underlying specific aspects of activity-dependent structural remodeling during development.

2. Résumé

La construction d'un cerveau qui contient des neurones correctement connectés est cruciale pour la survie d'un animal dans son environnement. Les mécanismes génétiques et dépendants d'expérience tous deux contribuent à l'établissement et au raffinement des connexions neuronales (synapses) pendant le développement. L'expérience sensorielle traduite en modèles d'activité neuronale instruit divers aspects du raffinement de la carte topographique, qui est cruciale pour une représentation ordonnée du monde extérieur dans le cerveau. La formation et le raffinement de la connectivité cérébrale appropriée dépendent de la communication entre la projection d'un neurone et ses futurs partenaires postsynaptiques. Dans cette thèse, nous avons demandé comment les modèles d'activité sont traduits en un code moléculaire qui instruit l'affinement des circuits. Le facteur neurotrophique dérivé du cerveau (BDNF) a été identifié comme un des candidats moléculaires les plus importants sur lesquels repose le raffinement du circuit neuronal dépendant de l'activité. Le BDNF est synthétisé comme protéine précurseur proBDNF qui est censée jouer un rôle dans la facilitation de l'affaiblissement synaptique par la signalisation de p75NTR, alors que le clivage résultant à la forme mature mBDNF signale via p75NTR et TrkB et est crucial pour le renforcement synaptique. Dans l'ensemble, la signalisation du BDNF est essentielle pour le remodelage structurel de dendrites et d'axones pendant le développement, mais les voies par lesquelles l'activité neuronale est traduite à l'expression du BDNF et par la suite à la plasticité des circuits structurelle et fonctionnelle demeure incertaine.

Nous avons utilisé l'imagerie multiphotonique de cellules ganglionnaires rétiniennes (CGR) qui projettent vers le tectum optique chez le têtard albino *Xenopus laevis* pour observer leur remodelage structurel in-vivo. Un seul axone de CGR mal ciblé à l'hémisphère ipsilatérale était visuellement stimulé de manière synchrone ou asynchrone avec ses entrées voisines, tout en bloquant la signalisation du BDNF avec TrkB-Fc ou en supprimant la formation de ses récepteurs TrkB ou p75NTR dans les CGRs. Nous avons montré que la signalisation aigüe du BDNF est nécessaire pour la suppression de l'addition de branche axonale en réponse à un déclenchement corrélé.

p75NTR dans les CGRs est nécessaire pour l'ajout de ramifications induit par l'asynchronie, alors que la signalisation TrkB dans les CGRs agit comme un suppresseur d'élimination des ramifications dépendant de l'activité. p75NTR dans les RGC est essentiel pour la croissance exploratoire pendant plusieurs jours. p75NTR et TrkB semblent avoir une signalisation distincte dans l'obscurité par rapport à l'activité évoquée visuellement. Ces résultats fournissent des détails de structure cellulaire pour la signalisation du BDNF, TrkB et p75NTR en tant que mécanismes sous-jacents à des aspects spécifiques du remodelage structurel dépendant d'activité pendant le développement.

3. List of Abbreviations

4E-BP1	4E-binding protein 1
5mC	5-methylcytosine
AMPARs	α-amino-3-hydroxy-5-methyl-4-isoxazolepropionic acid type glutamate receptors
APV	D-2-amino-5-phosphonovalerate
ARNT2	Aryl hydrocarbon receptor nuclear translocator 2
ATP	Adenosine triphosphate
AtT-20	Pituitary corticotrope tumor cells (AtT20)
BDNF	Brain-derived neurotrophic factor
bHLH	Basic helix-loop-helix
bHLH-PAS	bHLH-Per-Arnt-Sim
BHLHB2	Basic helix-loop-helix factor
blu	*blumenkohl* mutant containing a mutation in vglut2a
BSA	Bovine serum albumin
Ca^{2+}	Calcium ions
CA1	Cornu Ammonis, zone 1
CaM kinases	Ca2+-calmodulin-regulated protein kinases
CaMKII	Ca-calmodulin kinase type II
CANDLE	Collaborative approach for Enhanced denoising under low-light excitation
CaRF	Calcium-responsive transcription factor
CBP	CREB bindning protein
Cholera toxin B	Cholera toxin subunit B
cis-signaling	Signaling within the same axon
CNS	Central nervous system
CoREST	RE1-silencing transcription factor corepressor 1
CpG	5'-Cytosine-phosphate-Guanine-3'
cr-proBDNF	Cleavage resistant-proBDNF
CREB	(ATF)/cAMP/Ca 2+ -response element

CTCF	CCCTC-binding factor
DAG	Diacylglycerol
DAS	Dark/asynchronous/synchronous
DiI	1,1-dioctadecyl-3,3,3′,3′-tetramethylindocarbocyanine perchlorate
DNA	Desoxyribonucleic acid
DRG	Dorsal root ganglion
dsRed	Discosoma Red
DTT	Dithiothreitol
ECD	Extracellular domain
EDTA	Ethylenediaminetetraacetic acid
eEF2K	Eukaryotic elongation factor 2 kinase
EGFP	Enhanced green fluorescent protein
eIF4E	Eukaryotic initiation factor 4E
ELISA	Enzyme-linked immunosorbent assay
Elvax	Ethylene vinyl acetate copolymer
Eph	Erythropoietin-producing human hepatocellular receptors
EphA	Family of tyrosine kinase receptors EphA
EphB	Family of tyrosine kinase receptors EphB
ephrin-A	Ligand for EphA
Ephrin-B	Ligand for EphB
EPR	Endoplasmic reticulum
EPSC	Excitatory postsynaptic current
Fas	First apoptosis signal receptor
GaAsP PMTs	Gallium arsenide phosphide photo-multiplier tubes
Gab1	Grb2-associated binder-1
GEF	Guanine nucleotide exchange factor
GFP	Green fluorescent protein
GFP-VAMP2	Vesicle-associated Membrane Protein-2/green fluorescent protein, linked in a fusion protein
Grb2	Growth factor receptor-bound protein 2

GDP	Guanosine diphosphate
GTP	Guanosine triphosphate
H2A, H2B, H3 and H4	Histone2A, Histone 2B, Histone 3, Histone 4
H3K27	Lysine-27 on Histone 3
HCG	Human chorionic gonadotropin
HCl	Hydrochloric acid
HDAC	Histone deacetylase
HEPES	2-[4-(2-hydroxyethyl)piperazin-1-yl]ethanesulfonic acid
ICD	Intracellular domain
ICV	Intracerebroventricularl
IP3	Inositol tris-phosphate
Islet2+	LIM homeodomain protein, Islet 2-positive
JIP3	c-Jun NH2-terminal kinase-interacting protein 3
K^+	Potassium ions
k252a	Protein kinase inhibitor, (9S,10R,12R)-2,3,9,10,11,12-Hexahydro-10-hydroxy-9-methyl-1-oxo-9,12-epoxy-1H-diindolo[1,2,3-fg:3',2',1'-kl]pyrrolo[3,4-i][1,6]benzodiazocine-10-carboxylic acid methyl ester
Kd	Dissociation constant
kDa	Kilodaltons
Kir2.1	Inward-rectifying potassium channel
lakritz	Zebrafish mutant, containing mutation in Ath5
LGN	Lateral geniculate nucleus
Lingo-1	Ig domain-containing Nogo Receptor-interacting protein-1
LTD	Long-term depression
LTP	Long-term potentiation
mA	Milliampere
MAG	Myelin-associated glycoprotein
MAPK/Erk	Mitogen-Activated Protein Kinase/Extracellular Signal Kinase
mBDNF	Mature BDNF
MBSH	Modified Barth’s saline with HEPES
MeCP2	Methyl-CpG binding protein 2

MEK	Mitogen-activated protein kinase kinase
mEPSC	Miniature EPSC
Met-propeptide	Methionine66-containing BDNF prodomain
Mg^{2+}	Magnesium ions
mi-30a-5p	MiRNA-30a-5p
miRNA	Microribonucleic acid
MK-801	Dizocilpine
mM	Millimolar
MMP	Matrix metalloproteinase
MO	Morpholino oligonucleotides
mRNA	Messenger ribonucleic acid
MS-222	Tricaine methanesulfonate
mTOR	Mechanistic target of rapamycin
Na^{+}	Sodium ions
NaCl	Sodium chloride
NaOH	Sodium hydroxide
NF-κB	Nuclear factor κB
NFAT	Nuclear factor of activated T cells
NGF	Nerve growth factor
NMDAR	N-methyl D-aspartate receptor
NMJ	Neuromusclular junction
NogoR	Nogo receptor-1
NP40	Nonyl phenoxypolyethoxylethanol
NPAS4	Neuronal PAS domain protein 4
NRSE	Neuron-restrictive silencer element
NT-3/4/6/7	Neurotrophin-3/4/6/7
O_2 -bubbled	Oxygen-bubbled
OMgp	Oligodendrocyte-myelin glycoprotein
p-Trk	Phosphorylated Trk
p75NTR	p75 neurotrophin receptor

PAGE	Polyacrylamide gel electrophoresis
PDMS	Polydimethylsiloxane
PDZ	Protein domain found in postsynaptic density protein (PSD-95), Drosophila disc large tumor suppressor (Dlg1), and Zonula occludens-1 protein (zo-1)
PI(4,5)P2	Phosphatidylinositol(4,5)bisphosphate
PKB	Protein kinase B/Akt
PKC	Protein kinase C
PLC-γ	Phospholipase C-γ
PNS	Peripheral nervous system
proBDNF	Precursor of BDNF
proNGF	Precursor of NGF
PSD-95-GFP	Postsynaptic density-95/green fluorescent protein, linked in a fusion protein
PVDF	Polyvinylidene fluoride
Rab	Subfamily of guanosine triphosphate hydrolases
Raf	Rapidly accelerated fibrosarcoma kinase family
Ras	Rat sarcoma family of guanosine triphosphate hydrolases
RGC	Retinal ganglion cells
Rho-GDI	Rho GDP dissociation inhibitor
ROUT test	Robust regression and Outlier removal test
RRVR	Aminoacid sequence Arginine-Arginine-Valine-Arginine
Rxβ2-cKO	Conditional knockout mouse in which β2-nAChR is deleted only in the retina
SC	Superior colliculus
SDS	Sodium dodecyl sulfate
Ser/Thr-X-Val	Aminoacid sequence Serine/Threonine-Unspecified aminoacid-Valine
Shc	SH2-containing collagen-related protein
SOS	Son of sevenless
synaptophysin-GFP	Synaptophysin/green fluorescent protein, linked in a fusion protein
tCaMKII	Truncated form of CaMKII

TGN	Trans-Golgi network
tLTD	Spike-timing-dependent long-term depression
tLTP	Spike-timing-dependent long-term potentiation
TNF	Tumor necrosis factor
TNFR	TNF receptor
tPA	Tissue plasminogen activator
TRAF	TNFR associated factors
Tris	Tris(hydroxymethyl)aminomethane
Trk	Tropomyosin-related kinase
TrkB	Tropomyosin-related kinase B
TrkB-Fc	Recombinant human chimera TrkB protein
TrkC	Tropomyosin-related kinase C
TRPC3/6	Transient receptor potential canonical subfamily channel 3/6
TTX	Tetrodotoxin
USF	Upstream stimulatory factor
UTR	Untranslated region
Val propeptide	Valine66-containg BDNF prodomain
Vglut2a	Vesicular glutamate transporter homologous to mammalian VGLUT2
β2-nAChR	β2 nicotinic acetylcholine receptor subunit
β2(TG)nAChR	Transgenic mouse with restored expression of β2-nAChR in RGC

4. Author Contributions

Chapter 1: Literature review: Sections 6.1.1 - 6.1.3 in this chapter are modified from the published review article “Rules for Shaping Neural Connections in the Developing Brain” which is part of the collection of articles under the research topic “Spontaneous Activity in the Sensory System”, Frontiers in Neural Circuits, 10 January 2017. I am first author of this review article. This article was written jointly by Elena Kutsarova and Edward S Ruthazer in consultation with Martin Munz. Figures were made by Elena Kutsarova and Martin Munz. Copyright © 2017 Kutsarova, Munz and Ruthazer. Edward S Ruthazer and Martin Munz granted their permission for this review article to be included in this thesis. I wrote section 6.1.4 and 6.2 of Chapter 1 with suggestions from Dr. Edward Ruthazer. I made Figures 4 and 5, summarizing information reviewed by Roux and Barker (2002); Deinhardt and Chao (2014).

Chapter 2: Methodology: I wrote Chapter 2 with suggestions from Dr. Edward Ruthazer. Anne Schohl provided details on the 2-cell stage injection protocol. I made the figure.

Chapter 3: The low-affinity neurotrophin receptor p75NTR, but not TrkB, in RGCs participates in baseline axonal branch dynamics and long-term axonal exploration in the developing visual system. Together with Dr. Edward Ruthazer, I developed the rationale and conceived the experiments. I performed the imaging experiments, traced axonal arbors, carried out the analysis and presentation of the data. Dr. Edward Ruthazer provided guidance for data analysis and presentation. Anne Schohl (Laboratory Technician), Dr. Edward Ruthazer and I developed the rationale for the experiments related to validation of the receptor knockdown. Anne Schohl performed the morpholino injections in 2-blastomere stage embryos. Anne Schohl and I jointly carried out and analysed the Western Blot experiments. Yuan Yuan Zhang (Undergraduate Student) helped with some axonal tracing. I wrote Chapter 3 with suggestions from Dr. Edward Ruthazer.

Chapter 4: Roles of BDNF signaling, presynaptic p75NTR signaling and presynaptic TrkB signaling in neural activity correlation-dependent axonal branch dynamics: Dr. Edward Ruthazer and I conceived all the experiments. I carried out the imaging experiments, axonal tracing, data analysis and presentation. Dr. Edward Ruthazer provided guidance for data analysis and presentation. Olesia Bilash (Undergraduate Student) was instrumental for the design and making of a novel imaging chamber, which decreased the lethal rate of tadpoles during setup and the course of imaging. Tasnia Rahman provided useful suggestions for improvement of the chamber design. I reanalyzed data acquired by Dr. Martin Munz (Munz et al., 2014) and combined it with data acquired by me to create Figure 1. Dr. Edward Ruthazer and Dr. Martin Munz provided these data and granted permission to reanalyze it and include it in this thesis. Carmelia Lee (Undergraduate Student) performed some axonal tracing included in Figure 2. I wrote Chapter 4 with suggestions from Dr. Edward Ruthazer.

5. Acknowledgements

This work was supported by the Canadian Institutes for Health Research (CIHR) Foundation Grant to Edward Ruthazer; Integrated Program in Neuroscience (IPN) Graduate Excellence Award to Elena Kutsarova, McGill University; NSERC-CREATE Neuroengineering Studentship Grant to Dr. Edward Ruthazer; Jeanne Timmins Costello Award to Elena Kutsarova, Montreal Neurological Institute; Molson Neuroengineering Award to Elena Kutsarova, Montreal Neurological Institute; Tom Gevas Travel Award to Elena Kutsarova, Montreal Neurological Institute and Graduate Research Enhancement and Travel Award to Elena Kutsarova, IPN, McGill University.

I would like to thank my advisory committee members Drs. Wayne Sossin, Anne McKinney and Philip Barker for their advice, guidance and useful suggestions. Special thank you for Dr. Sossin, who made himself available, so I could just go to his office and ask him a question.

I would like to express my immense gratitude to my supervisor Dr. Edward Ruthazer for his guidance and support throughout this journey. Ed, you believed in me and the project at times when I didn't. Your support led me out of dark periods. Your curiosity and faith in science and the scientific method brought me back to why I wanted to be a scientist at the first place.

I would like to thank Dr. Etienne de Villers Sidani for generously providing the 3D printer used to print the chamber mould, Dr. Kelly Sakaki for providing files with example design of imaging chambers.

Very special thank you to the Ruthazer lab members, past and present, who made the lab a great place to work in and for their suggestions about my project. Thank you to Martin, who took me under his wing and spent a lot of time teaching me how to do the imaging experiments. Thank you for starting this project. Thank you for being a great friend and for hanging out and discussing the project with me endlessly. Anne, thank you for being the most amazing technician the universe has known and for being my "older sister" in the lab and in life. Thanks for the experiments, scientific and non-scientific talk,

the lunches and coffee breaks. Thanks to Phil, who is the best labmate anyone could ever wish for, for allowing me to rely on you for lab duties and for listening to me when I was not happy. Thank you for helping me take the image included in Figure 1*D*, Methodology. Thanks to Delphine and Nasr for being sarcastic and funny and for hanging out and chatting in the lab and for keeping in touch, I miss you a lot. Thanks to Zahraa for being a great desk neighbor and for sharing tea and lots of life conversations, and for being a labmate I could rely on for favors. Thanks to Tasnia for many, many things: endless discussions about stabilization, darkness and what it all means, for helping me take the pictures included in Figure 1*B*-*C*, Methodology and for translating the abstract in French! Thanks to Lois, with whom I worked on a side project and who taught me how to do calcium imaging. Thanks to Marion, who is always positive and who set an example that a woman, mum and scientist are possible roles for the same human. Thanks to Mari and Tony for being the odd ones in the corner of the office, who always brought some joy or maybe a toy with them and made the mundane life of experiments so much better. Thanks to Stephen, who proofread one of the essays for class. Thanks to Valerie, Nick, Ryan, Sarah and Vanessa for being good labmates. Thanks to Cynthia who taught me new words in English. Thanks to the undergrads that worked with me: Alex Wang, Olesia Bilash, Yuan Yuan Zhang and Carmelia Lee, you were great.

Thanks to the Rotons, 2012 - Ana, Eva, Miguel, Peter and Reiko for being great peers and friends. Thank you to Ana and Eva with whom I studied for different classes.

Благодаря на приятелите си от България, които въпреки че не съм там, не ме забравиха и винаги бяха щастливи да ме посрещнат на летището. Кате, Люби, Ицо и София, Цвети, Анди, Ая и Едиа, Ивче, Тикварски, Тони и Галя, благодаря, че заради вас имаше толкова много причини да се прибирам, за прекрасните ваканции и за неизмерната подкрепа и милите думи, които винаги намирахте за мен.

Благодаря на преподавателите си през годините, които запалиха интереса ми към науката. Госпожи Бонева, Божилова, Бобева, Антонова, Апостолова, Ялъмова. Професори Оджакова, Лалчев, Василиев, Панков, Иванов и доценти Георгиев, Евтимова и Христакудис. Thanks to my supervisors at Imperial, Drs. Brickley and Djamgoz for having me in their labs and teaching me techniques and scientific

method. Special thanks to the director of my program there, Dr. Ushkaryov for teaching me scientific rigor.

Мамо, нищо нямаше да бъде възможно без теб! Благодаря ти безкрайно и завинаги! Благодаря на татко за всичко, което ми остави и съм наследила от него. Благодаря на всички от семейството ми, баба Елена, Васко, вуйчо Васко, вуйна Елена, леля Светла, чичо Христо, Емо, Яна, Ицко, Неви, Ицко, Сашко, Гери, Стилиан, Йоана, Маги и всички, които не са сред нас вече, но живеят в сърцето ми: баба Ненка и дядо Стоян, дядо Гого.

Peter, thank you for your immense support, love, care and for sharing this and everything else. This wouldn't have been possible without you. Thanks for all the Python and MATLAB code you patiently helped me with. I will always be thankful for having you around.

Малък бебчо, благодаря ти за издръжливостта и извинявай за стреса, под който те подложих, докато растеше в корема ми. Благодаря, че ми позволи да работя и пиша. Чакам те с нетърпение.

На Лиляна Куцарова

В памет на Иван Куцаров

Für Peter Donhauser

На сина ми

6. Chapter 1: Literature Review

6.1. Neural Circuit Refinement in the Developing Brain

In this review, we propose a detailed set of cellular rules that govern activity-dependent circuit refinement. This list of rules synthesizes what has been learned in the extensive experimental literature on the development of the visual system, with a strong emphasis on data obtained from live imaging of the retinotectal projection in fish and frogs. Because of their external development and largely translucent bodies, permitting high-resolution in vivo imaging of developing neurons and their associated glial cells, albino tadpoles of the African clawed frog (*Xenopus laevis*) and larval zebrafish (*Danio rerio*) in particular have been popular models for studying activity-dependent circuit development and remodeling. Moreover, unlike mammals, these animals rely extensively on vision for survival from very early developmental stages and use this same visual information to direct circuit refinement.

While molecular guidance cues are critical for establishing the initial crude topographic projections from the eye to the brain, even greater precision of neuronal maps is achieved through the involvement of activity-dependent mechanisms. Because neighboring retinal ganglion cells (RGCs) in the eye are more likely to exhibit temporal correlation in their firing patterns than are distantly separated RGCs, the pattern of firing of action potentials in the developing visual system contains important information about the relative position of the RGC somata in the retina. The system therefore is able to use patterned neural activity in RGCs to instruct the orderly mapping of their axons onto postsynaptic partners in the optic tectum (OT). This results in a more precise map of the retina onto the OT. This review will discuss classic studies and more recent experimental insights from *in vivo* imaging that reveal fundamental details about how activity-dependent structural and functional refinement takes place. The refinement of the retinotectal circuit achieves a remarkably accurate retinotopic representation that contributes to effective visual processing and ultimately to the generation of visually-guided behaviors. Here, we define refinement as the process of establishing precise anatomical wiring (i.e., the

representation most closely reproducing the input space), which allows for the optimal function of neural circuits in the animal.

6.1.1. Retinotopic maps and eye-specific segregation in the developing central nervous system

In fish and frogs the RGCs project to at least 10 distinct tectal and pretectal arborization fields believed to mediate important behavioral responses such as eye movements and prey capture (Easter and Taylor, 1989; Burrill and Easter, 1994; Kubo et al., 2014; Semmelhack et al., 2014). By far, the most extensive projection terminates in the contralateral optic tectum, where the organization of axonal terminals reconstitutes a topographic map of the retina. The axons of RGCs whose somata are located in the temporal retina project to the rostral tectum, whereas RGCs residing in the nasal retina send their axons to the caudal tectum (Attardi and Sperry, 1963). Similarly, the dorsoventral axis of the retina is represented medio-laterally in the optic tectum. The retinocollicular projection in mammals forms a retinotopic map with a similar coordinate system in the analogous structure to the optic tectum, the superior colliculus (SC). [N.B., The term optic tectum is applied generically to represent the analogous retinorecipient structure in all vertebrates.] The SC is involved in directing eye and head movements in mammals (Schiller, 1972).

Unlike amphibians, in which the retinofugal projection is almost exclusively contralateral, in mammals a fraction of the RGCs does not cross at the optic chiasm but projects to the ipsilateral hemisphere of the brain. This fraction ranges from 3-5% in mice, around 15% in ferrets to up to nearly 40% in humans (Petros et al., 2008). Interestingly, anterograde and retrograde tracing of RGCs also reveals a substantial transient ipsilateral projection during embryonic development in mammals and chicks, much of which is lost during subsequent maturation (Land and Lund, 1979; Dräger and Olsen, 1980; McLoon and Lund, 1982). In the mammalian brain, inputs from both eyes project to the deep part of the stratum griseum superficiale and to the stratum opticum of the SC. These binocular projections segregate into alternating eye-specific bands in the rostral colliculus (Godement et al., 1984). The more superficial part of the stratum griseum superficiale of

the SC normally receives exclusively contralateral eye input. In addition to providing afferents to the SC, RGC axons also project to the visual thalamus in mammals. A distinct visual processing pathway, the retinothalamic (retinogeniculate) projection terminates in both the ventral and in the dorsal lateral geniculate nuclei (LGN) in the thalamus. The dorsal LGN is thought to serve as the fundamental relay station through which visual information is passed to higher order cortical visual centers where increasingly complex features are extracted from visual scenes (Felleman and Van Essen, 1991). The afferents in the LGN, much like in the SC, project retinotopically but segregate into eye-specific laminae (Linden et al., 1981).

This review focuses primarily on the retinotectal projection and outlines the evidence supporting a specific set of rules for projection refinement based on activity-dependent cellular mechanisms involved in the establishment and refinement of the functional retinotopic map in the optic tectum. Experimental perturbations and live observations of labeled neurons in the developing brains of small transparent tadpoles and fish larvae constitute the main source of data that explain how map development proceeds at the cellular level. However, the same mechanisms responsible for retinotectal development in these simpler vertebrates are also likely to play essential roles in mammalian development. We have highlighted experiments from multiple species that have provided particularly important insights into projection refinement mechanisms throughout this review. In addition, it is important to note that the most prominent activity-dependent stages of brain circuit refinement do not necessarily take place at the same time in development (e.g., the retinal projection to the SC achieves its mature organization earlier than that in the LGN) and therefore the rules that control retinotectal refinement may be fundamentally different, or manifest themselves differently, during later refinement events.

We begin by outlining a list of fundamental mechanistic events that the experimental evidence indicates are likely to occur during retinotectal map refinement. Each of these is elaborated in greater detail below.

6.1.2. Rules for retinotectal structural plasticity:

6.1.2.1. Molecular guidance cues provide information for coarse axonal targeting

6.1.2.2. Inputs compete for available synaptic target space.

6.1.2.3. Axonal and dendritic arbors are highly dynamic, even after seemingly mature morphology is attained.

6.1.2.4. Patterned neuronal activity provides instructive cues that help refine inputs:

6.1.2.4.1. Synchronous firing stabilizes synapses and prolongs branch lifetimes while actively suppressing branch dynamics via N-methyl D-aspartate receptor (NMDAR)-dependent retrograde signaling (Hebbian mechanisms).

6.1.2.4.2. Asynchronous activity weakens synapses (LTD) and actively promotes axonal branch dynamics, including addition and elongation, as well as branch elimination (Stentian mechanisms).

6.1.2.5. In the absence of sensory input, correlated spontaneous firing provides surrogate patterned activity.

6.1.2.6. New axonal branch tips emerge near existing synapses.

6.1.2.7. Stronger synapses help stabilize the axons and dendrites on which they form (Synaptotropism)

6.1.2.8. Homeostatic mechanisms help maintain the overall level of functional synaptic input to the target.

6.1.2.1. Molecular guidance cues provide information for coarse axonal targeting

The classic experiments of Roger Sperry and co-workers, studying the developing and regenerating retinotectal projection in fish and amphibians, led Sperry to propose the “Chemoaffinity Hypothesis” in which the molecular tagging of presynaptic and postsynaptic partners with a kind of address code guides the establishment of the retinotopic maps in the optic tectum (Sperry, 1963). Sperry observed that following optic

nerve section, regenerating RGC axons projected back to roughly correct, retinotopically appropriate sites in the optic tectum irrespective of whether the whole retina was still present, even if the eye had been rotated to provide erroneous information about the visual environment (Sperry, 1943). Furthermore, even upon initial entry to the OT, RGC inputs are already coarsely retinotopically distributed within the optic tract (Holt and Harris, 1983), suggesting the presence of molecular guidance cues throughout the developing visual system.

Concrete support for this model came initially with the identification of a candidate molecular activity expressed in membranes isolated from posterior optic tectal cells that could serve as one of Sperry's tags (Walter et al., 1987). Ultimately, the molecule was identified to be a ligand of the EphA family of receptor tyrosine kinases, and together with related EphA binding molecules, this group of ligands was labeled as the ephrin-A family (Drescher et al., 1995; Feldheim and O'Leary, 2010). In mammals, there are 9 members of the EphA subclass (EphA1-EphA8 and EphA10) and 5 members of the EphB subclass (EphB1-EphB4 and EphB6), the molecular properties and signaling of which have been exhaustively reviewed (Egea and Klein, 2007). Studies in numerous species have demonstrated that EphA and ephrin-A members are expressed in complementary gradients across the retina and the tectum (Brennan et al., 1997; Monschau et al., 1997; McLaughlin et al., 2003a a; Higenell et al., 2012). The expression levels of EphA are highest in temporal retina and decline in a graded manner toward the nasal retina; A decreasing gradient of ephrin-A from the caudal to the rostral tectum is also present. Ephrin-A and EphA family members are expressed at the surface of both RGC axons and tectal cells. Once bound, the receptor-ligand couple activates a signaling pathway that results in axon repulsion (Drescher et al., 1997). Therefore, temporal axons expressing high EphA levels avoid the caudal tectum where the ephrin-A levels peak.

Interestingly, the complementary expression gradients of ephrins and Ephs mean that they are co-expressed at differing ratios within cells across the retina and the tectum (Marcus et al., 1996; Rashid et al., 2005). Ephrin-A5 is expressed in a strong graded fashion (nasal > temporal) in the mouse retina (Suetterlin and Drescher, 2014). Thus, cis-signaling mediated by Eph-ephrin binding within the same RGC axon may serve to

effectively sharpen the nasotemporal gradient of trans-neuronal ephrin signaling (Hornberger et al., 1999). Moreover, the high levels of ephrin-A5 expressed on nasal axons allow them to also participate in the repulsion of temporal axons that express high levels of EphA (Bonhoeffer and Huf, 1980; Raper and Grunewald, 1990; Suetterlin and Drescher, 2014).

Just as the interaction of EphA and ephrin-A mediates the mapping of the temporal-nasal axis of the retina along the rostral-caudal dimension of the tectum, the interaction of EphB with ephrin-B has been proposed to contribute to the dorsoventral mapping of RGC terminals along the mediolateral axis of the optic tectum. However, the underlying interaction appears to mediate axonal attraction rather than repulsion and may also involve reverse signaling from EphB to ephrin-B (Hindges et al., 2002; Mann et al., 2002). While the importance of EphA-ephrin-A signaling in establishing the anteroposterior axis of the retinotectal topographic map has been well validated with knockout and misexpression studies (Feldheim and O'Leary, 2010), there remains some uncertainty about the specific roles played by EphB-ephrin-B signaling. In frogs, the actual gradient of expression during development is not consistent with that predicted by the cell biology. The proposed reverse signaling model, based on *in vitro* observations, suggested that dorsal RGCs expressing ephrin-B should be attracted to putative high levels of EphB in the ventral tectum (Mann et al., 2002). However, labeling the expression pattern of EphB in the *Xenopus laevis* tadpole brain using ephrin-B-alkaline phosphatase fusion proteins revealed that, to the contrary, there is instead a dorsal > ventral expression gradient of EphB and no detectable ephrin-B gradient in the optic tectum (Higenell et al., 2012). Furthermore, the dorsoventral axis of the retinofugal projection appears to presort in the optic tract prior to encountering any gradient in the tectum, suggesting that EphB-ephrinB signaling may have a role to play in axon guidance in the optic tract (Plas et al., 2005).

6.1.2.2. Inputs compete for available synaptic target space

Aside from the chemoaffinity and chemorepulsive mechanisms that direct RGC axons to arborize roughly within topographically appropriate locations in the target,

several lines of evidence indicate that mapping of the projection is subject to an additional fundamental influence that is most likely independent of neural activity. There appears to be a competition for available target space that has the important consequence of rendering the retinotectal projection free of discontinuities and innervation gaps. One striking example of this phenomenon can be seen in the retinotectal projection of the ephrin-A2/A5 double knockout mouse, which has severely disrupted mapping of RGC inputs along its rostrocaudal axis, such that injection of the anterograde tracer DiI into one site in the eye results in multiple discrete patches of axon terminal labeling along the entire axis instead of a focused single termination zone in the target as seen in wildtype animals (Feldheim et al., 2000). Despite the complete topographic disorganization of retinal inputs, bulk labeling the entire retinotectal projection by intraocular cholera toxin B injection produces a uniform and uninterrupted pattern of afferent labeling across the entire area of the tectal neuropil which is indistinguishable from that in wildtype animals. Thus, the ability of the inputs to occupy all available target space is unperturbed despite the absence of the ephrin-A signaling that is essential for ordering the map.

An extreme version of this phenomenon, which offers some insights into the importance of this competition over target space in map formation is the so-called “EphA ki/ki” transgenic mouse in which two overlapping gradients of EphA expression are induced in the retina, one normal and one elevated by uniform high expression of EphA3 in a subset of RGCs (Islet2+ cells) throughout the eye (Reber et al., 2004). In these mice, RGCs expressing the normal levels of graded EphA project to the tectum and form a complete, topographically ordered map that is restricted to the caudal half of the tectum. In the rostral tectum a second complete and well-ordered map is formed by the Islet2+ RGCs. This double map reveals that in distinction to the pure chemoaffinity model put forth by Sperry, it is relative, rather than absolute, levels of EphA receptor expression that organize the map. The fact that two full maps form in the space that normally accommodates one further supports the idea that maps can expand or contract as necessary to fill available territory.

In animals capable of central nervous system regeneration like fish and frogs it has long been known that if half the retina is ablated and the remaining half allowed to regrow

into the tectum, the resulting half-map expands to fill the territory formerly occupied by afferents from the intact retina (Schmidt and Easter, 1978). Similarly, ablation of part of the tectum results in a compressed retinotectal map that fits within the remaining area (Yoon, 1976; Schmidt and Coen, 1995). It appears that this process of map regulation, by which input and target size are matched, may occur without the benefit of patterned neural activity, as injection of the sodium channel blocker tetrodotoxin (TTX) failed to prevent the map rescaling (Meyer and Wolcott, 1987). These observations support the notion of activity-independent competitive interactions in the optic tectum, perhaps analogous to the competition of peripheral axons for nerve growth factor in the skin (Lewin and Barde, 1996). The reorganization of the map that occurs after ablations therefore appears to represent an independent influence that the system imposes on the afferents through competition for space.

Map plasticity has also been examined at the single axon level in a clever experiment in zebrafish in which a single arbor from a transplanted RGC is allowed to innervate the optic tectum of a *lakritz* mutant fish that is incapable of generating its own RGCs. This single axon is free to innervate its target in the complete absence of competition from other retinal afferents (Gosse et al., 2008). Interestingly, these axons managed to target their topographically appropriate termination zones in the tectum but formed abnormally large terminal arbors. This result suggests that retinal axons do at least have a crudely defined inherent preferred termination zone within the target, presumably due to chemoaffinity cues, but that in the absence of competition for space, arbors can enlarge their coverage area, at least to a limited extent.

Is there a role for neural activity in the competition between afferents? This question was addressed in an experiment in which the Kir2.1 potassium channel which reduces neuronal excitability and firing was overexpressed in just a few RGCs together with GFP in zebrafish larvae (Hua et al., 2005). These silenced RGC axons failed to elaborate arbors in the optic tectum that were as large as those from control GFP-expressing neurons. But blocking all activity in the network by rearing the animals in TTX restored normal arbor size to the Kir2.1-expressing cells, indicating a competition based on overall activity levels can also regulate arbor elaboration. Electroporation to express

Kir2.1 in RGCs in mice, produces a similar result, with axon arbor elaboration greatly reduced compared to control cells (Benjumeda et al., 2013).

Interestingly, partial ablation of the SC at birth in the Syrian hamster results in an enhancement in the steepness of the ephrin-A gradient in the remaining part of the colliculus that is consistent with the accompanying compression of the retinotectal map (Tadesse et al., 2013). Implantation of a slow-release Elvax polymer to deliver the NMDAR blocker D-2-amino-5-phosphonovalerate (APV) to the SC during development fails to prevent map compression in response to partial SC ablation, as measured electrophysiologically (Huang and Pallas, 2001). Thus, the compression of the map appears to depend more upon molecular than on activity-dependent cues. However, receptive field sizes are enlarged in these APV-treated animals, consistent with neural activity playing an important role in map refinement. Thus, the experimental evidence indicates that the rough retinotopic mapping of axon arbors, as well as map compression and expansion, is largely the result of activity-independent mechanisms, including guidance molecule expression and competition for space in the overall target structure. Axon arbor size, important for the precision of connectivity, is regulated by activity-dependent competitive interactions.

6.1.2.3. Axonal and dendritic arbors are highly dynamic, even after seemingly mature morphology is attained.

The remarkable potential for structural plasticity observed in the developing and regenerating retinotectal projections reflects the cellular mechanisms by which retinal axons ramify within the optic tectum. Static images of labeled cells, reconstructed from fixed histological specimens, reveal convoluted trajectory changes and the frequent presence of interstitial branches throughout the axonal arbor which hint at the fact that axon growth and arbor development result from a highly exploratory process involving extensive axon remodeling over time (Sakaguchi and Murphey, 1985; Nakamura and O'Leary, 1989; Cline and Constantine-Paton, 1990; Dhande et al., 2011). However, live imaging of axonal and dendritic remodeling in intact, transparent zebrafish and *Xenopus laevis* embryos has revealed a far more dynamic reality in which axons are perpetually

extending and retracting extensive interstitial branch tips to probe the target area (O'Rourke and Fraser, 1990; Kaethner and Stuermer, 1992; Dingwell et al., 2000). In zebrafish, the process by which an axon arrives at and elaborates extensive branch tips within its final termination zone is not directed growth as one might find with chemoattraction, but rather what appears to be a process of random branch extension in which the overall progression of branch elongation and stabilization favors the future termination zone (Kita et al., 2015). The process is similar in *Xenopus* except that individual arbors occupy a relatively larger proportion of the total tectal neuropil from earlier stages, creating a situation in which the topographic map increases in precision with age, not only by restricting axonal branches to appropriate locations, but also by constant growth of the total retinorecipient field with age (Sakaguchi and Murphey, 1985). As the tectum expands by adding cells at its caudomedial pole, the RGC arbors adjust and improve their relative retinotopic order by gradually shifting their positions within the tectum. This creates a need for ongoing structural dynamism and plasticity at least until metamorphosis in order to optimize the map. The dendritic arbors of tectal neurons and even the filopodial processes extended by radial glial cells are similarly labile during this period, consistent with the notion that dynamic process remodeling can combinatorially increase the potential set of connections available for the network to sample and also reduce the steric interference that may result when multiple cells are actively rewiring within the same volume (Rajan et al., 1999; Chklovskii et al., 2004; Tremblay et al., 2009). Thus, even in relatively mature tadpoles, in which most RGC axons have attained their mature size and complexity, time lapse imaging still reveals ongoing remodeling and exploratory probing at branch tips, albeit at considerably slower rates than are observed during the initial establishment of the retinotectal projection.

6.1.2.4. Patterned neuronal activity provides instructive cues that help refine inputs

The relative contributions of molecular signaling versus neuronal activity in topographic map establishment and refinement have long been a subject of debate. The apparent lack of a requirement for action potential firing in the initial establishment of retinotopy has renewed questions about the overall importance of activity in map formation (Harris, 1984; Stuermer et al., 1990; Benjumeda et al., 2013). In this section,

we have made an effort to describe the various experimental approaches, covering nearly a half-century, that have contributed to the conclusion that patterned neuronal activity is indeed instructive for precise retinotopic map refinement. We further discuss recent efforts from *in vivo* imaging to dissect how specific properties of patterned neuronal activity instruct different aspects of retinotectal refinement.

6.1.2.4.1. Effects of dark rearing

Dark-rearing repeatedly has been shown to have no significant impact on topographic precision in the retinotectal projections in fish or amphibians, measured either electrophysiologically or morphologically. In the optic tectum of *Xenopus laevis* frogs, dark-rearing produced no significant modifications in multiunit tectal receptive field sizes or in the laminar segregation of RGC inputs defined by specific stimulus selectivities (Keating et al., 1986). There are also no obvious alterations in the proper laminar targeting of RGC inputs within the superficial layers of the optic tectum in dark-reared compared to control zebrafish (Nevin et al., 2008). Furthermore, visual deprivation following optic nerve crush in adult goldfish does not impair the gradual sharpening of the initially diffuse termination field of regenerating retinal afferents into fine patches (Olson and Meyer, 1991). At first glance, these data appear consistent with the possibility that visual experience, and patterned neural activity, may not play a meaningful role in directing RGC axons to refine their projections to topographically appropriate tectal partners, and that the precise spatial organization of inputs in the tectum is exclusively determined by graded molecular guidance cues. However, it is critical to bear in mind that dark rearing does not necessarily deprive the visual system of all activity as spontaneous activity may be sufficient to provide the necessary activity-dependent cues needed for normal retinotopic map refinement. Work in the mammalian visual system certainly suggests that the maintenance of receptive field properties in the SC requires ongoing patterned visual input (Carrasco et al., 2005).

6.1.2.4.2. Blockade of action potential firing

In contrast to dark-rearing, experiments using chronic pharmacological blockade of voltage-gated sodium channels with TTX can directly test the requirement for action

potential firing in development. Schmidt and Edwards (1983) reported that, unlike dark-rearing, intraocular injection of TTX during optic nerve regeneration in adult goldfish prevented the refinement of multiunit receptive field sizes in the TTX-treated animals. It also resulted in the degradation of precision in the anatomical projection (Meyer, 1983). At the single cell level, TTX treatment resulted in significantly enlarged regenerated axonal arbors, but failed to induce any detectable alterations in an intact projection (Schmidt and Buzzard, 1990).

In *Xenopus laevis* tadpoles, retinal action potential blockade with TTX leads to a rapid increase in axonal branch dynamics measured both as number of branches added and lost per 2 hours (Cohen-Cory, 1999). The TTX-treated arbors also undergo greater net growth and branch addition over 24 hours. In zebrafish larvae, however, the size and topographic location of individual RGC terminal arbors is not altered when action potential firing is blocked or in *macho* mutant fish with reduced sodium channel activity during development, perhaps reflecting the relatively faster pace of development in this species (Stuermer et al., 1990; Gnuegge et al., 2001). Interestingly, however, both TTX treatment and the macho mutation result in greater divergence of the retinotectal axons as they project into the tectum from the same quadrant of the eye, suggesting that while individual axon arbors are morphologically normal, they fail to converge precisely within their correct termination zone. In the mouse, silencing RGCs by *in utero* electroporation of Kir2.1 also does not prevent axonal pathfinding or targeting in the SC, but this manipulation does result in less elaborate, more diffusely arborizing axon terminals, indicative of a degraded retinocollicular map (Benjumeda et al., 2013).

6.1.2.4.3. Blockade of NMDA receptors

Locally-correlated, patterned firing in the retina, whether mediated by visual stimuli or spontaneous retinal waves, carries information about the relative locations of RGCs with respect to one another that the system can use to instruct map refinement. The notion of correlated firing between pre- and postsynaptic cells leading to strengthening of connection efficacy was originally articulated by Canadian psychologist Donald Hebb in the context of learning and memory (Hebb, 1949). The idea of a “Hebb synapse” capable

of modifying its synaptic strength in response to co-activation of pre- and postsynaptic partners is in fact borne out by the basal occlusion by Mg^{2+} of the ion channel of NMDA receptors, the principal glutamate receptor type found at newly formed synapses. Only when the dual requirements of glutamate binding and simultaneous postsynaptic depolarization to relieve the Mg^{2+} block of the pore are satisfied can the NMDAR flux current (Nowak et al., 1984). This property of the NMDAR means that it can function as a molecular detector of correlated activity. The fact that NMDAR activity appears to be required for many forms of neural plasticity, including long-term potentiation (LTP) of excitatory synaptic transmission is consistent with this role.

One of the first demonstrations that correlation detection by NMDARs likely contributes to retinotectal map refinement involved the implantation of a slow-release polymer to continuously deliver the NMDAR antagonist APV over the optic tectum in *Rana pipiens* frogs and tadpoles. After several weeks of tectal NMDAR blockade a focal injection of a retrograde tracer was made into the optic tectum in order to reveal the convergence of inputs from the eye, a measure of map refinement. Compared with sham treated control animals, the animals that had undergone tectal NMDAR blockade exhibited a pronounced degradation of input convergence resulting in less precise retinotectal maps (Cline and Constantine-Paton, 1989). A similar experiment performed on early postnatal rat SC gave consistent results, leading to many mistargeted retinocollicular axon terminals and disrupting the normal refinement of termination zones of RGC axons (Simon et al., 1992). Electrophysiological analysis of OT and SC receptive fields in the *Xenopus laevis* tadpole and in the Syrian hamster respectively, provided functional evidence that NMDAR blockade during development also prevents the normal refinement of receptive field size (Huang and Pallas, 2001; Dong et al., 2009). Thus, Hebb's postulate that "cells that fire together, wire together" indeed appears to be implemented by NMDARs, presumably acting as correlation detectors.

6.1.2.4.4. Dually innervated tectum

The normal retinotectal projection in fish and frogs is almost exclusively contralaterally projecting and monocular. Surgical ablation of one of the tectal lobes or

surgical deflection of the optic fibers from one tectal lobe to the other forces both eyes to map onto a single lobe, resulting in a dually innervated tectum (Sharma, 1973; Levine and Jacobson, 1975; Springer and Cohen, 1981). Alternatively, implanting a supernumerary third eye during embryogenesis results in a projection that must share the optic tectum with the animal's normal retinal inputs (Constantine-Paton and Law, 1978). The retinal afferents in dually innervated tectal lobes segregate into alternating ocular dominance bands, each dominated by inputs from one eye (Higenell et al., 2012). Because the tectum is normally monocular, it seems unlikely that any cryptic molecular patterning exists to program the segregation of retinal afferents into ocular dominance bands. Instead, it has been proposed that ocular dominance bands in the dually innervated tectum reflect a compromise between Sperry's chemoaffinity cues and a Hebbian convergence of co-active inputs. Presumably each eye expresses the full complement of graded molecular guidance cues and therefore their axons seek to target topographically appropriate sites in the optic tectum. When two such axons from the same eye terminate in the same part of the tectum, Hebbian mechanisms should facilitate their convergence, but in the case where two axons from different eyes attempt to terminate in the same location they may be forced apart by competitive mechanisms as a consequence of their poorly correlated firing patterns. Evidence that neuronal activity indeed mediates the segregation into ocular dominance bands comes from experiments in which the firing of action potentials in retinal axons in 3-eyed frogs was chronically blocked by TTX, which resulted in the desegregation of inputs into a uniform, overlapping field in the tectum (Reh and Constantine-Paton, 1985). Moreover, the activation of tectal NMDARs specifically is also required, as chronic delivery of APV from a slow-release polymer placed over the tectum also desegregated the afferents from both eyes (Cline et al., 1987). Though it remains formally possible that neural activity and tectal NMDAR activation are merely permissive for segregation into ocular dominance bands, at least no band-like pattern of ephrin-A expression in the tectum, which would foreshadow the formation of eye-specific bands, has been observed in the dually innervated tecta (Higenell et al., 2012).

6.1.2.4.5. Stroboscopic rearing

Further evidence for activity patterns being instructive rather than merely permissive for activity-dependent retinotectal projection refinement comes from strobe-rearing experiments, in which an atypically high degree of correlation in the firing activity of RGCs is induced across the entire eye. The retinotectal projections in goldfish reared by stroboscopic illumination after hatching overlap substantially and fail to refine throughout development (Schmidt and Buzzard, 1993). Labeling of single RGCs in strobe-reared fish revealed axonal arbors that are long and diffusely branched without forming the characteristic dense clusters of branches at the termination zone. Multiunit receptive field maps in these animals also showed poor topographic refinement, with atypically large response fields. Regenerating projections exhibit a similar failure to refine under conditions of stroboscopic illumination (Schmidt and Eisele, 1985). Interestingly, the effects of strobe rearing on ocular dominance bands in the dually innervated fish or frog tectum has not to our knowledge been reported, though differences in axonal path length from the two eyes could produce sufficiently asynchronous synaptic activation in the tectum to reinforce segregation. On the other hand, a study in mice, which normally do have binocular innervation of the SC, found that in animals that had experienced optogenetic simultaneous co-activation of the two eyes during the period of retinotectal axon ingrowth prior to eye-opening, ipsilateral eye afferents were no longer restricted to deeper tectal layers but instead appeared able to stabilize inputs within the more superficial layers where contralateral inputs normally terminate exclusively (Zhang et al., 2011).

6.1.2.4.6. HEBBIAN MECHANISMS: Synchronous firing stabilizes synapses and prolongs branch lifetimes while actively suppressing branch dynamics via NMDAR-dependent retrograde signaling.

The amenability of the intact *Xenopus laevis* tadpole retinotectal system to live imaging and whole-cell electrophysiology makes it an ideal system in which to ask questions about the fundamental cellular events that underlie Hebbian structural plasticity. The retinotectal synapse was one of the first synapses shown to exhibit spike-

timing-dependent long-term potentiation (tLTP) and depression (tLTD) *in vivo* (Zhang et al., 1998; Tsui et al., 2010). During the period of retinotectal map refinement, repeated visual stimulation can be used to induce conditions favorable for tLTP and this results in a shift in receptive field structure toward the potentiated subfield (Vislay-Meltzer et al., 2006). As in many other brain areas, tLTP in the retinotectal system is pathway-specific and NMDAR-dependent. One advantage of tLTP as a model for experience-dependent plasticity is the fact that it is far more physiological than protocols like tetanic stimulation and therefore more likely to resemble the actual mechanisms by which sensory input and patterned activity alter synaptic strengths in the developing visual system. As in the hippocampal Schaffer collateral-CA1 synapse, induction and expression of retinotectal LTP are both mediated by signaling events in the postsynaptic cell, which involves activation of NMDARs, Ca^{2+} influx, activation of Ca-calmodulin kinase type II (CaMKII), and trafficking of α-amino-3-hydroxy-5-methyl-4-isoxazolepropionic acid type glutamate receptors (AMPARs) to the synapse (Wu et al., 1996; Mu and Poo, 2006). In order for these phenomena to be relevant to map refinement, however, such postsynaptic signaling must be able to drive changes in the presynaptic axons through the production of one or more retrograde signals that can act back on the presynaptic terminal.

Normal visual experience during the period of developmental refinement can activate postsynaptic NMDARs. Indeed, blockade of NMDARs by bath application of APV results in a rapid upregulation of presynaptic RGC axon branch dynamics visualized *in vivo* by confocal microscopy, with a greater number of new branch tips added and retracted at the axon terminal over minutes to hours (Rajan et al., 1999). Application of the non-competitive NMDAR blocker dizocilpine (MK-801) in zebrafish at 3 days post-fertilization when the retinotectal projection is first established is reported to result in an overall expansion of RGC axon arbor size (Schmidt et al., 2000). However because NMDARs are present not only in postsynaptic tectal neurons, but also in the retina and potentially at presynaptic terminals of RGCs in the tectum (Corlew et al., 2008; Banerjee et al., 2016) pharmacological blockade of NMDARs is not conclusive evidence for the existence of retrograde signaling.

More conclusive evidence for a retrograde signal originating in the postsynaptic cell that can modify the growth of presynaptic axons comes from an impressive series of *in vivo* time lapse imaging studies in *Xenopus* tadpoles by Zou and Cline (1996). Viral overexpression in tectal neurons of a constitutively active truncated form of CaMKII (tCaMKII), which lacks the autoinhibitory regulatory domain, mimics the activation of CaMKII that takes place in LTP induction. Animals in which the postsynaptic tectal neurons, but not the presynaptic RGCs, were virally infected with tCaMKII showed the expected enhancement in synaptic AMPAR currents as NMDAR-only "silent synapses" matured *en masse* to become AMPAR-containing functional synapses (Wu et al., 1996). Interestingly, the RGC axon arbors were visualized in these animals and found to grow far less and exhibit much lower branch tip densities than control cells, indicating the existence of a retrograde signal downstream of CaMKII activation that stabilizes existing branches and suppresses branch elaboration as it drives synaptic maturation. Furthermore, expression of Kv1,1 in tectal neurons led to an enlargement of the receptive fields of those neurons, suggesting that dampening the output of the target neuron prevents the process of refinement of its inputs (Dong et al., 2012).

The process of ocular dominance band formation in dually innervated fish and frog tectum (described above) almost certainly requires retrograde signaling, as correlation detection is most likely performed by NMDAR activation in postsynaptic neurons. At the level of single axon branch dynamics, time-lapse imaging of *Xenopus* RGC axon arbors in dually innervated tectum reveals a preferential stabilization of branches that extend into same eye territory, compared to territory dominated by the other eye (Ruthazer et al., 2003). This preference is eliminated when NMDARs are pharmacologically blocked, a result that conforms with the idea that NMDARs mediate axon branch stabilization via retrograde signaling.

6.1.2.4.7. STENTIAN MECHANISMS: Asynchronous activity weakens synapses (LTD) and actively promotes axonal branch dynamics, including branch addition, elongation, and elimination.

To date, the most direct elucidation of how correlated firing among retinal afferents can instruct the refinement of the retinotectal map at the level of individual RGC axon branch dynamics has come from a study that took advantage of the fact that although the retinotectal projection in *Xenopus* tadpoles is almost purely contralateral, in the occasional animal one or two individual RGC axons can be found to project by accident to the ipsilateral optic tectum (Munz et al., 2014). These misguided axons arborize and form synaptic contacts within the ipsilateral tectum, presumably responding to the same molecular cues that guide the contralateral RGC axons to form a crude map. This creates a unique experimental system in which, by visually stimulating the two eyes independently and systematically varying the degree to which stimulation is correlated between the two eyes, it becomes possible to directly test the Hebbian "fire together, wire together" hypothesis. Because the contralateral eye drives most of the inputs, a flash of light presented to that eye will cooperatively recruit activation of postsynaptic tectal neurons. In contrast, for the lone ipsilateral RGC to participate in firing the tectal neurons, it must fire at the same time as the contralateral inputs.

In his 1973 treatise on Hebbian plasticity, Gunter Stent argued that there must exist a complementary rule to Hebb's postulate to explain the case where a presynaptic axon repeatedly fails to excite a postsynaptic partner that is actively firing under the influence of another input (Stent, 1973). Stent proposed that this condition should be punitive, resulting in the weakening of that non-contributing input. This is sometimes referred to as the "Stentian extension" of Hebb's postulate. The lone ipsilaterally projecting RGC axon allows for both Hebbian and Stentian forms of correlation-based plasticity to be examined by applying synchronous or asynchronous stimulation to the two eyes.

Electrophysiological recordings from tectal neurons that receive synaptic input from both the ipsilateral and contralateral eyes revealed that the ipsilateral input maintains

or even slightly increases its synaptic strength relative to the contralateral inputs when both eyes are stimulated together. However, when the two eyes were stimulated 1 sec apart, the ipsilateral eye input, which by itself is usually not strong enough to drive the postsynaptic neurons to fire action potentials, very rapidly declines in synaptic strength and in many cases entirely loses its ability to evoke an AMPAR-mediated postsynaptic current, suggesting that a phenomenon like tLTD can be induced by asynchronous visual stimulation of the two eyes in this case.

In vivo multiphoton time-lapse imaging of the misdirected ipsilateral axon was also performed while concurrently presenting these same synchronous or asynchronous visual stimuli to the two eyes. Remarkably, asynchronous stimulation resulted in a rapid (within 30 min) and dramatic upregulation of new branch additions and a significant increase in branch tip elongation compared with axon dynamics during a preceding period of darkness. Elimination of branch tips was also enhanced, indicating that rather than producing a larger arbor, asynchronous stimulation makes the axon more dynamic and exploratory. Thus, asynchronous visual stimulation produced an enhancement in growth and dynamics akin to the effects of NMDAR blockade. This makes sense as it is unlikely that the lone ipsilateral axon would by itself be able to drive sufficient depolarization of the postsynaptic tectal cell to permit Ca^{2+} flux through NMDARs. Consistent with this notion, addition of MK-801 to block NMDARs did not prevent the increased rate of branch additions in response to asynchronous stimulation. It is therefore possible that the source of the branch promoting signal may not be postsynaptic in origin, but could, for example be released by surrounding glial cells or come directly from nearby axon terminals.

In contrast, synchronous stimulation of the two eyes resulted in a rapid decrease in the rate of branch additions to levels seen in darkness. This decrease in branch dynamic behavior was completely prevented in the presence of MK801 or if tetanus toxin was expressed in the ipsilateral axon to render it incapable of releasing neurotransmitter, indicating that the activation of postsynaptic NMDARs likely leads to the release of a retrograde branch suppressing factor. In addition, branches that did form during synchronous stimulation had longer lifetimes on average that those that emerged during periods of asynchronous stimulation, indicating that they were more stable overall.

This experimental protocol tests the full range of growth responses that patterned activity might be able to induce, as it creates a set of extreme differences in firing correlation with synchronous stimulation resembling the conditions that might be produced by strobe rearing where all inputs are artificially correlated, and asynchronous stimulation creating a set of correlations that might only be found if the RGC were to ramify in an entirely inappropriate part of the tectum or what occurs in the dually innervated tectum. In the normal process of activity-dependent developmental refinement a typical axon might be expected to experience a more modest range of local correlation and asynchrony that would lead to a slight upregulation of exploratory branching and synapse disassembly on those branches that extend away from the proper termination zone (promoting them to keep growing until they land in more welcoming territory), and a stabilization and synaptic strengthening on those branches that extend into the appropriate part of the map where inputs with similar activity patterns converge (promoting consolidation and further synaptogenesis at this site). Figure 1 portrays several plausible models for how these mechanisms could promote projection refinement.

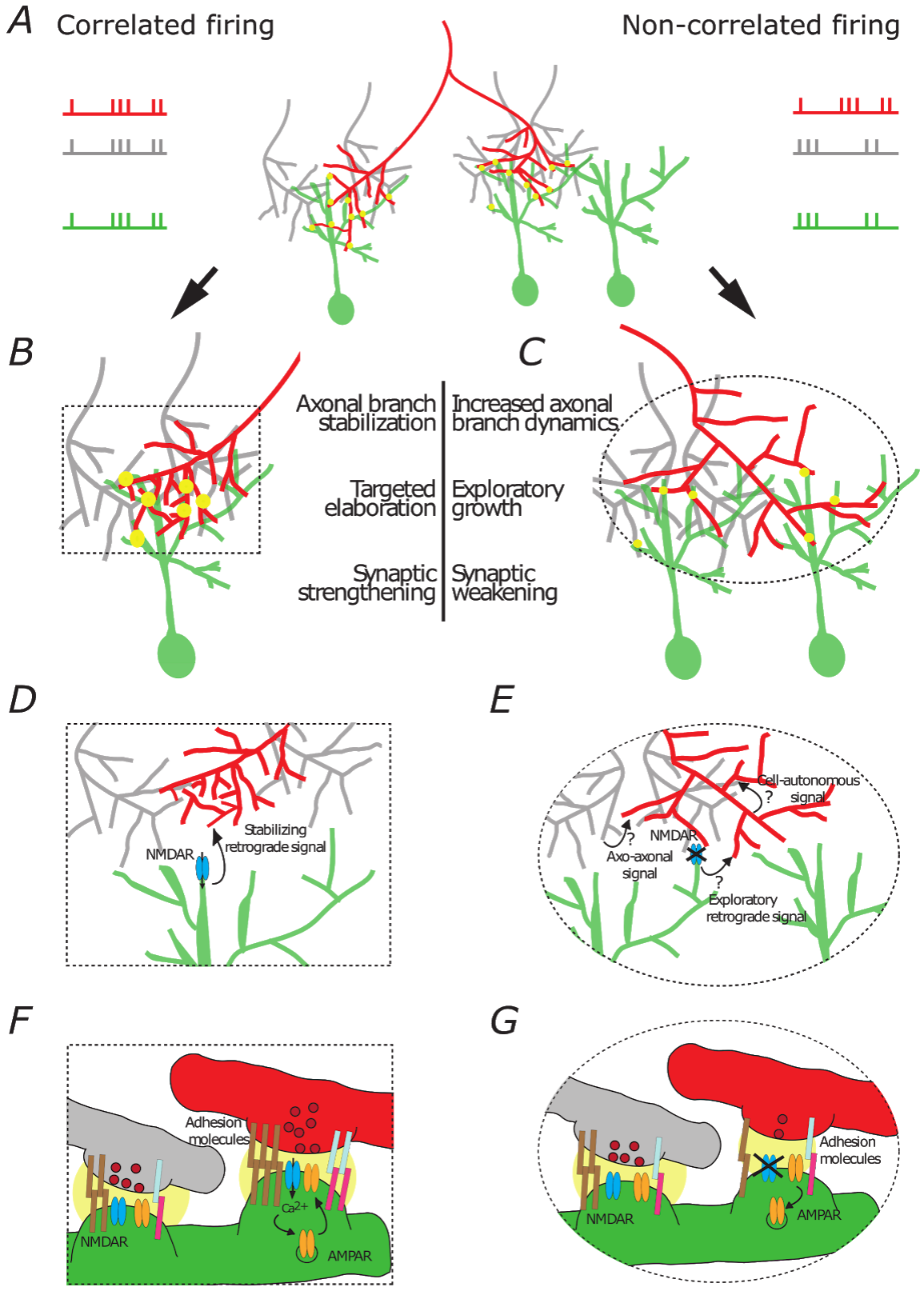
A
Correlated firing
Non-correlated firing
B
C
Axonal branch stabilization
Increased axonal branch dynamics
Targeted elaboration
Exploratory growth
Synaptic strengthening
Synaptic weakening
D
NMDAR
Stabilizing retrograde signal
E
Cell-autonomous signal
NMDAR
Axo-axonal signal
Exploratory retrograde signal
F
Adhesion molecules
NMDAR
Ca2+
AMPAR
G
Adhesion molecules
NMDAR
AMPAR

Figure 1: **Cellular and molecular mechanisms underlying the instructive role of patterned neuronal activity in retinotectal map refinement.**

An RGC axon of interest (red) synapses onto tectal neuron dendrites (green) in *A*. The red axon (left branch) is co-active with its neighboring RGCs (grey) and its firing pattern is therefore correlated with the firing pattern of the tectal neuron on which it synapses. The right branch of the red axon is not co-active with its neighbors and its firing pattern is not correlated with the firing pattern of its synaptic partner. Synapses are depicted as yellow circles. The effects of patterned neuronal activity on structural remodeling and synaptic efficacy are schematized in *D-E* and *F-G*, respectively. *B.* Correlated firing patterns of an RGC with its partnering tectal neuron instruct an increase in synaptic strength and stabilization of the axonal arbor allowing for local targeted arbor elaboration as new branches tend to form at existing synapses. *C.* Non-correlated firing of an RGC with its neighboring axons and its postsynaptic partner instructs synaptic weakening and an increase in axonal branch dynamics, accompanied by exploratory growth in search of a better partner. Synaptic strength is represented by the size of the yellow circles. *D* shows a zoom-in of the area of the box in B depicting a "stabilizing retrograde signal" downstream of activation of NMDAR which encodes axonal branch stabilization and targeted elaboration. *E.* Zoom-in of the ellipse in *C.* Plausible mechanisms instructing axonal exploratory growth and branch destabilization due to the lack of correlated firing with the neighboring RGC inputs and the postsynaptic partner include: 1. Axo-axonal signal, released by the firing neighboring inputs (grey); 2."Exploratory retrograde signal", unmasked by the inactivation of NMDAR; 3. Cell-autonomous activity-dependent signal, released by the red neuron, or acting intracellularly. F. zoom-in depicting molecular mechanisms underlying synaptic strengthening and stabilization of the red axon from B. Correlated firing of the RGC axon (red) with its neighboring axons (grey) and the tectal neuron (green) results in both release of glutamate containing vesicles (dark red) and postsynaptic depolarization. This satisfies the conditions required for release of the Mg^{2+} block from the channel pore of the NMDAR (blue), allowing for cation influx. Ca^{2+} triggers a molecular cascade resulting in insertion of more AMPAR (orange) in the membrane. A retrograde signal downstream of NMDAR encoding higher probability of vesicle fusion in the red axon (depicted as higher number of vesicles in dark red). Increase in synaptic efficacy is accompanied by strong homophilic (brown) and heterophilic interactions of adhesion molecules (light blue and pink). The strength of the interaction is represented by the number of pairs of adhesion molecules. *G* zoom-in showing the change is synaptic efficacy in *C*. Non-correlated firing of the red axon with its neighbors and its partnering tectal neuron prevents opening of the channel pore of NMDAR, leading to AMPAR endocytosis, lower probability of glutamate release and weaker interaction of adhesive molecules.

6.1.2.5. In the absence of sensory input, correlated spontaneous firing provides surrogate patterned activity.

The pattern of action potential firing in the developing visual system contains information about the relative positions of the RGC somata in the retina and thus can instruct the precise mapping of the axons onto their postsynaptic partners in the optic tectum. Anamniotes, which include fish and amphibians, develop exclusively externally which allows for the possibility of neuronal activity driven by natural visual scenery (see review by Pratt et al., 2016). Unlike fish and frogs, amniotes are hidden behind thick shells or develop *in utero*, which leads to a general deprivation of visual experience during the time when visual circuit refinement takes place. It is reasonable to speculate that spontaneous activity in the retina may have arisen as an evolutionary adaptation to provide replacement patterns of neuronal activity in amniotes that lower vertebrates are able to experience by visually interacting with their surrounding environment after hatching. The first evidence for locally correlated spontaneous activity in the fetal retinal came from extracellular retinal recordings made in rat pups while still attached to the uterus via the umbilical cord (Maffei and Galli-Resta, 1990). They have subsequently been confirmed and meticulously characterized using *in vitro* multielectrode array recordings and calcium imaging of retinal explants (Meister et al., 1991; Wong et al., 1993; Feller et al., 1996). These spontaneous activity patterns exhibit a high degree of local correlation in firing and consequently have been dubbed “retinal waves” (Meister et al., 1991). RGCs located in close proximity overlap their bursting activity in time, whereas RGCs that reside further away from each other are less likely to be co-active. This spatiotemporal pattern of RGC activity results from a local initiation of depolarization, which propagates to adjacent neurons spreading over long distances across the retina.

The definitive demonstration of this phenomenon was recently implemented in the intact mouse by loading RGCs out to their axon terminals with a calcium indicator to permit retinal waves in the eye to be detected by imaging their calcium transients in the SC (Ackman et al., 2012). This study revealed that the initiation point of the waves is biased to the ventrotemporal region of the retina, an observation that is particularly interesting in light of the fact that a locomoting fish or tadpole in the wild would typically

experience natural visual stimuli as optic flow similarly sweeping from temporal to nasal retina, further arguing that retinal waves may have evolved as a replacement for natural vision prior to eye-opening. In tadpoles, it has been shown directly that visual stimulation which includes optic flow in this more natural direction is far more effective at refining the retinotopic projection of RGCs than an identical amount of stimulation oriented in the opposite direction (Hiramoto and Cline, 2014). During different periods of development the mechanisms generating retinal waves differ: embryonic type I waves depend on gap junctions; type II waves are initiated by starburst amacrine cells and spread through activation of nicotinic acetylcholine receptors; and type III waves utilize glutamate (Feller et al., 1996; Bansal et al., 2000; Torborg et al., 2005); see reviews by Arroyo and Feller (2016) and Kerschensteiner (2016).

While there is abundant evidence that patterned activity has an instructive role in topographic map refinement, an important remaining problem is to dissect the specific aspects of spontaneous activity that instruct retinocollicular refinement. Genetic deletion of the β2 nicotinic acetylcholine receptor subunit (β2-nAChR) in mice results in abnormal retinal waves with impaired spatiotemporal properties (Rossi et al., 2001; McLaughlin et al., 2003b ; Chandrasekaran et al., 2005; Mrsic-Flogel et al., 2005). These perturbations result in severe defects in both the topographic refinement and eye-specific segregation in the SC and LGN. Unexpectedly, it was also reported that between-eye correlations in wave activity are enhanced in these β2-nAChR knockout mice, which may partially account for the failure of eye-specific segregation (Burbridge et al., 2014).

Xu and colleagues examined a transgenic mouse line (β2(TG)nAChR) in which expression of the β2-nAChR was restored specifically in the RGCs in β2-nAChR knockout animals (Xu et al., 2011a). Although retinal waves in these mice occur with the same frequency and overall level of activity as in wild-type animals, their propagation is truncated and thus the correlation between the firing patterns of neighboring cells decreases steeply with distance. The very local correlations in RGC spiking are still intact, but the large-area within-eye correlations are lacking. These “smaller” retinal waves are sufficient to permit the refinement of retinotopy in the monocular zones of SC. Interestingly, however, RGC projections to the binocular zone fail to refine normally. This

is apparently a result of an interaction between inputs from the two eyes, as monocular enucleation permits the full refinement of the remaining eye's afferents. Eye-specific segregation is also strongly disrupted in these mice.

They also tested animals (Rxβ2-cKO) in which β2-nAChR expression was conditionally deleted specifically in the retina (Xu et al., 2015). Much like the β2(TG)nAChR mice, Rxβ2-cKO mice exhibit only small residual retinal waves that have high local correlation but much lower long-distance correlations in firing. Retinotopy in Rxβ2-cKO mice was normal in the monocular SC, but eye-specific segregation was disrupted, phenocopying the β2(TG)nAChR animals. The rescued retinotopy and impaired eye-specific segregation in the SC compared to full β2-nAChR knockouts suggest that topographic precision of the visual map depends primarily on local correlation in spiking patterns, whereas eye-specific segregation requires global within-eye correlations that differentiate the two eyes. It remains to be tested whether the abnormal between-eye correlations seen in full β2nAChR knockout mice might also occur in β2(TG)nAChR or Rxβ2-cKO lines. This binocular correlation could perhaps help explain the failure of RGC inputs to refine topographically in the binocular zone of the SC, as inappropriately correlated inputs would be converging on postsynaptic cells in the SC.

Spontaneous retinal waves occurring before the onset of vision have been observed across numerous amniote species: turtle, chick, rat, mouse, ferret, cat, and monkey. However, they are not present in fish and frogs, species that are able to rely on photoreceptor-driven vision from the onset of development of the retinotectal projection (Ackman and Crair, 2014). Interestingly, Demas and colleagues used multielectrode arrays to record retinal activity across the eye, and discovered that rearing *Xenopus* tadpoles in complete darkness induces an increase in the amount of correlation in the spontaneous activity between neighboring RGCs (Demas et al., 2012). However, dark rearing prevents the developmental increase in correlated neural activity over large groups of tectal neurons in the OT (Xu et.al, 2011b). The former observation supports the notion that the retinal circuitry may exhibit a tendency to favor retinal waves as a natural means of compensating for an absence of early visual stimulation. This critical discovery by Demas and colleagues finally helped make sense of several decades of earlier dark-

rearing experiments in fish and frogs that had concluded that visual experience was dispensable for normal refinement of the developing retinotectal projection.

6.1.2.6. New axonal branch tips emerge near existing synapses.

At the same time as the retinotectal axons are dynamically remodeling by constant exploratory branch addition and withdrawal, fish larvae and tadpoles are already using their visual system to interact with the environment. Zebrafish are avid predators that can track and capture tasty paramecia and other organisms for food, a behavior that requires precise tectal function (Gahtan et al., 2005). This raises the paradox of how a functional circuit can at once be wired to reliably perform essential behavioral tasks while actively adding and eliminating synaptic contacts to refine connectivity. Insights into this process have come from time-lapse imaging of RGC axons and tectal neurons expressing fluorescently labeled synaptic marker proteins to reveal synapse locations. This powerful approach was pioneered in the retinotectal system by Alsina and co-workers (2001) who expressed GFP-VAMP2 in *Xenopus* RGCs to reveal that many putative synaptic sites along the developing axonal arbor are added and eliminated rapidly over time, the rate of which can be regulated by BDNF signaling. These authors made the important observation that new axonal branch tips almost always emerged from GFP-VAMP2 positive puncta, a finding that was later confirmed using a better targeted synaptic marker, synaptophysin-GFP (Meyer and Smith, 2006; Ruthazer et al., 2006). This result has profound implications as a mechanism for map refinement because it means that wherever a synapse strengthens (or weakens) through activity-dependent plasticity, it will be available (or not) to nucleate new branches from which new synapses can form. This constitutes a positive feedback loop that will lead to the targeted elaboration of axonal arbor at sites where that axon has formed effective, strong synaptic contacts and the scaling back of branch initiation at inappropriate sites where synapses may form transiently but are subsequently eliminated.

6.1.2.7. Stronger synapses help stabilize the axons and dendrites on which they reside (Synaptotropism)

Postsynaptic dendritic growth and remodeling was studied in zebrafish tectal neurons co-expressing PSD-95-GFP to mark postsynaptic sites (Niell et al., 2004). These investigators made the critical observation that synaptic sites were fairly labile. They observed that the dendritic tree elaborated through a process of dynamic filopodial extensions followed rapidly by synapse formation. As synapses formed, those synapse-bearing branches became consolidated. Further branch extension then proceeded by building upon these more stable sites. Thus, the presence of a synapse appears to confer stability onto the branch on which it forms, a phenomenon referred to as “synaptotropism” (Vaughn et al., 1988; Cline and Haas, 2008). Further support for the synaptotropic model of dendritic growth was solidified by experiments where synaptogenesis or synapse maturation, respectively were prevented by blocking neurexin/neuroligin signaling or AMPAR trafficking in *Xenopus* tectal neurons, resulting in a failure to elaborate normal complex dendritic arbors (Haas et al., 2006; Chen et al., 2010).

Time lapse imaging of dsRed/synaptophysin-GFP-expressing RGC axons in zebrafish and *Xenopus* tadpoles showed that synaptotropism is equally applicable at the presynaptic side (Meyer and Smith, 2006; Ruthazer et al., 2006). Within minutes of axonal branch extension, synaptophysin-GFP puncta could be observed accumulating in the wake of the advancing growth cone. Some synaptic puncta were later lost while others became more mature over time, indicated by the bright accumulation of synaptophysin-GFP positive vesicles. When these branches later attempted to retract, the presence of a mature synaptic site conferred structural stability, preventing the branch from withdrawing beyond that site.

6.1.2.8. Homeostatic mechanisms help maintain the overall level of functional synaptic input to the target.

Both the Hebbian and Stentian mechanisms in the context of changes in synaptic efficacy are inherently unstable. Correlated firing between a presynaptic neuron and its postsynaptic partner would induce synaptic strengthening as described above. An increase in synaptic efficacy would result in an even higher probability of correlation between the firing patterns of the pre- and postsynaptic neuron. Thus, applying only the Hebbian plasticity rules, the positive feedback loop would become unsustainable. Applying the same logic to Stent's extension to the Hebbian postulate, we will find ourselves in a similar situation where each time the synapse weakens, it will be less likely that the pre- and the postsynaptic firing patterns will be correlated. The brain overcomes this inherent instability by applying additional rules which ensure a healthy dynamic range of synaptic transmission within which bidirectional changes in synaptic efficacy can occur. These rules are referred to as homeostatic plasticity and have been extensively studied in the neocortex and the hippocampus (Bienenstock et al., 1982; Turrigiano and Nelson, 2004; Kaneko et al., 2008). An example of homeostatic regulation in the developing *Xenopus* retinotectal projection can be found in experiments where the intrinsic excitability of tectal neurons was manipulated either by overexpression of leak K^+ channel or by modifying synaptic efficacy by application of a peptide that hinders AMPAR trafficking. Both manipulations lead to upregulation of voltage-gated Na^+ currents (Pratt and Aizenman, 2007), suggesting a homeostatic mechanism regulating intrinsic excitability that counteracts Hebbian/Stentian plasticity rules.

Further evidence for homeostatic regulation of the retinotectal circuit during development was obtained using zebrafish *blumenkohl* mutants (*blu*). The *blu* mutation disrupts *vglut2a*, encoding a vesicular glutamate transporter homologous to mammalian VGLUT2 (Smear et al., 2007). *Blu* mutants exhibit a decrease in TTX miniature ecxitatory postsynaptic current (mEPSC) amplitudes in tectal neurons, suggesting a reduction in glutamate concentration per vesicle. Interestingly, mEPSC frequency in mutant animals is increased, consistent with a higher probability of glutamate vesicle release or with upregulation in the number of release sites. These observations allude to a compensatory

mechanism that helps normalize glutamatergic transmission in these animals. In accordance with this homeostatic regulation, the RGC arbors in the *blu* mutant zebrafish are larger, spanning a greater area of the optic tectum and tectal neurons exhibit larger receptive fields. In tectal *blu* animals neurotrophin-3 (NT-3) protein levels are upregulated in the optic tectum, suggesting that it could act as a homeostatic retrograde signal through TrkC receptor promoting axonal branch elaboration (Auer et al., 2015).

6.1.3. Summary

Thanks to many decades of experimentation on retinotectal development in models ranging from fish to mammals, in conjunction with modern technology permitting live imaging of developing axons in the intact animal, we now have a much clearer understanding of the mechanisms that regulate the developmental fine-tuning of the retinotectal map. The decisions faced by a growing retinotectal axon are summarized in the form of a flow-chart in Figure 2. While it is likely that other brain regions will apply slightly different strategies for activity-dependent refinement, the rules we have outlined here should prove a useful template for further investigation.

6.1.4. Candidate molecular mechanisms underlying activity-dependent circuit refinement

A few molecular mechanisms have been suggested to regulate or instruct activity-dependent circuit refinement. It has become apparent that a phenomenon as crucial for the individual's survival in its specific environment is likely not under the control of a single mechanism, increasing the chance of survival of animals possessing genetic polymorphisms. However, an overarching mechanism regulating activity-dependent refinement throughout the visual system is the activation of the NMDAR (Cline et al., 1987; Hahm et al., 1999; Berardi et al., 2003). Protein synthesis has been shown to be crucial for cortical ocular dominance plasticity (Taha and Stryker, 2002). Experience-dependent plasticity also produces long-term epigenetic changes. In particular, inhibition of histone deacetylases, which are often linked to enhanced transcription is able to fully restore visual acuity in monocularly deprived rats (Silingardi et al., 2010). The

neurotrophin BDNF was also implicated in activity-dependent refinement. The evidence that it acts as a regulator of protein synthesis and it can be expressed in an activity-dependent manner made it an attractive target for numerous studies (Karlsson and Hallböök, 1998; Ruiz et al., 2014). In the visual cortex, BDNF signaling regulates inhibitory neuron maturation during the critical period (Huang et al., 1999b; Gianfranceschi et al., 2003; Baho et al., 2019).

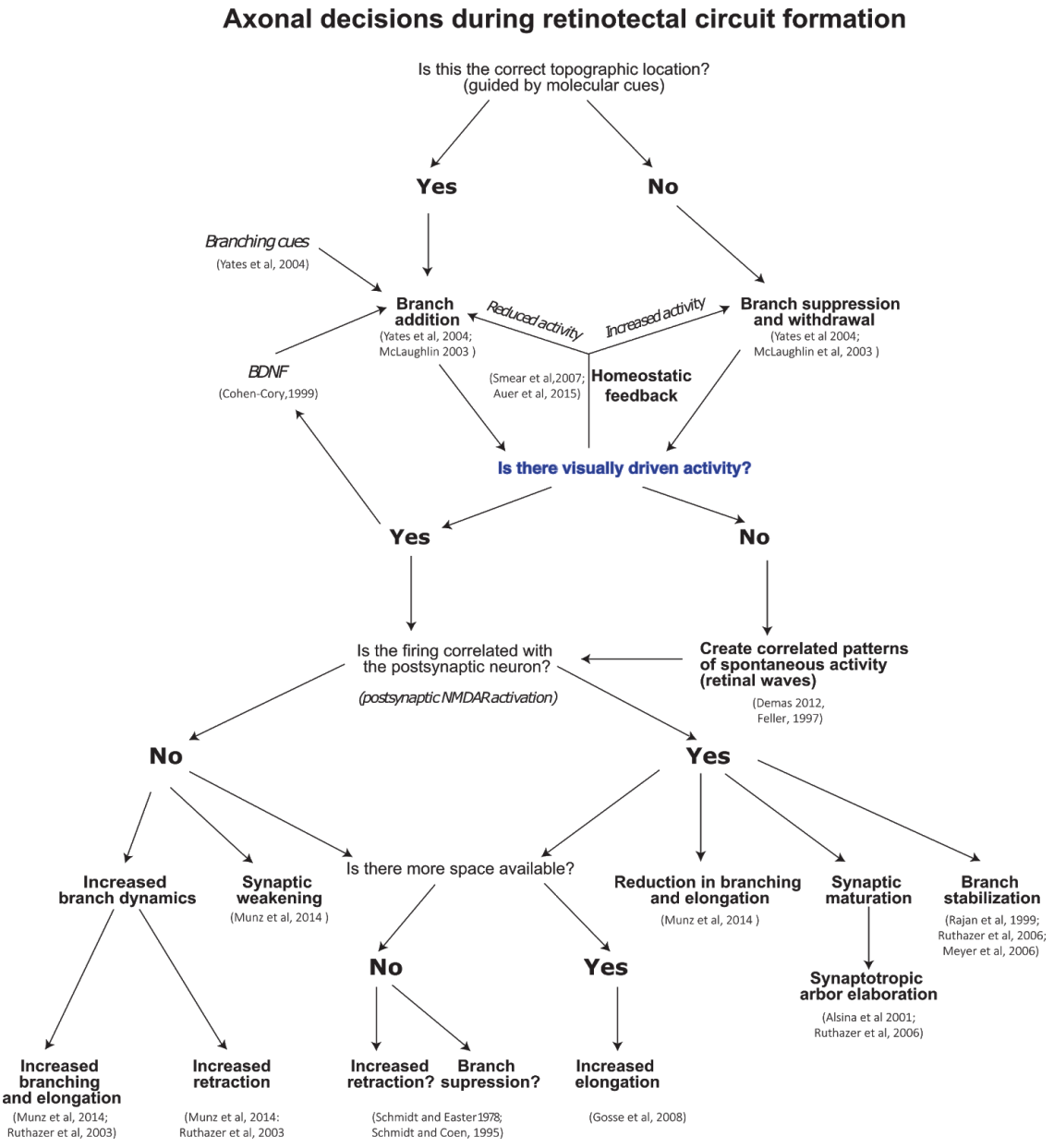

Figure 2: **Flow-chart of decisions RGCs face during retinotectal map formation and refinement.**

6.2. BDNF -- biology, signaling and functions

In this part, I will review the literature related to genetic regulation, translation and post-translational regulation of BDNF, its signaling through both TrkB and p75NTR receptors and its functions in the nervous system, with a specific focus on neural circuit development and synaptic plasticity, in the context of the family of neurotrophic factors. The specific properties of BDNF and its signaling cascades described below make it an excellent molecular candidate that could instruct or regulate various cellular processes in circuit remodeling in the developing brain.

6.2.1. The history of the discovery of the neurotrophin family

The “neurotrophic hypothesis” comes originally from experiments in which the removal of the limb bud of a chick embryo led to a reduction in the number of motor neurons, whereas the transplantation of additional limb buds resulted in an increase in the number of efferent and afferent projecting neurons. These early experiments led to a search for the identities of the players signaling this “neurotrophism” (Hamburger, 1934, 1939; Bothwell, 2014 p.4). Nerve growth factor (NGF) was first identified as a soluble, thermolabile factor isolated from snake venom that could induce marked neurite outgrowth in cultured sympathetic and sensory ganglia (Cohen and Levi-Montalcini, 1956; Levi-Montalcini and Cohen, 1956). Later, another member of the family, coined BDNF was purified from pig brain based on its additive effect on outgrowth (Barde et al., 1982) when applied to chick sensory ganglia together with NGF (Barde et al., 1982). This protein did not bind to NGF and was later shown to have structural similarity with NGF (Leibrock et al., 1989). Neurotrophin-3 (NT-3) and neurotrophin-4/5 (referred to as NT-4 henceforth), neurotrphin-6 (NT-6) and neurotrophin-7 (NT-7) were subsequently discovered and added to the neurotrophin family (Hohn et al., 1990; Berkemeier et al., 1991; Hallböök et al., 1991; Götz et al., 1994; Nilsson et al., 1998). NT-6 and NT-7 are only observed in fish, whereas NT-4 is likely absent in chicks and other birds (Sehgal and Lovette, 2003).

6.2.2. Structural properties of BDNF as p75NTR and TrkB ligand

Similarly to the other members of the neurotrophic family, BDNF is synthesized as a precursor protein (proBDNF) of approximately 35 kDa (Marcinkiewicz et al., 1998) which is then cleaved at a well-conserved RRVR site intracellularly in the trans-Golgi network (TGN) by furin protease or in secretory vesicles by prohormone convertases (Rouillé et al., 1995; Mowla et al., 1999) to yield the mature form (mBDNF or just BDNF). Analogously to NGF, a cysteine-knot in the mature domain is responsible for the formation of homodimers in BDNF at physiological concentration. Post-cleavage mature BDNF homodimers are very stable in denaturing conditions: both in high urea concentration and at high temperatures. Each protomer is about 14 kDa (Marcinkiewicz et al., 1998). BDNF is able to heterodimerize with other neurotrophin monomers *in vitro*, however to date it remains unclear whether this phenomenon is physiologically relevant (Bothwell and Shooter, 1977; Radziejewski et al., 1992).

There are two major families of receptors with which neurotrophins are known to bind and signal: the high-affinity Trk receptor tyrosine kinases and the low-affinity neurotrophin receptor p75NTR. Several reports compare the biological activity of neurotrophin heterodimers on the phosphorylation of the Trk receptor and on survival essays. Conflicting studies show that BDNF/NT-3 heterodimers are about 10-times less effective than homodimers of the two neurotrophins (Jungbluth et al., 1994; Robinson et al., 1999) or that the heterodimers are as active as the homodimers (Arakawa et al., 1994). BDNF/NGF heterodimers also form but are considerably less stable, which raises questions about the physiological relevance of this particular heterodimer. There are two plausible physiological functions of neurotrophin heterodimers: to ensure a fast on-demand switch of production and action of two neurotrophins, or to ensure compensation of the function of a certain neurotrophin under unfavorable circumstances (Robinson et al., 1995, 1999). The solved crystal structure of NGF homodimer brought insights into the molecular structure and interactions of neurotrophins and their receptors (McDonald et al., 1991). Later on, NT-3 and NT-4 homodimers and NT-4/BDNF, NT-3/BDNF heterodimers further showed that although there is only 50% amino acid homology between the neurotrophins, their structure in homo- and heterodimers is highly similar

(Robinson et al., 1995, 1999). It consist of eight β-strands that form four pairs of antiparallel β-strands supported by three cysteine bonds establishing a cysteine knot (McDonald and Hendrickson, 1993; Lou et al., 2005). The highly conserved regions are located at the β-sheet interface of the protomers forming a dimer and the variable regions are located in loops.

The residues crucial for p75NTR binding are positioned in the loop regions, suggesting that binding to the receptor might modify the neurotrophin structure (Ibáñez et al., 1991; Urfer et al., 1994; Robinson et al., 1999). Residues forming the binding region with p75NTR are not located in close proximity between the two protomers in a dimer. In the case of Trk-neurotrophin binding, the residues forming the common motif and the ones ensuring specificity of each neurotrophin to its preferred Trk receptor are contributed by both of the protomers in a dimer (Ibáñez, 1995; Robinson et al., 1999).

6.2.3. Synthesis, post-translational modifications, sorting and secretion

As mentioned above, proBDNF is cleaved at a highly conserved basic sequence RRVR to yield mBDNF. Consistent with the synthesis of a secretory protein, BDNF translation starts at the rough endoplasmic reticulum (EPR). The precursor form is further subjected to *N*-glycosylation in the Golgi apparatus at a site 6 residues upstream of the cleavage site (Mowla et al., 2001). This glycosylation seems to be crucial for the proper folding and/or stabilization of BDNF, as impeding this process leads to decreased amounts of both proBDNF and mBDNF. BDNF is also glycosulfated, however the sulfation does not seem to affect neither the processing, nor the stability of mBDNF and its precursor. Once in the TGN, BDNF and NGF are sorted into the secretory pathway. There are two distinct modes of secretion in endocrine cells and in neurons, which assure their ability to function as specialized secretory cells: the regulated and the constitutive pathways. The constitutive pathway is responsible for consistent replenishment of proteins on the plasma membrane, whereas vesicles undergoing the regulated pathway are stored until a specific signal triggers their release (Moore et al., 1993)

Much has been revealed about the conversion of proneurotrophins to mature neurotrophins and their secretion over the last 20 years. NGF seems to be sorted

preferentially in the constitutive pathway and BDNF to the regulated pathway (Goodman et al., 1996; Mowla et al., 1999). Cleavage by furin in the TGN drives neurotrophins into the constitutive secretion mode, thus most of proNGF is processed by furin. ProBDNF is mainly cleaved by prohormone convertases (PC) either in the TGN or in immature secretory vesicles. Recent study suggests that mature BDNF and its pro-peptide can be observed in dense core vesicles in neuronal cultures (Dieni et al., 2012). A four-residue motif ($I_{16}E_{18}I_{105}D_{106}$) in BDNF likely interacts with a membrane carboxypeptidase E in the TGN which ensures the preferential sorting of BDNF to the regulated pathway (Lou et al., 2005). In NGF one of the two acidic residues is missing from a similar sorting motif preventing efficient interaction with carboxypeptidase E. Formation of multimolecular complexes and self-aggregation in acidic pH together with higher Ca^{2+} concentration also likely aid the sorting of proBDNF to secretory granules for exocytosis (Lessmann and Brigadski, 2009). Another Golgi-residing receptor -- sortilin enhances proBDNF targeting to regulated secretion (Chen et al., 2005). Such multiplayer control of BDNF secretion is crucial in order to achieve an on-demand release in time and space.

6.2.4. Activity-dependent release

Mounting evidence demonstrates that BDNF release takes place in an activity-dependent manner. Using high K^+ concentration Lou and colleagues showed a 3-fold increase in secreted BDNF (both pro- and mature) by AtT-20 cells using Western blot analysis (Lou et al., 2005). In hippocampal rat cultures electrical stimulation of increasing frequencies caused a linear increase in the released amount of mBDNF measured by enzyme-linked immunosorbent assay (ELISA; Balkowiec and Katz, 2000, 2002). Theta-burst stimulation, which is considered a physiologically relevant electrical stimulation protocol, had a comparable effect on mBDNF release to 100 Hz high-frequency stimulation. The mechanisms underlying the described activity-dependent BDNF secretion involve intracellular mobilization of Ca^{2+} from internal calcium stores (Balkowiec and Katz, 2002). Further studies relying on exogenous expression of BDNF fusion proteins such as BDNF-GFP showed that BDNF in hippocampal culture could be released postsynaptically from glutamatergic synapses following high-frequency electrical stimulation, supporting the idea that BDNF serves as a retrograde or paracrine mediator

during synaptic plasticity (Hartmann et al., 2001; Kohara et al., 2001; Kojima et al., 2001). Interestingly, much stronger stimuli are required for axonal compared to dendritic BDNF release (Zakharenko et al., 2003; Kuczewski et al., 2008; Matsuda et al., 2009). Moreover, a common human polymorphism Val66Met occurring in the prodomain of BDNF leads to an inefficient sorting of BDNF into the regulated secretory pathway and thus impairs activity-dependent release (Egan et al., 2003; Chen et al., 2004). Humans carrying this polymorphism have compromised episodic memory.

6.2.5. Subcellular localization and trafficking

There has been a long-standing debate on the exact site of BDNF release with contradictory evidence supporting release from either presynaptic or postsynaptic excitatory sites as mentioned before. Rigorous detection of endogenous BDNF due to its low levels in adult animals has been the main challenge to conclusively show the subcellular localization and secretion mode of this neurotrophin. BDNF has been detected in synaptosomes but it is still a matter of debate whether it is secreted pre- or postsynaptically (Fawcett et al., 1997). Most of the data suggesting that both axonal and dendritic BDNF secretion is plausible come from exogenous expression systems (Haubensak et al., 1998; Hartmann et al., 2001; Brigadski et al., 2005; Dean et al., 2009; Harward et al., 2016). In contrast, studies both in hippocampal cultures and adult slices assessing endogenous release using electron microscopy and super resolution imaging have shown that BDNF is released solely by the presynaptic terminal (Dieni et al., 2012; Andreska et al., 2014). In line with axonal secretion, BDNF secretory vesicles have been shown to be preferentially transported anterogradely by kinesin-1 within axons, but seem to be more stunted in dendrites (Zhou and Rush, 1996; Altar et al., 1997; Adachi et al., 2005; Butowt and von Bartheld, 2007). Recent work of Vignoli and colleagues looking at the distribution of endogenous proBDNF and mBDNF has revealed that in cortical slices BDNF (both pro- and mature) are mainly localized to presynaptic terminals in baseline conditions, but after theta-burst stimulation, the distribution shifts towards similar levels of the neurotrophin in presynaptic, postsynaptic and astrocytic sites (Vignoli et al., 2016). Although the dendritic BDNF might be a result of endocytosed BDNF-bound TrkB, it is also plausible that local protein synthesis or dendritic trafficking are activated upon theta-

burst stimulation. Interestingly, even post-endocytic BDNF could be released in an activity-dependent manner (Wong et al., 2015). This is not the first experimental evidence supporting the hypothesis that axonal versus dendritic secretion of BDNF are differentially regulated by neuronal activity (Dean et al., 2009; Matsuda et al., 2009). However, previous reports relied on overexpression of fusion proteins, calling into question the physiological relevance of processes like protein sorting and trafficking under these conditions.

6.2.6. Transcriptional regulation

6.2.6.1. Bdnf expression

The *bdnf* gene is expressed at its highest levels in the brain during development (Kaisho et al., 1991). In adult animals, *bdnf* expression has also been identified in non-neuronal tissues such as heart, lung, liver, skeletal muscles and others. As certain brain regions mature they increase their *bdnf* expression (Maisonpierre et al., 1990a, 1990b; Katoh-Semba et al., 1997).

6.2.6.2. Alternative splicing

In rodents and humans, the *bdnf* gene contains eight exons and eleven exons, respectively, that are alternatively spliced to yield the 5'-untranslated region (UTR) of the mRNA and a last exon that encodes the protein and contains the 3'UTR (Aid et al., 2007; Pruunsild et al., 2007; Cattaneo et al., 2016). The *bdnf* gene in *Xenopus laevis* consists of six non-coding exons alternatively spliced and transcribed into the 5'UTR of the mRNA and seventh exon containing the coding sequence (Kidane et al., 2009). Although there are more non-coding exons in mammals than in *Xenopus laevis*, the principle of alternative splicing to increase the variability between transcripts is evolutionary conserved. *Xenopus* exons I-IV share high degree of homology with mouse, rat and human *bdnf* exons I-IV. Furthermore, in zebrafish larvae, the above described mechanism of generating *bdnf* mRNA is also present (Huynh and Heinrich, 2001). The evolution of this genetic structure containing multiple promoters possibly contributes to specific

regulation of *bdnf* transcription in response to numerous stimuli (West et al., 2014, p.76). In mammals, promoter I,II and III are regulated by various pharmacological treatments such as kainic acid-induced seizures, AMPAR, NMDAR and metabotropic glutamate receptor activation (Metsis et al., 1993). It is likely that neuronal activity controls transcription of exon I through (ATF)/cAMP/Ca^{2+}-response element binding protein (CREB) and the basic helix-loop-helix (bHLH) proteins upstream stimulatory factor (USF) 1 and USF2 (Tabuchi et al., 2002). Other Ca^{2+}-responsive proteins binding promoter I upstream from the transcription start site and regulated by neuronal activity include bHLH-Per-Arnt-Sim (bHLH-PAS) transcription factors aryl hydrocarbon receptor nuclear translocator 2 (ARNT2) and neuronal PAS domain protein 4 (NPAS4; Pruunsild et al., 2011). Promoter II is regulated by neuron-restrictive silencer element (NRSE) which interacts with transcriptional co-repressors mSin3A and CoREST and histone modifying proteins such as histone deacetylase (HDAC; Palm et al., 1998; Andrés et al., 1999; Huang et al., 1999a; Timmusk et al., 1999). Promoter IV is the most studied of all *bdnf* promoters regulated by neuronal activity. It is under the control of myriad Ca^{2+} -responsive proteins such as calcium-responsive transcription factor (CaRF), NPAS4, ARNT2, basic helix-loop-helix factor BHLHB2, nuclear factor κB (NF-κB), nuclear factor of activated T cells (NFAT) and others (Lipsky et al., 2001; Tao et al., 2002; Jiang et al., 2008; Vashishta et al., 2009; Pruunsild et al., 2011). Exon IV - containing *bdnf* transcripts seem to be preferentially expressed during activity-dependent neuronal development, more specifically affecting inhibitory interneuron development (Hong et al., 2008; Sakata et al., 2009).

6.2.6.3. Chromatin Remodeling

Apart from regulation via transcription factors, chromatin remodeling is another mechanism to control gene expression at the level of DNA transcription. Modifications in the DNA itself such as methylation and hydroxymethylation or acetylation of the histone proteins are referred to as chromatin remodeling. Histones serve as a scaffold for DNA folding, forming a complex DNA-protein structure referred to as chromatin. There are four proteins that form the core structure of chromatin H2A, H2B, H3 and H4 (West et al., 2014, p.82).

6.2.6.3.1. DNA methylation

DNA methylation was originally discovered as a means for permanent X-chromosome repression. However, recently 5-methylcytosine (5mC) in CpG islands has been identified as a transcription suppressor in active gene regions (Hellman and Chess, 2007; Meissner et al., 2008). Membrane depolarization as a model of neural activity in neuronal cultures results in a reduction in CpG methylation in *bdnf* promoter IV associated with an increase in BDNF expression (Martinowich et al., 2003). In more physiologically relevant models, CpG demethylation in *bdnf* promoters was observed in response to associative learning, early life adversity and fear conditioning (Lubin et al., 2008; Roth et al., 2009, 2014; Ambigapathy et al., 2015). The mechanism underlying stimulus-dependent transcriptional regulation via DNA methylation includes recruitment of various factors that exert transcriptional control. Methyl-CpG binding protein 2 (MeCP2) and CCCTC-binding factor (CTCF) are among the factors that regulate the transcription of *bdnf* (Martinowich et al., 2003; Chang et al., 2010). Interestingly, MeCP2 and CTCF are both responsible for alternative splicing of exons in *bdnf* triggered by classic conditioning in turtles (Zheng et al., 2017).

6.2.6.3.2. Histone acetylation

Acetylation of certain lysine residues in H3 (K9, K14) and H4 (K5, K8 and K12) are associated with increases in transcription (Roh et al., 2004). These modifications in *bdnf* are often the result of neuronal activity such as following epileptic seizure or fear extinction (Tsankova et al., 2004; Bredy et al., 2007). In neuropathologies such as Alzheimer's disease, the presence of amyloid fibrils seems to increase deacetylation of H3 in *bdnf*, leading to a decrease in *bdnf* expression, accompanied by memory impairment (Wang et al., 2014). Histone acetylation or deacetylation in response to the above-mentioned stimuli often targets different *bdnf* promoters, permitting specific transcriptional outcomes for each stimulus. HDAC1, HDAC2 and the histone acetyltransferase CREB binding protein (CBP) are implicated in the described modifications (Hong et al., 2008; Guan et al., 2009; Tian et al., 2010; Wang et al., 2014; Palomer et al., 2016).

6.2.6.3.3. Histone methylation

Another important way to regulate chromatin is histone methylation. Specific H3 lysine residue methylation could result in activated or repressed gene transcription with K3 and K36 leading to activation, whereas K9, K20 and K27 leading to repression (Lachner and Jenuwein, 2002; Greer and Shi, 2012). A further layer of regulation of transcription through methylation comes from the possibility for mono-, di- or trimethylation of the lysine residues. An example of activity-dependent histone modification comes from experiments in which dark rearing led to an increase in H3K27 methylation in the visual cortex paired with a decrease in *bdnf* expression (Karpova et al., 2010).

6.2.7. Translational Regulation

In addition to transcriptional regulation the expression of proteins is also subject to translational regulation. MicroRNAs are small non-coding RNA molecules that bind to specific complementary sequences of the 3'UTR of mRNAs. In most cases, this interaction impedes the early stages of translation and further recruits machinery which degrades the targeted mRNA (Djuranovic et al., 2012; Bazzini et al., 2012). Example miRNAs that regulate BDNF protein levels are miR-30a-5p and miR-195 (Mellios et al., 2008).

An intriguing hypothesis in the field has been that neuronal activity may induce local protein synthesis of BDNF in dendrites. Although it is still unclear how such translation might occur, what molecular factors might support it and importantly what type of cellular organelles might be responsible for post-translational modifications of locally translated BDNF, there is increasing evidence that BDNF could be synthesized on demand in dendrites. *Bdnf* mRNA has been identified in dendrites and in synaptosomes (Tongiorgi et al., 1997; Gharami and Das, 2014). Two alternative 3'UTR of *bdnf*, a result of two separate polyadenylation signals, are the plausible determinants of the differential trafficking of *bdnf* mRNA (Hofer et al., 1990; Metsis et al., 1993; An et al., 2008). The mRNA containing long 3'UTR seems to be preferentially targeted to the dendrites,

whereas the short 3'UTR containing mRNA is restricted to the somatic compartment (An et al., 2008; Orefice et al., 2013). Interestingly, the same group has recently reported that membrane depolarization or activation of NMDARs results in the specific dendritic translation of long 3'UTR-containing *bdnf* mRNA which is then translated and released as proBDNF to contribute to dendritic spine pruning (Orefice et al., 2016). However, experiments from another group show essential dendritic trafficking elements in the short 3'UTR of the mRNA (Oe and Yoneda, 2010). Furthermore, the same authors identified a novel cellular compartment that fails to co-label with markers for EPR, Golgi, endosomes and TGN which contains the locally translated BDNF. Bicaudal-D2, which forms complexes with the members of the family of dynein motors is co-localized with this compartment and is likely crucial for dendritic protein synthesis (Oe et al., 2016). Oe and colleagues suggest that this discrepancy might be due to the fact that they investigated the distribution of BDNF fusion proteins as opposed to the previous studies which were using mRNA reporter constructs. Another plausible mechanism of differential *bdnf* mRNA trafficking involves specific 5'UTR. Blockade of visual activity in the visual cortex leads to a decrease in dendritic targeting of exon-IV-containing mRNAs, whereas exon-III-containing mRNAs also go down, but stay restricted to the soma (Pattabiraman et al., 2005). Epileptogenic seizures in the hippocampus result in an increase of exon-II and exon-VI *bdnf* mRNA in the dendrites, whereas exon-I and exon-IV transcripts are somatically restricted (Chiaruttini et al., 2008). Analysis of the dendritic morphology of CA1 and CA3 pyramidal neurons in animals in which the specific exons of interest were knocked out support the functional relevance of differential *bdnf* mRNA trafficking (Maynard et al., 2017). It is unclear whether *bdnf* mRNA is present in axons likely due to difficulties in detection in this cellular compartment (Tongiorgi et al., 1997; Ma et al., 2012). A molecular mechanism involving eukaryotic elongation factor 2 kinase-induced (eEF2K) phosphorylation of eEF2 was proposed as a plausible regulation of activity-dependent protein translation of BDNF in dendrites (Verpelli et al., 2010). On the other hand, application of the NMDAR antagonist ketamine leads to an inactivation of eEF2K and consequently to a decrease in phosphorylated eEF2. The decreased levels of phosphorylated eEF2 lead to a lift of the translation block of *bdnf* (Autry et al., 2011).

6.2.8. Evolutionary conservation

Neurotrophins and neurotrophin receptors have been identified in arthropods, annelids and molluscs (Wilson, 2009). It appears that neurotrophins and Spätzle proteins (described in *Drosophila melanogaster*) which also contain cysteine knots, are paralogous and form a neurotrophin/Sptzl superfamily (Zhu et al., 2008).Neurotrophin signaling components are likely also present in early deuterostomes such as *Strongylocentrotus purpuratus* (sea urchin; Bothwell, 2006; Wilson, 2009). Trk/Trkl receptor family is present in protostomes but the three paralogous Trk receptors in vertebrates seem to have evolved due to a duplication in the early vertebrates (Benito-Gutiérrez et al., 2006; Hallböök et al., 2006). The different functional domains of Trk receptors (kinase domain, extracellular/ligand-binding domain and signaling domain) have distinct evolutionary histories, where the kinase domain is the most conserved (Sossin 2006). The p75NTR receptor has also been described in protostomes, suggesting that the neurotrophin signaling pathway developed in the bilaterian ancestor and is still present in modern vertebrates where it has crucial functions in the nervous system and beyond (Wilson, 2009).

6.2.9. BDNF signaling via its receptors

6.2.9.1. TrkB receptor signaling

6.2.9.1.1. Structure and ligand binding properties

The above mentioned three vertebrate isoforms TrkA, TrkB and TrkC share similar structure and are around 140-160 kDa (Lamballe et al., 1991; Luberg et al., 2010). They contain a highly glycosylated extracellular region which consist of 5 distinct domains, a single-pass transmembrane region, and an intracellular tyrosine kinase region (Figure 3). The extracellular region contains two cysteine-rich domains on the two sides of a leucine-rich domain, two immunoglobulin-like C2 domains followed by the transmembrane and intracellular regions (Schneider and Schweiger, 1991; Hubbard et al., 1994; Deinhardt and Chao, 2014). TrkB interacts with BDNF, NT-3 or NT-4 through its immunoglobulin-

like juxtamembrane domain (Ultsch et al., 1999; Banfield et al., 2001; Wehrman et al., 2007). Upon binding of the ligand, the Trk receptor dimerizes, initiating intracellular autophosphorylation of three tyrosine residues on an autoregulatory loop. This loop, when phosphorylated, increases the kinase activity of the receptor, thus resulting in activation of its downstream signaling (Hubbard et al., 1994; Deinhardt and Chao, 2014). Another two regulatory regions within the intracellular region contribute to the kinase activation state of Trk receptors. One of them is responsible for the proper positioning of a Mg^{2+} in the catalytic site of the kinase and the other for stabizing the α-phosphate of an adenosine triphosphate (ATP) molecule upon interaction with the receptor (Cherry and Williams, 2004; Noble et al., 2004; Bertrand, 2017). As mentioned earlier, BDNF has higher affinity to TrkB than to p75NTR. The dissociation constant (Kd) of BDNF binding to p75NTR is 1.3×10^{-9} M and to TrkB ranges between 1.5×10^{-11} M and 9.9×10^{-10} M depending on the expression system (Rodriguez-Tébar and Barde, 1988; Dechant et al., 1993).

6.2.9.1.2. Alternative splicing of trkb

Interestingly, the 11-amino acid motif from the Ig-like domain closest to the cell membrane is regulated through alternative splicing of exon IX of the *trkb* gene (Strohmaier et al., 1996; Boeshore et al., 1999). When present, this motif confers promiscuity of TrkB binding to BDNF, NT-3 and NT-4. However, in the case when TrkB lacks this motif it exhibits specificity solely to BDNF. Another intriguing control over TrkB signaling through alternative splicing is the truncated TrkB (TrkB.T1), which lacks the tyrosine kinase domain (Middlemas et al., 1991; Ohira et al., 2005). This isoform seems to function beyond being a simple neurotrophin “sponge” which regulates the levels of TrkB activation (Yacoubian and Lo, 2000; Ohira et al., 2005). Upon binding of BDNF to TrkB.T1, Rho GDP dissociation inhibitor (Rho-GDI) is released from the C-terminus of TrkB.T1 leading to an inhibition of the small GTPase Rho. This event in turn has been associated with changes in astrocytic and dendritic morphology (Ohira et al., 2005; Carim-Todd et al., 2009). The alterations in dendritic morphology in mice lacking TrkB.T1 in the amygdala have been linked to an increase in anxiety.

6.2.9.1.3. Subcellular localization and trafficking

After its translation in the rough ER, post-translational modification and maturation in the Golgi, TrkB is sent to the plasma membrane in axons, presynaptic terminals, dendritic spines and cell somata (Drake et al., 1999). In recent years, a few molecular players that participate in this transport have been identified. The molecular motor kinesin-1 likely mediates the anterograde transport of TrkB in axons through an interaction with c-Jun NH2-terminal kinase-interacting protein 3 (JIP3; Huang et al., 2011). Furthermore, interaction of TrkB with sortilin enhances anterograde trafficking (Vaegter et al., 2011). This transport is likely dependent on Rab27, part of the Rab family of small GTPases which govern vesicular transport throughout the cell (Arimura et al., 2009).

6.2.9.1.4. Endocytosis of BDNF-TrkB complexes

Upon BDNF binding to TrkB, the TrkB-BDNF complex is subject to endocytosis dependent on clathrin, adapter protein 2 (AP2) and dynein (Zheng et al., 2008). The internalized receptors, which continue to signal in these vesicles, referred to as “signaling endosomes”, are trafficked to other cellular compartments, are targeted for degradation or are recycled back to the cell membrane (Grimes et al., 1996). These signaling endosomes are likely essential messengers responsible for informing the cell body of a synaptic event that occurred far away in a presynaptic bouton or a dendritic spine. Retrograde axonal transport of signaling endosomes containing BDNF-bound active TrkB is mediated by the molecular motor myosin VI and dynein, the small GTPases Rab5 and Rab7 and AP2 (Yano et al., 2006; Valdez et al., 2007; Bucci et al., 2014; Kononenko et al., 2017). In *Xenopus laevis* tadpoles, application of BDNF in the optic tectum results in a TrkB-dependent synaptic potentiation at the RGC dendrites (Du and Poo, 2004). Intriguingly, neuronal activity enhances translocation of TrkB signaling endosomes and their association with the postsynaptic density. This process is Rab11-dependent and myosin Va-dependent and is specific to the full length TrkB isoform but not to TrkB.T1, suggesting that those endosomes could serve as a reserve pool of TrkB during synaptic strengthening (Huang et al., 2013; Sui et al., 2015). Furthermore, secretion of BDNF

endocytosed through TrkB takes place in response to physiologically relevant stimuli, such as theta-burst stimulation in hippocampal neurons (Wong et al., 2015). The release of endocytosed versus newly-synthesized BDNF is differentially regulated by synaptotagmin-6 and synaptotagmin-4, respectively. Endocytosis of BDNF-bound TrkB.T1 expressed by astrocytes and oligodendrocytes provides a mechanism of tight regulation of the tonic concentration of BDNF (Alderson et al., 2000). Glial cells are able to sequester BDNF through endocytosis and release it in the extracellular space on demand (Biffo et al., 1995; Fenner, 2012).

Another interesting regulation of TrkB signaling comes from the differential levels of ubiquitination of the receptor by BDNF and NT-4, where BDNF binding to TrkB induces substantially higher level of ubiquitination. Ubiquitination makes TrkB less stable at lower pH, targeting the receptor for degradation and shortening the lifetime of active TrkB in the signaling endosome (Proenca et al., 2016). Arguably, the rapid degradation of BDNF-activated TrkB provides a tighter control of TrkB signaling which might be crucial for time-sensitive processes such as Hebbian plasticity.

6.2.9.1.5. Downstream signaling pathways of activated TrkB

6.2.9.1.5.1. Phospholipase C-γ (PLC-γ)

Binding of BDNF to TrkB initiates a similar molecular cascade to binding of NGF to TrkA (Chuang et al., 2001; Deinhardt and Chao, 2014 p.106). Phosphorylation of the tyrosine most proximal to the C-terminus of TrkB is crucial for interaction with and activation of PLC-γ. Activated PLC-γ results in hydrolyzation of the phospholipid phosphatidylinositol(4,5)bisphosphate ($PI(4,5)P_2$) yielding diacylglycerol (DAG) and inositol tris-phosphate (IP_3; Irvine et al., 1986; Goldschmidt-Clermont et al., 1991; Obermeier et al., 1994). IP_3 is known to trigger the release of Ca^{2+} from intracellular stores such as the smooth ER and this increase in the cytosolic concentration of Ca^{2+} leads to the activation of Ca^{2+}-dependent catalytic proteins such as calcineurin and Ca^{2+}-calmodulin-regulated protein kinases (CaM kinases; Stewart et al., 1982; Klee et al., 1988; Miyazaki, 1988; Hanson and Schulman, 1992). Protein kinase C (PKC) is cooperatively activated by DAG and cytosolic Ca^{2+} and in turn initiates the mitogen

activated protein kinase kinase/extracellular signal kinase (MEK/Erk) cascade which is crucial for NMDAR delivery to the membrane and probability of opening (Xiong et al., 1998; Lan et al., 2001; Slack et al., 2004). Furthermore, DAG and elevated cytosolic Ca^{2+} contribute to the activation of transient receptor potential canonical subfamily channel 3/6 (TRPC3/6) that in turn leads to increase in cytosolic Ca^{2+} in growth cones and to the formation of dendritic spines (Li et al., 2005; Amaral and Pozzo-Miller, 2007; Yoshii and Constantine-Paton, 2010). Mutation of the specific tyrosine which binds specifically to PLC-γ (Y816) resulted in impairment in synaptic plasticity in the hippocampus (Minichiello et al., 2002).

6.2.9.1.5.2. Mitogen-Activated Protein Kinase/Extracellular Signal Kinase (MAPK/ERK)

Phosphorylation of the tyrosine closest to plasma membrane (Y515) on TrkB leads to recruitment of SH2-containing collagen-related protein (Shc) which interacts with growth factor receptor-bound protein 2 (Grb2). Grb2 in turn activates the Ras guanine nucleotide exchange factor (GEF) son of sevenless (SOS; Yoshii and Constantine-Paton, 2010). Upon GDP exchange to GTP the small GTPase Ras activates the Raf, MEK and MAPK/Erk molecular cascades (Huang and Reichardt, 2003). MAPK modulates translation initiation by phosphorylation of eukaryotic initiation factor 4E (eIF4E), the 4E-binding protein 1 (4E-BP1) and ribosomal protein S6 (Kelleher et al., 2004). The MEK-MAPK/Erk pathway is also crucial for activation of CREB and is thus involved in transcription regulation (Ying et al., 2002). BDNF activation of TrkB and subsequent MAPK signaling likely serves to achieve longer-lasting molecular and cellular changes in response to external stimuli. TrkB-induced activation of MAPK/Erk is involved in the process of synaptic strengthening in the hippocampus (Ying et al., 2002; Kelleher et al., 2004).

6.2.9.1.5.3. Phosphatidylinositol 3-kinase (PI3K)

The docking of Shc to phosphorylated Y515 and subsequent phosphorylation of Grb2 results in the recruitment of Grb2-associated binder-1 (Gab1) which in turn leads to the activation of PI3K (Reichardt, 2006). Phosphorylation of inositol phospholipids by PI3K changes the local composition of the plasma membrane. Protein kinase B (PKB) is

then shuttled to the membrane where it is activated (Yoshii and Constantine-Paton, 2007, 2010). Active PKB induces protein synthesis via mechanistic target of rapamycin (mTOR) exerting neuroprotective effects (Chen et al., 2013). Interestingly, all the three pathways described above are involved in BDNF-induced TrkB-dependent translocation of PSD-95 to synapses, suggesting that BDNF is crucial for synaptic maturation (Yoshii and Constantine-Paton, 2007, 2014).

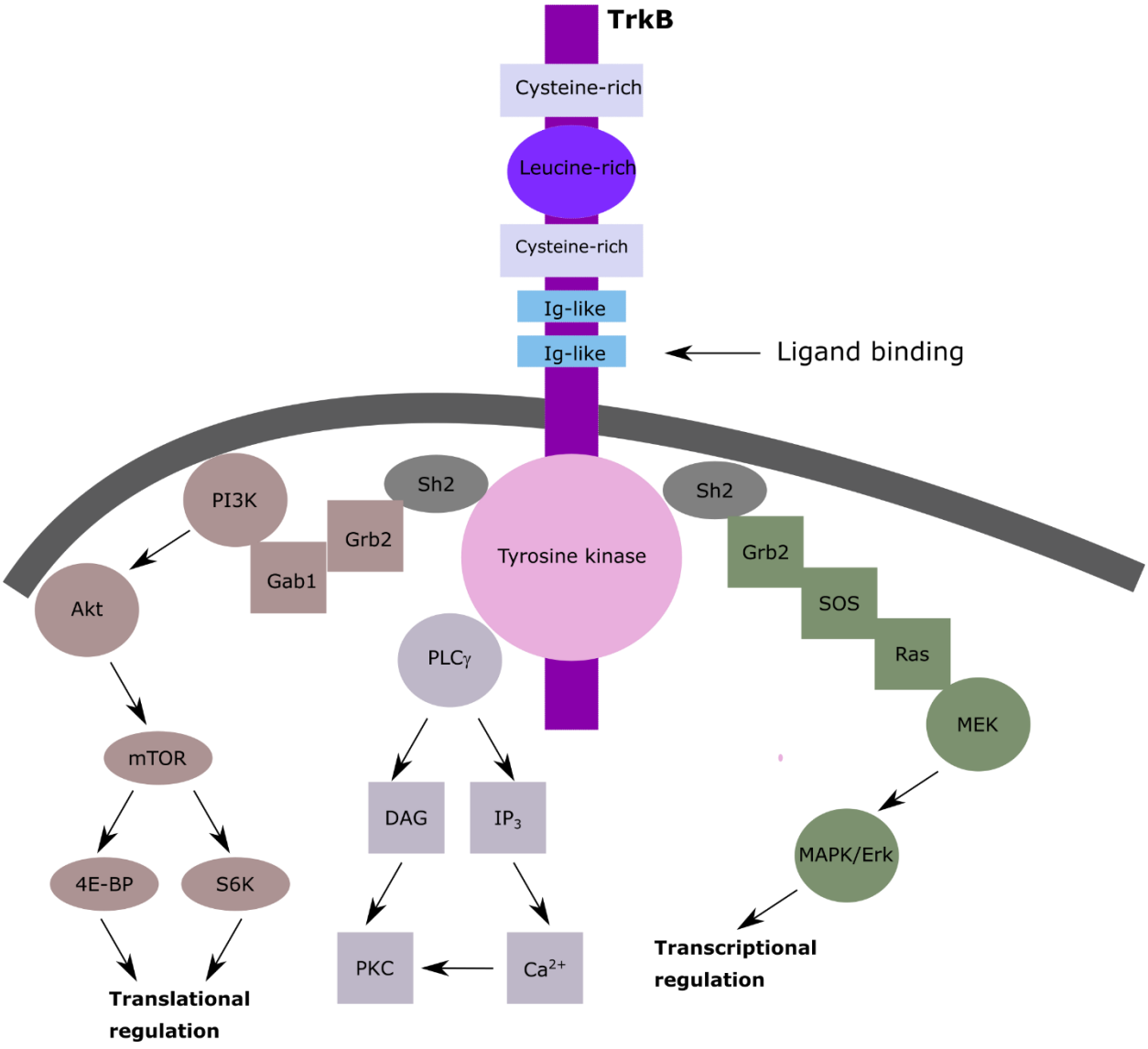

Figure 3: **TrkB receptor signaling**

6.2.9.1.6. Alternative non-ligand dependent activation of TrkB

It has been shown that TrkB is also activated in the presence of zinc via a neural activity-dependent mechanism that does not require ligand binding and it is localized to the postsynaptic density where it may modulate synaptic strength (Huang et al., 2008).

6.2.9.2. p75NTR receptor signaling

6.2.9.2.1. Structure and ligand binding properties

The other neurotrophin receptor, p75NTR, was identified as a lower affinity binding receptor and, as mentioned above, the Kd characterizing this interaction for BDNF is 1.3 x 10^{-9} M (Grob et al., 1983; Chao et al., 1986; Radeke et al., 1987; Rodriguez-Tébar and Barde, 1988). It is likely that the high affinity of TrkB receptor binding to BDNF is due to the interaction with p75NTR, suggesting that a complex of both receptors forms a high affinity binding site (Chao, 1994; Chao and Hempstead, 1995). p75NTR is a 70-80 kDa protein that belongs to the tumor necrosis factor (TNF) superfamily and can bind all neurotrophins and with similar affinity (Ross et al., 1984; Rodríguez-Tébar et al., 1992; Bothwell, 1995). Similarly to the other TNF superfamily members, p75NTR contains a cytosolic domain, variable between species, a single transmembrane domain, and a well-conserved extracellular domain (ECD) incorporating four cysteine-rich domains (Large et al., 1989; Baldwin and Shooter, 1995). p75NTR is also likely post-translationally modified by both *O*-linked and *N*-linked glycosylation (Grob et al., 1985). It forms dimers through disulfide bonds connecting two cysteine residues or through noncovalent interaction of a conserved sequence located in the transmembrane domain. The intracellular domain (ICD) of p75NTR has high structural resemblance to the “death domains” of TNF receptor (TNFR) and first apoptosis signal receptor (Fas; Chapman, 1995). Unlike the death domain of Fas, p75NTR’s does not show self-aggregation which in turn implicates different downstream mechanisms (Liepinsh et al., 1997; Wang et al., 2001). Both the ECD and ICD of p75NTR and of TrkB participate in the interaction of the receptors. The tyrosine kinase activity is also implicated for the formation of the two-receptor complex. Furthermore, the presence of p75NTR increases the specificity of TrkB binding to BDNF,

compared to NT-3 and NT-4 (Bibel et al., 1999). The ICD of p75NTR contains an amphipathic α-helix resembling GTPase activation domains in other proteins such as the wasp toxin mastoparan (Feinstein and Larhammar, 1990; Myers et al., 1994; Roux and Barker, 2002). This motif is likely responsible for p75NTR-induced RhoA inhibition and underlies BDNF-driven growth cone filopodia dynamics (Yamashita et al., 1999; Gehler et al., 2004). The C-terminal motif Ser/Thr-X-Val of p75NTR ICD has been identified as crucial for interaction with the postsynaptic density protein PSD-95 in other proteins such as NMDARs (Kornau et al., 1995).

6.2.9.2.2. Transcriptional regulation of p75NTR

6.2.9.2.2.1. Expression profile

p75NTR is highly expressed in the central and the peripheral nervous system (CNS, PNS, respectively) as well as in non-neuronal tissues. In the retina, the expression is highest in the retinal ganglion cells (Roux and Barker, 2002). The expression of the receptor peaks prenatally with a substantial decrease postnatally. In *Xenopus laevis*, two different sequences of p75NTR, named p75NTRa and p75NTRb, were identified. Since they show a higher degree of similarity to each other than to sequences in other species including zebrafish, rat and human, it was proposed that these two genes are two alleles evolved by duplication and reflect the recently proposed allotetraploidism of *Xenopus laevis*, instead of the earlier view that those animals are pseudotetraploidic (Graf and Kobel, 1991; Hutson and Bothwell, 2001; Session et al., 2016). p75NTR expression initiates at stage 14 (neurula), and until stage 28 p75NTRa and p75NTRb expression appear to mirror each other with higher levels of p75NTRa. At stage 39 p75NTR expression, determined using a probe that binds both isoforms, appears in anterior telencephalon and the ganglion cell layer, the inner and the outer layers of the retina. Contrary to the role of p75NTR in cell death in other species, overexpression of full length p75NTR in the retina enhances cell survival (Frade and Barde, 1999; Hutson and Bothwell, 2001).

6.2.9.2.2.2. Alternative splicing

Alternative splicing of exon III of *ngfr* (p75NTR gene) in mice leads to two p75NTR isoforms one of which produces mRNA encoding the full length of the receptor and the other one a truncated version, which lacks three of the cysteine-rich ECDs, including the ligand interacting domains (von Schack et al., 2001). It is still unclear what the exact physiological function of the truncated receptor is, however, mice lacking both isoforms of p75NTR exhibit more severe phenotypes in motor function and PNS development, as well as a novel phenotype related to blood formation. In general, p75NTR knockout mice are subject to increased perinatal lethality (Phenotypes associated with Ngfr/Ngfr, Alliance of Genome Resources). Among other visual system abnormalities, they exhibit alterations in SC morphology and increased number of photoreceptors.

6.2.9.3. Subcellular localization of p75NTR

Although the PDZ-containing ICD of p75NTR was predicted to interact with PSD-95, very low levels of p75NTR labeling are observed in postsynaptic densities and dendritic shafts *in vivo* (Dougherty and Milner, 1999). The receptor is mostly located in axons and axonal terminals, with a small fraction localized to astrocytes. p75NTR has been shown to undergo both anterograde and retrograde transport in axons (Johnson et al., 1987; Mok et al., 2013). Furthermore, the receptor seems to be crucial for internalization and retrograde transport of BDNF, which unlike the TrkB-BDNF complex is dependent on beta-caveolin-1 in caveolae, suggesting that trafficking of TrkB-BDNF and p75NTR-BDNF complexes is regulated by distinct mechanisms (von Bartheld et al., 1996; Hibbert et al., 2006)

6.2.9.4. Downstream signaling pathways of activated p75NTR

6.2.9.4.1. Soluble p75NTR ECD

The ECD can be cleaved by matrix metalloproteinases (MMPs) leading to a soluble ECD capable of binding and sequestering neurotrophins and an ICD that continues to

interact with cytosolic partners (Zupan et al., 1989; DiStefano et al., 1993). This mechanism seems to be prevalent during development (Roux and Barker, 2002).

6.2.9.4.2. p75NTR interactor TRAF activate JNK and NF-κB

Upon ligand binding p75NTR recruits TNFR associated factors (TRAF), specifically TRAF6 (Khursigara et al., 1999). TRAFs have an E3 ubiquitin ligase domain that induces the formation of lysine-linked ubiquitin chains which enhance protein-protein interactions instead of tagging the TRAF downstream binding partners for proteasomal degradation (Ha et al., 2009; Häcker et al., 2011). TRAF6 is then crucial for the activation of the stress kinase c-Jun N-terminal kinase (JNK), which leads to apoptosis, and of the transcription factor NF-κB, which enhances the transcription of pro-survival genes (Bamji et al., 1998; Dempsey et al., 2003; Yeiser et al., 2004). This makes TRAF6 activation via neurotrophin-p75NTR binding a pivotal point between cell death and survival (Figure 4).

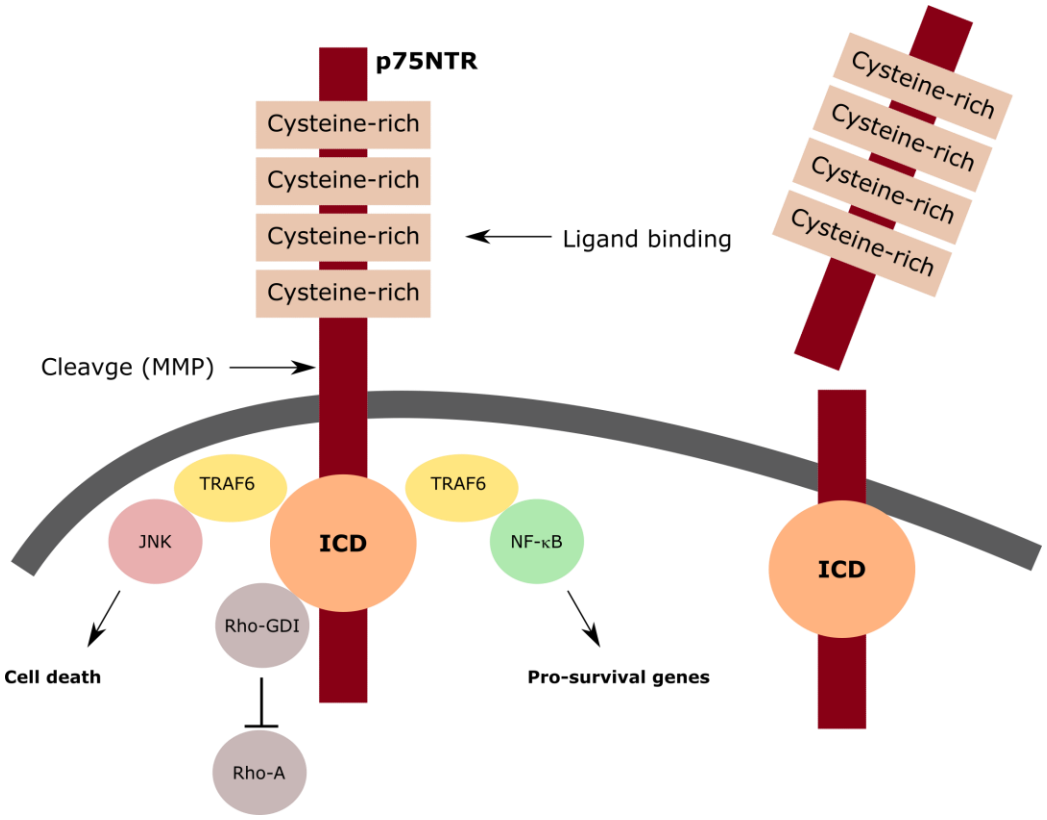

Figure 4: **p75NTR receptor signaling**

6.2.9.5. p75NTR forms complexes with other receptors

A small fraction of the p75NTR dimers are formed prior to interaction with neurotrophins, however, it is likely that p75NTR dimerizes to bind a neurotrophin dimer through an intermediate state of p75NTR monomer bound to a neurotrophin dimer (He and Garcia, 2004; Gong et al., 2008; Feng et al., 2010). Upon neurotrophin binding, the disulfide bond leads to separation of the cytosolic domains allowing for enhanced interaction of the receptor with downstream partners (Vilar et al., 2009). Neurotrophin but not myelin-associated glycoprotein (MAG) binding to p75NTR seems to trigger this mechanism providing some specificity of the activation of downstream signaling between ligands. Notably, p75NTR is a promiscuous receptor forming complexes with Trk, Nogo receptor-1 (NogoR), LRR and Ig domain-containing Nogo Receptor-interacting protein-1 (LINGO-1) and sortilin, thus directly or indirectly participating in ligand binding, not only of all pro- and mature neurotrophins, but also Nogo-66, MAG, oligodendrocyte-myelin glycoprotein (OMgp; Wang et al., 2002a; Mi et al., 2004). Arguably, the interaction of p75NTR with other receptors could provide an explanation for the various functions attributed to p75NTR. As mentioned above, the interaction between p75NTR and TrkB leads to an increased specificity of TrkB binding to BDNF over its other ligands and to higher affinity of the ligand binding (Chao and Hempstead, 1995; Bibel et al., 1999). Similarly to the p75NTR-TrkA complex, p75NTR-TrkB perhaps underlies cell survival (Bronfman and Fainzilber, 2004; Nykjaer et al., 2004). Interestingly, the function of p75NTR as cell death-promoting receptor is likely achieved through its interaction with sortilin. Both proBDNF and proNGF require the cooperative action of p75NTR and sortilin to promote cell death (Nykjaer et al., 2004; Teng et al., 2005). Interestingly, sortilin has high affinity binding to both proNGF, its cleaved prodomain, and proBDNF. In the absence of sortilin, proNGF displays lower affinity to p75NTR, suggesting that the interaction with sortilin, which by binding the prodomain of NGF, is what confers the previously observed higher affinity of p75NTR to proNGF, than to mature NGF (Lee et al., 2001; Beattie et al., 2002; Nykjaer et al., 2004). Interestingly, sortilin was shown to be predominantly localized to the somato-dendritic compartment, potentially providing spatial control over the distinct functions of p75NTR (Sarret et al., 2003; Bronfman and Fainzilber, 2004). A complex of

the p75NTR and NogoR was shown to interact with the transmembrane protein LINGO-1, and to inhibit neurite outgrowth via activation of RhoA (Mi et al., 2004). A model explaining the contradictory results regarding p75NTR-induced activation or blockade of RhoA, suggests that binding of neurotrophins to the p75NTR/NogoR/LINGO-1 results in Rho-GDI translocation from the complex which inhibits RhoA, whereas binding of MAG or Nogo-66 induces RhoA activation (Mathew et al., 2009). Furthermore, unlike sortilin, NogoR is localized on the plasma membrane in axons, indicating that p75NTR's function in neurite outgrowth might be executed by axonal p75NTR (Wang et al., 2002b). A recent study, however, challenged the proposed p75NTR/NogoR/LINGO-1 receptor complex, as LINGO-1 was demonstrated predominantly intracellularly (Meabon et al., 2015). However, it is possible that LINGO-1 affects aspects of p75NTR endosomal properties.

6.2.9.6. proBDNF signaling through TrkB and p75NTR

A lot of the findings related to binding affinity of pro- and mature neurotrophins come from surface plasmon resonance studies on NGF. As mentioned above, in the presence of sortilin p75NTR has subnanomolar affinity to proNGF, and up to 20 nM affinity to TrkA (Nykjaer et al., 2004). In the absence of sortilin, the affinities of both TrkA and p75NTR to proNGF are similar. However, less is known about the exact binding properties of proBDNF to p75NTR and TrkB. ProBDNF, applied in concentrations at which mBDNF induces robust phosphorylation of TrkB measured by Western blot, fails to increase TrkB phosphorylation above control (without neurotrophin added) levels in TrkB-positive PC12 cells (Teng et al., 2005). In these cells, neurite outgrowth is triggered with higher efficacy by mBDNF than by proBDNF. In this thesis, we show analogous specificity effects of proBDNF and mBDNF on Trk phosphorylation in *Xenopus laevis* tadpoles (Chapter 3, Figure 1). Furthermore many of the phenomena in which proBDNF and the cleaved prodomain were implicated, such as LTD, apoptosis, spine and axon remodeling, have been attributed to p75NTR, or p75NTR and sortilin signaling (Teng et al., 2005; Woo et al., 2005; Schwartz et al., 2011; Je et al., 2013; Yang et al., 2014). Detailed review of the functions of proBDNF and mBDNF in the brain follows.

6.2.10. Functions of BDNF signaling in the adult and developing nervous system

6.2.10.1. Synaptic plasticity

There has been considerable interest in the role of BDNF in synaptic plasticity, specifically in the hippocampus as understanding the molecular mechanisms of LTP and LTD in this brain region can provide important insights about learning and memory. Secretion of BDNF has been observed with neuronal depolarization, and with LTP-inducing electrical stimulation paradigms, e.g. high-frequency stimulation and theta-burst stimulation (Balkowiec and Katz, 2000; Gärtner and Staiger, 2002; Edelmann et al., 2015). As described above, the presence of alternative polyadenylation sites of *bdnf* mRNA results in transcripts that are equivalent in their coding regions but vary in their UTRs, generating mRNAs with long and short 3' UTRs. These alternative splice variants seem to be differentially trafficked to and released from the cellular compartments. The transcript containing the long 3'UTR has been reported to be enriched in dendrites, suggesting that BDNF protein could be synthesized locally on demand in this neuronal compartment (An et al., 2008; Lau et al., 2010). The presence of translation machinery in close proximity to dendritic spines supports a model where BDNF could be synthesized locally in response to a synapse-restricted activation of NMDAR or metabotropic glutamate receptors that lead to downstream activation of CaMKII or MAPK (Besse and Ephrussi, 2008; Park and Poo, 2013). Direct evidence for endogenous local dendritic BDNF synthesis in response to activity is yet to be obtained. The importance of BDNF in LTP has been clearly demonstrated (Figurov et al., 1996). Acute application of TrkB-Fc which sequesters the available endogenous BDNF impairs hippocampal LTP. Both homozygous and heterozygous *bdnf* knockout mice show reductions in hippocampal LTP which can be rescued by viral postsynaptic targeted overexpression or exogenous BDNF application (Korte et al., 1995, 1996; Patterson et al., 1996). Moreover, the effect of BDNF on LTP induction occurs through activation of TrkB and PLCγ and requires NMDAR activation and transient increase in postsynaptic Ca^{2+} (Kovalchuk et al., 2002; Minichiello et al., 2002). On the contrary, knockout mice lacking *bdnf* from only the postsynaptic CA1 neurons display normal LTP (Zakharenko et al., 2003). These contradictory results may

be explained either by differences in the LTP- induction protocols or by developmental alterations in connectivity of the full knockout mice (Korte et al., 1996). Recently, compelling evidence demonstrated that postsynaptically released BDNF acts in an autocrine manner to activate TrkB within the same dendritic spine which results in an increase in the spine volume, a structural change associated with LTP (Harward et al., 2016). The authors propose that this is not the sole source of BDNF that activates TrkB, but it is crucial for functional LTP induction. In the developing visual system of *Xenopus laevis* tadpoles, application of BDNF in the optic tectum potentiates the retinotectal synapse via TrkB-dependent increase in neurotransmitter release (Du and Poo, 2004). Furthermore, in these animals visual conditioning drives transcription and release of BDNF, which leads to facilitation of LTP, associated with increased visual acuity (Schwartz et al., 2011).

Although detection of secreted proBDNF has proved to be a challenging task due to its rapid extracellular processing, development of genetic tools and antibodies with high specificity over the last decade have permitted experiments showing that indeed proBDNF can be secreted into the extracellular milieu. In a study by Yang and coworkers (2009), the authors describe a developmental profile of both forms of BDNF, where the peak of proBDNF expression falls around the second postnatal week in mice, a period of intensive synapse formation in the hippocampus (Yang et al., 2009; Hempstead, 2014, p.24). However, the exact explanation for how proBDNF evades intracellular cleavage is still unclear. One hypothesis is that dendrites are the main location of proBDNF secretion. This model is based on the finding that *bdnf* mRNA is targeted to dendrites and it is plausible that classic somatic protein processing is modified in this compartment (Barker, 2009). Since neurons can release proBDNF in the extracellular matrix, it was reasonable to ask what the function of secreted proBDNF might be. A few studies have thoroughly described that proBDNF signaling through p75NTR enhances NMDAR-dependent LTD in the hippocampus (Rösch et al., 2005; Woo et al., 2005). Investigation of the behavioral relevance of proBDNF shows that the protein levels in the hippocampus seem to elevate with memory extinction and blockade of the extracellular cleavage of proBDNF facilitates extinction of fear-conditioned memories (Barnes and Thomas, 2008). Furthermore, proBDNF signaling through p75NTR also facilitates a form of LTD in the retinotectal

projection of *Xenopus laevis* tadpoles (Schwartz et al., 2011). In the hippocampus, asynchronous activation of neighboring synapses leads to synaptic weakening in a proBDNF/p75NTR-dependent manner (Winnubst et al., 2015). Interestingly, the propeptide domain of cleaved proBDNF was shown be released in an activity-dependent fashion and to facilitate LTD in the hippocampus, adding another layer of complexity in the signaling of BDNF (Anastasia et al., 2013; Mizui et al., 2015; Guo et al., 2016). This function of the propeptide is dependent on p75NTR activation and application of the propeptide in hippocampal slices of *bdnf* knockout mice produces the same effect as in wild-type mice, indicating that the propeptide functions as a ligand independently of proBDNF. Finally, the same group showed that propeptide possessing in the common human polymorphism Val66Met fails to facilitate LTD. On the other hand, the same Met-propeptide but not the regular Val propeptide is able to induce growth cone collapse in hippocampal cultures (Anastasia et al., 2013).

LTD often correlates with alterations in spine morphology. Consequently, it is reasonable that application of proBDNF leads to reduction in the number of dendritic spines in the hippocampus (Koshimizu et al., 2009). ProBDNF knockin mice were created in which one bdnf allele was substituted with cleavage-resistant proBDNF. This genetic manipulation results in an increase in the levels of secreted proBNDF. Higher levels of secreted proBDNF facilitate LTD which is accompanied by a decrease in the number of spines along with a decrease in the complexity of the dendritic arbor (Yang et al., 2014; Zagrebelsky and Korte, 2014). The observed pruning of dendritic spines could be a result of activity-dependent local translation of *bdnf* mRNA in the dendrites and subsequent secretion of proBDNF (Orefice et al., 2016). Analogously, application of the BDNF propeptide leads to a decrease in spine density and an increase in the relative number of long and thin spines at the expense of stubby spines (Guo et al., 2016). The propeptide could arise from extracellular cleavage by the tissue plasminogen activator (tPA)/plasmin system or could be released already cleaved by furin or PC, packaged together with mBDNF in dense core vesicles (Dieni et al., 2012). These last findings pose the question whether the effects of proBDNF observed so far are actually effects of extracellularly cleaved propeptide or the propeptide and proBDNF function distinctly, making BDNF one protein with three potentially different roles.

6.2.10.2. Cell survival

The role of neurotrophins in cell survival has been studied ever since the time when NGF was identified as a trophic factor (Cohen et al., 1954; Levi-Montalcini and Booker, 1960; Levi-Montalcini, 1965). Decades after their discovery, the neurotrophic factors were shown to play a dual role in cell survival and apoptosis, likely due to the differential signaling pathways activated by Trk and p75NTR receptors (Ceni et al., 2014 p.194). During development, both in the PNS and the CNS, there is a period of overproduction of neurons which then are subjected to programmed cell death. In the PNS, numbers of pruned neurons reach 50% for some neuronal populations. Different target-derived peripheral neurotrophins ensure the survival of specific populations of dorsal root ganglion (DRG) neurons expressing the corresponding Trk receptor (Huang and Reichardt, 2001). Interestingly, BDNF was shown to play a more autocrine function in cell survival of nociceptors as its expression was highest within the DRG rather than in the skin (Valdés-Sánchez et al., 2010). In the sympathetic nervous system, sympathetic neurons release BDNF which is crucial for the survival of their presynaptic partners, the preganglionic neurons (Causing et al., 1997). In the retinae of *Xenopus laevis* tadpoles, exogenous application of BDNF promotes RGC cell survival and sequestering endogenous BDNF results in an increase in cell death (Cohen-Cory et al., 1996). These experiments together with *in situ* hybridization showing *trkb* and *bdnf* expression in the ganglion cell layer, suggest a role for BDNF in RGC survival. Numerous studies have investigated the role of BDNF signaling through TrkB in cell survival in the brain (Xu et al., 2000; Baquet et al., 2004). TrkB knockout mice have increased apoptosis in the hippocampus. However, it appears it is the establishment and maintenance of proper neuronal wiring in the striatum and certain cortical regions such as the visual cortex, where BDNF's role is most crucial, rather than simply in ensuring neuronal survival (Gorski et al., 2003). Interestingly, BDNF signaling through TrkB may be essential for neuronal survival after injury. Sequestering BDNF after severing of the corticospinal projection leads to an increase in cortical neuronal apoptosis (Giehl et al., 1998). Furthermore, exogenous BDNF application leads to an increase in RGC survival after optic nerve crush in rats and cats (Di Polo et al., 1998; Chen and Weber, 2001).

On the other hand, a large body of literature indicates that p75NTR promotes naturally occurring or injury-induced apoptosis. p75NTR knockout mice display increased survival of sympathetic neurons, post-seizure hippocampal neurons and RGCs (Bamji et al., 1998; Frade and Barde, 1999; Roux et al., 1999). Both pro- and mBDNF signaling through p75NTR in superior cervical ganglionic neurons result in an increase in cell death through a mechanism involving p75NTR ICD domain cleavage (Kenchappa et al., 2006). In other systems, p75NTR enhances cell survival. In DRGs of p75NTR knockout mice there is a marked decrease in neuronal survival (Murray et al., 1999). As described above, p75NTR is a pro-survival receptor in the retina *Xenopus laevis* tadpoles (Hutson and Bothwell, 2001). One of the proposed mechanisms for p75NTR's role in cell survival is through NF-κB, which in turn initiates transcription of pro-survival genes as mentioned in Section 6.2.9.4.2 (Khursigara et al., 1999). Another model explains the pro-survival effects of p75NTR through a synergistic interaction with TrkA or TrkB, leading to enhanced activation of PKB (Ceni et al., 2010).

6.2.10.3. BDNF in circuit refinement during development

The main focus of this section is to describe the crucial role of BDNF and its signaling in the process of synaptic maturation and structural remodeling in developing neural circuits. In the primary visual cortex in cats, injection of TrkB-IgG led to a local disruption of ocular dominance bands (Cabelli et al., 1997). Interestingly, transgenic mice overexpressing BDNF display faster maturation of inhibitory circuitry in the visual cortex accompanied by an increase in visual acuity (Huang et al., 1999b). This precocious maturation is due to an increased perisomatic targeting of inhibitory basket cells (Huang et al., 1999b; Di Cristo et al., 2004). BDNF application results in an increase in the proportion of filopodia-like spines in developing Purkinje cells co-cultured with granule cells, whereas application of TrkB-IgG to sequester endogenous BDNF leads to a reduction in this type of spines (Shimada et al., 1998). These studies were the first to suggest that BDNF and its signaling pathways could be among the mechanisms underlying activity-dependent neural circuit refinement.

Further studies in *Xenopus laevis* tadpoles explored in more detail the roles of BDNF in structural remodeling of pre- and postsynaptic partners *in vivo. Bdnf* and *trkB* are expressed throughout the ganglion cell layer of the retina and in subset of neurons in the inner nuclear layer of *Xenopus laevis* tadpoles, as well as in chick embryos (Cohen-Cory et al., 1996; Garner et al., 1996). Exogenous application of BDNF in the optic tectum of tadpoles results in an increase in RGC axon branch additions and in total arbor length within 2 hours which persists for at least 24 hours (Cohen-Cory and Fraser, 1995). On the other hand, sequestering endogenous BDNF by application of anti-BDNF IgG leads to a reduction in branch additions and total arbor length both short- and long-term. Along with the changes in branch number and total arbor length, exogenous BDNF application induces an increase in synaptic density and in the number of presynaptic clusters of plausible presynaptic sites labeled by synaptobrevin-GFP (Alsina et al., 2001). Furthermore, sequestering BDNF with anti-BDNF IgG results in a fast reduction (within 2 hours) of stable synaptobrevin-GFP clusters along with a reduction in stable axonal branches. Interestingly, exogenous application of BDNF is able to reverse the decrease in synaptobrevin-GFP clusters induced by NMDAR blockade (Hu et al., 2005). Those studies reveal a role for BDNF in axonal branch and synapse stabilization. On the other hand, the observed branch initiation effect could involve addition of new branches from an already stable synapse, which might be more resistant to being retracted (Cohen-Cory, 1999; Ruthazer et al., 2006).

Elegant experiments indicated that the optic tectum rather than the retina is the source of BDNF which affects axonal morphology and synapse formation. Exogenous BDNF application in the retina resulted in a decrease in RGC dendritic branches and total dendritic length, however, failed to induce any alterations in RGC axon morphology (Lom et al., 2002). Another insight on the cellular mechanism of BDNF action came from a study from the same group suggesting that BDNF may act directly on the RGC axons since injection of exogenous BDNF in the optic tectum leads to an increase in the density of PSD-95-GFP puncta only 24-48 h post-treatment. These data point to a direct presynaptic role of BDNF in synapse stabilization which in turn later manifests itself postsynaptically (Sanchez et al., 2006). Expression in RGCs of the truncated TrkB receptor, TrkB.T1, which as described above can bind to BDNF, but lacks the tyrosine

kinase domain, results in an increase in axonal branch additions and a decrease in stable axonal branches and mature synapses (Marshak et al., 2007). This study is the only one in *Xenopus laevis* tadpoles that attempts to attribute the observed functions of BDNF in circuit refinement to TrkB receptor. However, as mentioned above, TrkB.T1 can activate non-canonical downstream targets, such as Rho-GDI, which in turn inhibits RhoA. Thus, overexpression of the truncated receptor might have more complicated outcomes than simply acting as a dominant-negative. Furthermore, overexpression of TrkB.T1 would act as a "sponge" of the endogenous BDNF, and thus the observed alterations in axonal remodeling potentially cannot be fully attributed to TrkB rather than to p75NTR signaling.

The finding that endogenous proBDNF could be released from neurons led to an increasing interest in its potential role in synaptic plasticity (Pang et al., 2004; Woo et al., 2005; Yang et al., 2009). Very few studies have investigated the functions of proBDNF in structural remodeling during development, especially *in vivo*. In the developing hippocampus, depression of asynchronously active synapses was achieved via p75NTR activation by proBDNF, whereas mBDNF signaling through TrkB results in stabilization of synapses highly co-active with their neighbors (Winnubst et al., 2015; Niculescu et al., 2018). Furthermore, differential roles in spine formation and spine maturation along with spine pruning have been attributed to mBDNF and proBDNF, respectively (Orefice et al., 2013). As mentioned above, long 3' UTR *bdnf* mRNA which is more likely to be trafficked to dendrites seems to lead to translation of proBDNF which is able to escape intracellular cleavage (An et al., 2008; Orefice et al., 2016). The dendritic secretion of proBDNF is dependent on neuronal depolarization. The authors of this study propose that upon release, proBDNF is converted to mBDNF, which signals through TrkB to promote spine head enlargement. On the other hand, proBDNF which does not get converted extracellularly binds to p75NTR on silent synapses and induces pruning of dendritic spines through activation of RhoA (Orefice et al., 2016). Analogously, proBDNF promotes growth cone collapse via Rho-activated kinase in DRG axons (Sun et al., 2012). Although, those experiments should be interpreted with caution because they were done in cell culture and relied on overexpression of fluorescently-tagged proteins which might alter their physiological trafficking, similar effects of proBDNF have been shown in knockin mice supporting the robustness of the findings. In these mice one of the *bdnf* alleles was

replaced with an allele encoding a mutation in cleavage site of proBDNF (Yang et al., 2014). Those animals displayed a reduction in spine density and dendritic complexity both in hippocampal and cortical neurons. Accordingly, an increase in dendritic complexity was described in p75NTR knockout mice (Zagrebelsky et al., 2005). In the PNS, proBDNF signaling through p75NTR and sortilin likely has similar functions. In *Xenopus laevis* motor neuron/myocyte co-cultures, proBDNF released postsynaptically leads to a retraction of non-stimulated axons via p75NTR, whereas stimulation leads to a MMP-dependent proBDNF cleavage (Je et al., 2012). Activation of TrkB through the mBDNF produced after MMP cleavage results in stabilization of the active “winner” motor neuron axon. Similar experiments were performed in the developing neuromusclular junction (NMJ) in mice, in which the model described above was validated, with the addition that for motor neuron retraction proBDNF requires the cooperative action of p75NTR and sortilin (Je et al., 2013).

7. Chapter 2: Methodology

7.1. Animals

The experiments described in this thesis were approved by the Animal Care Committee at the Montreal Neurological Institute and are in accordance with the guidelines of the Canadian Council on Animal Care. Animals of both sexes were used for the experiments, as at the stages of interest the two sexes could not be discriminated. Albino *Xenopus laevis* tadpoles were generated by induced mating of a sexually mature female frog, injected with pregnant mare serum gonadotropin (50 IU) 3 days before mating and with 400 IU human chorionic gonadotropin (HCG) immediately before mating, and a sexually mature male frog injected with 150 IU HCG up to 8 hours before mating. The produced fertilized eggs were reared in 0.1X modified Barth's saline with HEPES (MBSH).

7.2. Morpholinos

Xenopus p75NTR morpholino sequence: 5′-CCA TGC TGA TCC TAG AAA GCT GAT G-3′ (Je et al., 2012), referred to as p75-MO and *Xenopus* TrkB morpholino sequence: 5′-CCA CTG GAT CCC CCC TAG AAT GGA G-3′ (Du and Poo, 2004; Je et al., 2012), referred to as TrkB-MO, and standard control: 5'-CCT CTT ACC TCA GTT ACA ATT TAT A 3' (Gene Tools, LLC), referred to as Ctrl-MO, were generated as described previously and were tagged with lissamine on the 3'-end (Gene Tools, LLC).

7.3. Morpholino injections in 2-blastomere stage embryos

Each blastomere in albino *Xenopus laevis* 2-cell stage embryos was microinjected with 18 ng/injection TrkB-MO or Ctrl-MO using an automatic pressure microinjector (Harvard Apparatus) with micropipettes pulled from glass (6.66 µL, Drummond Scientific), using a Flaming Brown Micropipette Puller (P-97, Sutter Instruments CO.). The tadpoles were screened for lissamine fluorescence at stage 46 (Nieuwkoop and Faber, 1994).

7.4. Labelling of single or few contralaterally projecting RGC axons

Albino *Xenopus laevis* tadpoles (stages 40-42) were anaesthetized by immersion in 0.02% MS-222 (Sigma) diluted in 0.1X MBSH. The developmental stages were determined using the standard criteria of Nieuwkoop and Faber (1994). DNA plasmids or DNA and oligonucleotides were pressure-injected into the eye using micropipettes pulled from borosilicate glass with filament (outer diameter 1.0 mm, inner diameter 0.78 mm; Sutter Instruments) on PC-10 puller (Narishige, Japan) and attached to a custom-built manual pressure injection system. Upon pressure injection of plasmid/morpholino solutions into the eye, current was delivered across two custom-made platinum plates placed in parallel: one on the side of the eye and the other on top of the lens. A Grass 9 constant voltage stimulator with a 3 µF capacitor placed in parallel was used to deliver 2 pulses in each direction (1.6 ms duration, 36 V). After electroporation, the animals were placed in a 20ºC biological oxygen demand incubator in a 12h light/12h dark cycle. For short-term dynamic or long-term daily imaging of contralaterally projecting RGC axons, RGCs were co-electroporated with synthetic morpholino oligonucleotides (MO) and plasmid encoding EGFP (4.5 µg/µL : 1.5 µg/µL).

7.5. Labelling of single or few ipsilaterally projecting RGC axons

To label ipsilaterally projecting RGC axons the protocol for contralaterally projecting axons was modified only in the duration of current pulses delivered (2 pulses in both polarities, 2.5 - 3 ms, 36V). To express EGFP in ipsilaterally projecting RGC axons, 2 µg/µL plasmid was pressure-injected. Solution containing 3 µg/µL : 4 µg/µL MO and EGFP was injected into the eye in order to achieve efficient co-delivery.

7.6. Daily and dynamic imaging of morpholino-loaded/EGFP expressing RGC axons

Stage 39-41 animals were co-electroporated with MO and EGFP and were given 3 days for sufficient knockdown of the target protein and proper axonal labeling with the

fluorescent protein. For daily imaging, animals at st. 45-46 containing a single co-labeled RGC axon were selected and imaged over the next 4 days. After anaesthetizing the tadpoles by immersion in 0.02% MS-222 (Sigma) in 0.1x MBSH, they were positioned in custom-made polydimethylsiloxane (PDMS) imaging chambers. For dynamic imaging, pre-screened tadpoles at st. 46 were immobilized by immersion in 2 mM pancuronium dibromide (Tocris) and positioned in a custom-made PDMS imaging chambers. The animals were habituated in darkness for 30 min. Optical section z-series at 1 µm steps of the axons of interest were acquired using an Olympus FV300 confocal microscope converted for multiphoton use, equipped with 60x LUMPlanFL N 1.0NA water immersion objective. For optimal excitation of the axon-filling EGFP, imaging was carried out at 910 nm. For dynamic imaging, z-series were acquired every 10 min for 1 h, and for daily imaging -- once every day for 4 days. To confirm the presence of lissamine-tagged MO in the axons of interest and assure minimal cross-talk between the two channels (green: 500-550 nm and red: 593-668 nm) 3D fluorescence stacks were also acquired at 840 nm where the EGFP excitation is minimal and the lissamine excitation peaks.

7.7. Dynamic imaging of ipsilaterally projecting RGC axons combined with visual stimulation

Stage 39-41 animals were electroporated either with EGFP or were co-electroporated with MO and EGFP. Animals were given at least 4 days to assure labeling and proper knockdown in ipsilaterally projecting RGC axons and imaging was performed in stage 47-48 tadpoles. The animals were immobilized by intraperitoneal injection of 2.5 mM tubocurarine hydrochloride pentahydrate (Sigma). In the experiments including acute pharmacological blockade, 50 µg/mL TrkB-Fc (Recombinant Human Chimera, 688-TK, R&D Systems) was injected intracerebroventricularly (ICV). The animals were then placed in a custom-built imaging chamber (described below), fixed in place with a small drop of 1.8% UltraPure™ Low Melting Point Agarose (Invitrogen, 16520) and placed under the two-photon microscope where they habituated in darkness for 30 min. Optical section z-series at 1 µm steps of the EGFP labeled ipsilaterally projecting axons were acquired every 10 min for 1 hour in darkness followed by 1.5 h of asynchronous

stimulation: 10 ms flashes, alternating between the two eyes at a duty cycle of 0.5 Hz for each eye (as shown in Chapter 4, Figure 1), followed by 1.5 h of synchronous stimulation: simultaneous 10 ms flashes light in the two eyes presented at 0.5 Hz. For some experiments involving knockdown of proteins of interest, optical section z-series of EGFP and lissamine co-labeled RGC axons were acquired for 1 h in darkness, 2 h in asynchronous and 2 h in synchronous stimulation. Imaging was performed at 910 nm allowing optimal excitation of EGFP using a ThorLabs multiphoton microscope equipped with XLUMPlanFL N 1.0 NA 20x WI objective (Olympus), two channels with gallium arsenide phosphide photo-multiplier tubes (GaAsP PMTs) filtered to detect green and red emission (525/50 and 630/92) and ThorImage software. During the whole imaging session, the tadpoles were perfused with O_2-bubbled 0.1x MBSH. Light flashes were delivered separately to each eye using an FG365LEC-Custom optic fiber (ThorLabs) placed in a channel leading to each eye. To generate light flashes Red Rebel 102lm@700mA LEDs (Luxeon Star, Ltd) controlled by STG4002 and MC Stimulus-II software (Multichannel Systems) were used. For some experiments including co-electroporation of EGFP and MO, additional optical section z-series were collected at the end of each imaging session at 840 nm to ensure minimal excitation of EGFP and maximal excitation of lissamine leading to minimal spectral mixing and confirmation that the EGFP labeled RGC axons had the proteins of interest knocked down.

7.8. Design of custom-built imaging/stimulation PDMS chamber

To ensure a higher survival rate and reliable positioning of the tadpoles during imaging of ipsilaterally projecting RGC axons, we modified a previously described setup (Munz et al., 2014) by designing a new PDMS imaging/stimulation chamber allowing for both perfusion and stimulation of each eye of the animal using fiber optics. Initial AutoCad files of similar chamber moulds were generously provided by Dr. Kelly Sakaki (Kurt Haas laboratory, UBC) and modified to satisfy our specific needs. Using SolidWorks 2015 (Dassasault Systems) a three-dimensional mould was designed and printed using MakerBot software and MakerBot Replicator Desktop 3D printer (MakerBot), where a perfusion, spill-over compartment and channels for each fiber optic were included (Figure

1 in this chapter). The mould was then used to pour a PDMS (SYLGARD® 184, Dow Corning) imaging chamber used for imaging/stimulation. Careful pouring of the PDMS mixture was required in order to avoid air bubbles in the chamber and the PDMS was left to solidify for at least 3 days.

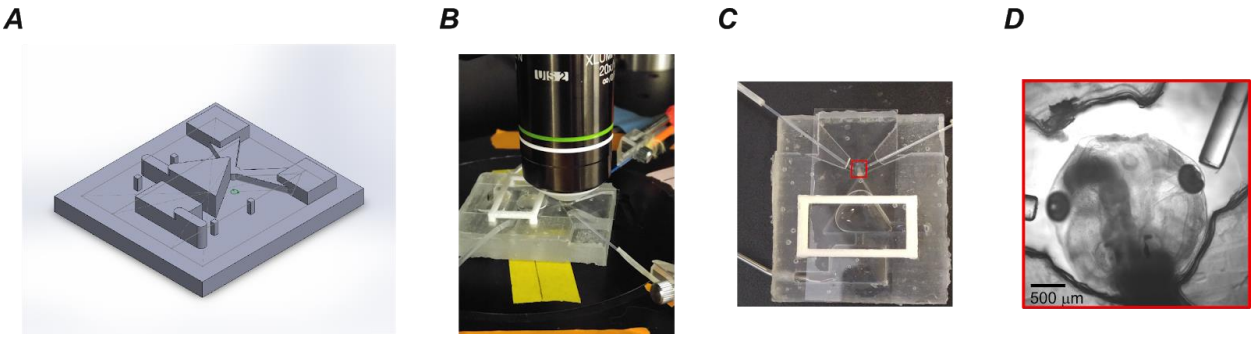

Figure 1: **Experimental setup with custom-made imaging chamber**

(*A*) Mould design for the imaging chamber, 3D view taken from SolidWorks. (*B*) Imaging setup, including perfusing with 0.1x MBSH. (*C*) Top view of the imaging chamber and the position of the optic fibers. (*D*) Zoom-in of the tadpole head with a fiber optic positioned in close proximity to each eye

7.9. Image Analysis

All multiphoton z-series were denoised using CANDLE software implemented in MATLAB (MathWorks) which relies on non-local means filtering methods (Coupé et al., 2012). Denoised 3D stacks were then used to reconstruct axonal arbors using “Autopath” and “Autodepth” features in Imaris 6.4.2 (Bitplane) for daily imaging experiments and by manual tracing in Dynamo software (Munz et al., 2014), implemented in MATLAB (MathWorks), generously provided by Drs. Kaspar Podgorski and Kurt Haas (UBC). For morphometric analysis of daily imaged RGC axonal terminal branch points, total arbor lengths and individual segment lengths were extracted from Imaris 6.4.2. Number of

axonal branches = number of terminal branch points - 1, since the software counts the initial point of the trace as terminal branch point. Segment length is defined by the software as the length between two branch points or between a branch point and a branch tip point. Length is measured in µm. The axonal reconstructions were performed blind to the experimental design. From the dynamic imaging experiments both of contralaterally and ipsilaterally projecting RGC axons branch additions and eliminations between two consecutive z-series (10 min) were extracted and further normalizations were performed as described in the Results sections for each individual case. A branch is counted towards any further analysis only if it attained a length of 1.5 µm at some point during the imaging session. Elongation is defined as the sum of the positive change of length (growth) between two consecutive timepoints where any change <2 µm for 10 min was excluded from further analysis. Retraction is defined as the absolute value of the negative change in length between two consecutive timepoints, where any change <2 µm for 10 min was excluded from further analysis. Elongations and retractions were then normalized as described in the Results sections for each individual case.

7.10. Western Blotting

Stage 46 *Xenopus laevis* were injected with either 200 ng/µL proBDNF (B-240, Alomone Labs), 200 ng/µL cleavage resistant proBDNF (B-243, Alomone Labs) or 100 ng/µL mature BDNF (B-250, Alomone Labs) using the same setup described for electroporation-related DNA injections. Brains of st. 46 animals were extracted in NP-40 extraction buffer (10 mM HEPES/NaOH pH 7.4, 150 mM NaCl, 2 mM EDTA pH 8.0, 0.05% NP40) with Halt™ protease/phosphatase inhibitor cocktail (ThermoScientific, P178442). Each brain was extracted in 10 µL buffer and at least brains from 8 animals were pooled together. Brain extracts were then homogenized using 10 s continuous 10% Amplitude on a Branson 250 Sonifier (Branson Ultrasonics™) equipped with microtip. The extracts were then centrifuged at 13,000 rpm at 4^{o}C for 10 min using a Biofuge 13 centrifuge (Heraeus Instruments). Laemmli sample buffer (50 mM Tris/HCl pH 6.8, 10% Glycerol, 2% SDS, 0.025% Bromphenol Blue, 100 mM DTT) was added to the supernatant and the protein sample was then boiled at 100^{o}C for 5 min for reduction and

linearization of the protein structure. 8% SDS-PAGE was run, and protein was transferred to PVDF membranes (Immobilon-P, 0.45 µm, Millipore) using wet transfer in transfer buffer (48 mM Tris base, 39 mM glycine, 0.037% SDS, 20% methanol) for 80 min, 400 mA. Gels were preincubated in transfer buffer for 12 min prior to transfer. Molecular markers of known size (Precision Plus Protein™ Dual Color Standard, Bio-Rad) were run in parallel with the proteins of interest. Blots were probed with 1:5,000 rabbit anti-p-Trk (Cell Signalling, 9141, AB_2298805) and, 1:10,000 peroxidase AffiniPure Goat Anti-Rabbit IgG (H+L; Jackson Immuno Research Laboratories, inc.) was used for visualization. Blots were blocked using 5% BSA (Fraction V, Fisher Scientific) in TBS-T (20 mM Tris/HCl pH 7.6, 135 mM NaCl, 0.05% Tween) for p-Trk, and with 5% fat-free milk in TBS-T for β-tubulin. To ensure equal loading the blots were probed with 1:20,000 anti-rabbit β-tubulin (sc-9104, Santa Cruz Biotechnology, AB_2241191) and 1:20,000 peroxidase AffiniPure Goat Anti-Rabbit IgG (H+L; Jackson Immuno Research Laboratories, inc.). Immobilon™ Western Chemiluminescent HRP Substrate (Millipore) was used to visualize the protein bands on the blots, diluted 1:1 in double distilled water. HyBlot Autoradiography films (Denville Scientific, Inc.) were used to collect images of the protein bands.

7.11. Statistics

Statistical analysis was performed using GraphPad Prism 7 and the specifics about the tests used for each experiment are described for each figure in Chapter 3 and Chapter 4.

8. Chapter 3: The low-affinity neurotrophin receptor p75NTR, but not TrkB, in RGCs participates in baseline axonal branch dynamics and long-term axonal exploration in the developing visual system

8.1. Overview and rationale

As reviewed in Section 6.2.10, BDNF has been identified as a pivotal player in structural and functional neural circuit development. However, most of these studies have either relied on exogenous application of high concentrations of BDNF, which may not be physiologically relevant or used overexpression of fluorescently-tagged BDNF. Studies utilizing sequestering of endogenous BDNF are difficult to perform *in vivo* and have been mostly performed in cell culture. Notably, as introduced in Sections 6.2.10.1 and 6.2.10.3, BDNF can activate both TrkB and p75NTR and could thereby exert opposing effects both on axonal and dendritic morphology, along with synaptic plasticity. Je and colleagues described the outcome of loss-of-function manipulations of either TrkB or p75NTR in parallel, both in co-cultures and in the developing NMJ (Je et al., 2012, 2013). In the CNS, Orefice and colleagues described opposing roles for proBDNF and mBDNF, acting through p75NTR and TrkB respectively (Orefice et al., 2016). However, these experiments were performed in hippocampal cultures. Although the significance of endogenous BDNF signaling has been examined in detail in *Xenopus laevis* tadpoles (reviewed in Section 6.2.10.3), including dynamic *in vivo* observation of circuit refinement through structural remodeling of RGC axons or tectal neurons, none of those studies provided a comparison between the roles of TrkB and p75NTR in this process (Cohen-Cory and Fraser, 1995; Lom and Cohen-Cory, 1999; Alsina et al., 2001; Hu et al., 2005; Sanchez et al., 2006).

Here, we have used *Xenopus laevis* tadpoles to study in detail whether TrkB and p75NTR exert differential roles in circuit refinement in the developing visual system,

specifically focusing on the retinotectal projection. As described in Section 6.1, amphibians provide important advantages that allow the investigation of living neural circuit remodeling: their transparent skin and skull provide a “window” into the brain allowing for *in vivo* imaging of both axons and dendrites, these animals also develop externally allowing for easy genetic and pharmacological manipulations, and also for manipulations of their sensory experience as the sensory systems develop.

Both *trkb* and *p75ntr* mRNA are expressed in the retina of *Xenopus laevis* tadpoles. Expression of *trkb* is mostly restricted to the ganglion cell layer with sparse expression present in the inner nuclear layer in a small subset of amacrine and/or bipolar cells (Cohen-Cory et al., 1996). RNA sequencing experiments detected *trkB* expression starting from stage 20 and peaking at stage 30 (*Xenopus* ntrk2; Session et al., 2016). Western blot analysis of extracts showed that TrkB protein is expressed in both the retina, including RGC and the optic tectum at stages 40-47 (Cohen-Cory et al., 1996). As described in Section 6.2.9.2.2.1, *p75ntr* mRNA is expressed throughout the retina and detectable levels by *in situ* hybridization were observed from st. 14 onwards (Hutson and Bothwell, 2001). The result of these experiments, taken together with cell biology studies indicating that both TrkB and p75NTR can be transported anterogradely in the axons suggest that it is reasonable to assume that not only are TrkB (Huang et al., 2011; Vaegter et al., 2011) and p75NTR (Johnson et al., 1987) expressed on the somato-dendritic compartments of RGCs, but are very likely also to be present along the axons.

As mentioned above, no study to date has addressed whether BDNF signaling through TrkB and p75NTR expressed in the presynaptic RGC have differential functions in dynamic structural remodeling during circuit refinement *in vivo.*

8.2. Results

8.2.1. RGC p75NTR but not TrkB facilitates axonal branch dynamics

We set out to determine whether signaling through TrkB and p75NTR expressed in RGCs have differential roles in regulating axonal branch dynamics under baseline conditions without stimulation. Both of the morpholino sequences which we utilized have been previously published (Du and Poo, 2004; Je et al., 2012). To validate that TrkB-MO knocks down TrkB, we microinjected lissamine-tagged TrkB-MO or Ctrl-MO into blastomeres in 2-cell stage embryos and reared them in normal light/dark cycle until they reached stage 46 (Figure 1*C*). We then injected mature BDNF intracerebroventricularly and allowed 1 h for sufficient diffusion of the protein in the brain. After brain dissection, we ran the brain extracts on SDS-PAGE and transferred the separated proteins on a membrane which we probed with an antibody for phosphorylated Trk (p-Trk), which recognizes autophosphorylation of both TrkA and TrkB. However, BDNF should not activate TrkA, thus the increase in the intensity of the bands we detect is likely due to TrkB activation. We observed a decrease in the intensity of TrkB-MO band compared to the Ctrl-MO band, which was independent on the sample loading as the β-tubulin bands displayed similar intensities (Figure 1*D*). Since the antibody against p-Trk has been shown to exhibit specificity to rat, mouse and human proteins, we ensured that we can detect a reasonable pattern of activation of TrkB in *Xenopus laevis* by injecting proBDNF, cleavage resistant-proBDNF (cr-proBDNF) and mBDNF (Figure 1*A*). Injection of mature BDNF led to the highest levels of p-Trk. Cr-proBDNF, even at double the concentration of mBDNF, did not induce an increase in p-Trk over control levels. Cleavable proBDNF injection induced an increase in p-Trk levels compared to Ctrl and cr-proBDNF, but the intensity of the band was markedly lower than that of the bands induced by mature BDNF (Figure 1*B*).

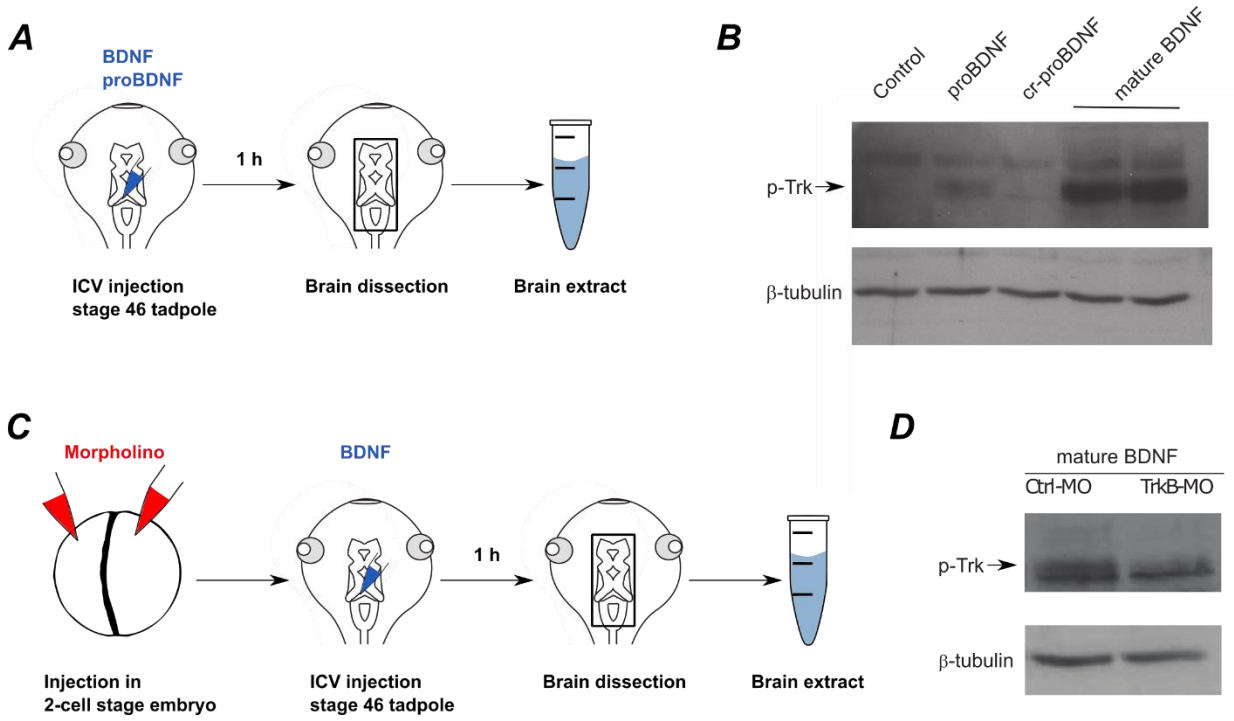

Figure 1. **Morpholino validation**

A. Schematic of the experimental procedure to assess specificity of p-Trk antibody in *Xenopus laevis*: proBDNF (200 ng/µL), cleavage resistant proBDNF (cr-proBDNF, 200 ng/µL) or mature BDNF (100 ng/µL) were injected ICV. One hour after injection, brain extracts were obtained after brain dissection. *B*. Western blot probed for p-Trk and β-tubulin as a loading control, of brain extracts from animals injected with proBDNF, cr-proBDNF and mature BDNF. *C*. Experimental procedure to validate TrkB-MO: injection of either Ctrl-MO or TrkB-MO in both cells in 2-cell stage embryos. The morpholino-injected animals reared to stage 46 and screened for lissamine fluorescence are injected with mature BDNF (100 ng/µL) and their brains are extracted 1 h post injection and homogenized to yield a brain extract. *D*. Western blot of brain extracts from animals injected with Ctrl-MO or TrkB-MO at 2-cell stage and treated with mature BDNF by ICV injection at stage 46, probed for p-Trk and β-tubulin as a loading control.

We co-electroporated lissamine-tagged morpholinos with EGFP in the retinae of albino *Xenopus laevis* tadpoles to achieve knockdown of TrkB or p75NTR in the RGCs. We reared the animals for three days after electroporation, allowing for a sufficient block of new translation and for the turnover of TrkB or p75NTR, synthesized prior to electroporation (Figure 2*A*). We then screened for tadpoles expressing EGFP in a single or couple of RGC axons and made sure these axons were co-labeled with lissamine, ensuring that the morpholino was present in the axons of interest (Figure 2*B*). We next performed short-interval *in vivo* multiphoton imaging of the RGC axon (Figure 2*A*-right) while the tadpole remained immobilized under the microscope objective in darkness -- the infrared light used to excite the fluorophore is not in the animals' visible range. We subsequently carried out 4-dimensional axonal tracing and performed dynamic morphometric analysis to assess axonal branch growth and dynamics at 10 min intervals over 1 h (Figure 2*B*). We observed significantly lower rates of branch additions (Figure 2*C*) and eliminations (Figure 2*E*) in p75NTR knockdown RGC axons (p75-MO) compared to TrkB knockdown RGC axons (TrkB-MO) or control axons (Ctrl-MO). Furthermore, we found evidence for a decrease in elongations (Figure 2*D*) and retractions (Figure 2*F*) in p75-MO axons compared to Ctrl-MO axons. These results show that p75NTR but not TrkB can promote basal axonal branch dynamics and growth, even in the absence of visual stimulation, and indicate that p75NTR signaling may play a crucial role in the process of dynamic RGC axon exploration that helps contact and select appropriate postsynaptic partners during development.

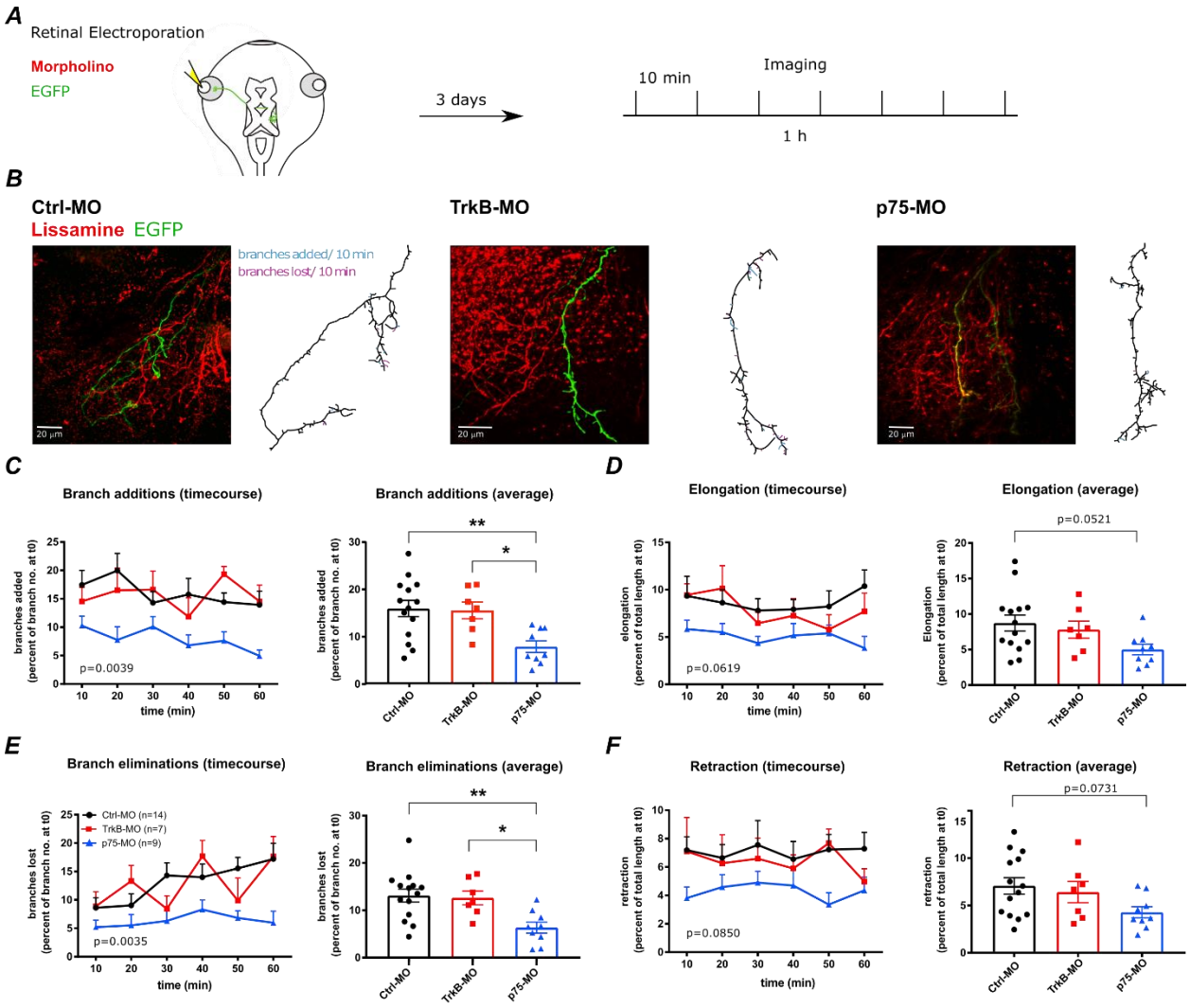
A
Retinal Electroporation
Morpholino
EGFP
3 days
Imaging
10 min
1 h
B
Ctrl-MO
Lissamine EGFP
TrkB-MO
p75-MO
branches added/ 10 min
branches lost/ 10 min
20 µm
C
Branch additions (timecourse)
branches added (percent of branch no. at t0)
p=0.0039
time (min)
Branch additions (average)
**
*
Ctrl-MO
TrkB-MO
p75-MO
D
Elongation (timecourse)
elongation (percent of total length at t0)
p=0.0619
time (min)
Elongation (average)
p=0.0521
E
Branch eliminations (timecourse)
Ctrl-MO (n=14)
TrkB-MO (n=7)
p75-MO (n=9)
branches lost (percent of branch no. at t0)
p=0.0035
time (min)
Branch eliminations (average)
F
Retraction (timecourse)
retraction (percent of total length at t0)
p=0.0850
time (min)
Retraction (average)
p=0.0731

Figure 2. **p75NTR but not TrkB in RGCs helps promote basal axon branch dynamics and growth**

A. Schematic of experimental procedure. Stage 39-41 tadpoles were co-electroporated in the eye with lissamine-tagged morpholino and EGFP to load RGCs. Multiphoton imaging of a single RGC axon co-labeled with lissamine and EGFP is performed 3 days post electroporation at stage 47. Images of the axons were obtained every 10 min for an hour. Merged maximum intensity projections of the red and the green channels acquired at 840 nm for Ctrl-MO (*B*-left), TrkB-MO (*B*-middle) and p75-MO (*B*-right) cases are shown. Next to each example image, a drawing of the axon depicting branch additions (cyan) and branch eliminations (pink) over 10 min is shown. (The traces show branch dynamics between timepoints 30 min and 40 min). Branch additions (*C*) and branch eliminations (*E*) per 10 min shown as percent of the number of axonal branches at the initial timepoint. The whole timecourse is shown on the left and the average normalized rates over the whole imaging session are shown on the right. Elongation (*D*) and retraction (*F*) represent the sum of positive or the absolute value of the negative change in length per 10 min, normalized to the total arbor length at the initial timepoint. Two-way mixed design ANOVA with time as within-subject and morpholino treatment as between-subject factor yielded significant main effect for MO-expression with $F(2,27)=6.874$ for branch additions (*C*), $F(2,27)=7.043$ for branch eliminations (*E*), $F(2,27)=3.089$ for elongation (*D*) and $F(2,27)=2.705$ for retraction (*F*). p-values for the ANOVAs are shown on the graphs. Tukey's post-hoc test was performed to find differences between morpholinos. The p-values are denoted as asterisks on the graph depicting the average additions (*C*-left), average eliminations (*E*-left), average elongation (*D*-left) and average retraction (*F*-left). Ctrl-MO (n=14), TrkB-MO (n=7), p75-MO (n=9). * $p \leq 0.05$, ** $p \leq 0.01$. Data in *C*-left, *D*-left, *E*-left, *F*-left are represented as mean+s.e.m and in *C*-right, *D*-right, *E*-right, *F*-right as mean±s.e.m

Scale bars: 20 μm

8.2.2. p75NTR but not TrkB in RGCs is necessary for normal RGC axon arbor elaboration over days

We further explored how the aforementioned changes in axonal branch dynamics may have led to long-lasting alterations of RGC axon elaboration. We again performed retinal co-electroporation of lissamine-tagged morpholino (TrkB, p75NTR or control) and EGFP and selected animals, in which a single or couple of axons were co-labeled with lissamine and EGFP at three days post electroporation. We then performed daily *in vivo* multiphoton imaging of RGC arbors in these tadpoles for a 4-day period (Figure 3*A-B*, Figure 4*A-B*). After reconstructing and measuring the axons we observed a significant interaction between p75NTR knockdown (p75-MO) and control (Ctrl-MO) RGCs for branch density (Figure 3*E*). As they grow, control axons showed a significant decrease in branch density by Day 4 compared to Day 1. In contrast, p75-MO RGC axons failed to decrease in branch density over the 4-day imaging period. We did not detect significant differences in total branch number (Figure 3*C*) or in total length (Figure 3*D*) between Ctrl-MO and p75-MO axons, though a trend toward smaller arbors was evident in RGCs knocked-down for p75NTR. To help explain the differences in branch density, we examined the distributions of axonal segment lengths over the 4-day imaging period. Axonal segment lengths were extracted from the reconstructions. These were defined as the lengths between any two branch points or between a branch point and a branch tip. (Figure 3*F*). The axonal segment lengths were binned into 4 bins: 0-5, 5-10, 10-20, >20 µm. We found significant differences between Ctrl-MO and p75-MO axons, particularly for the 0-5 µm and 5-10 µm bins (Figure 3*G-H*). Specifically, in control axons the distribution of branch segments seems to shift over time from the shorter to longer lengths, while in p75-MO cells, not only do the shortest length segments fail to reduce in number, but there is even a decrease in the number of longer 5-10 µm length segments, suggesting that short segments that normally would have either been pruned or grown into longer segments are instead retained.

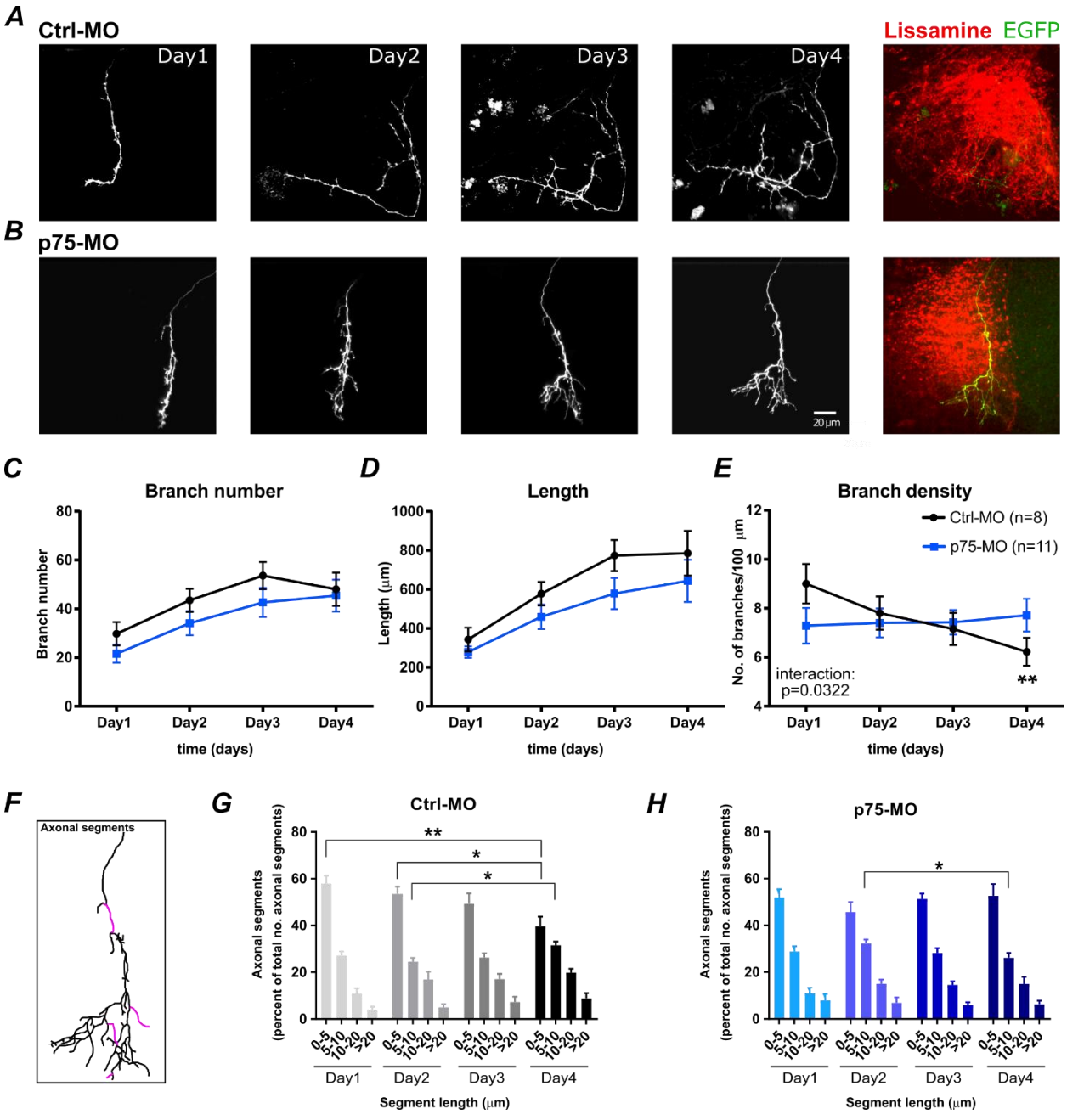
A
Ctrl-MO
Day1
Day2
Day3
Day4
Lissamine EGFP
B
p75-MO
20 µm
C
Branch number
Branch number
time (days)
D
Length
Length (µm)
time (days)
E
Branch density
Ctrl-MO (n=8)
p75-MO (n=11)
No. of branches/100 µm
interaction:
p=0.0322
**
time (days)
F
Axonal segments
G
Ctrl-MO
Axonal segments
(percent of total no. axonal segments)
**
*
*
0-5
5-10
10-20
>20
Segment length (µm)
H
p75-MO
*

Figure 3. **RGC p75NTR is necessary for axonal branch elaboration over days**

Example average intensity projections of images from RGC axons co-labeled with EGFP and lissamine from either Ctrl-MO (*A*) or p75-MO *(B*) over 4 days. To demonstrate the growth of single axon over 4 days, only the green channel image acquired at 910 nm is projected and the fluorescence is shown in greyscale. A merged average intensity projection of both the green and red channel acquired at 840 nm (*A*-*B*-right) shows the axon of interest surrounded by neighboring axons also filled with lissamine-tagged morpholino. Morphometric quantification of RGC axonal arbors: branch number (*C*), axonal length (*D*), branch density (*E*). Branch density is defined as the number of branches over 100 µm of axonal length. Schematic of axonal segments depicted in pink (*F*). Axonal segment is defined as a segment between two branch points or between a branch point and a branch tip point. Analysis of the axonal segment length distribution over 4 days of axons filled with Ctrl-MO (*G*) and p75-MO (*H*). The axonal segment length was binned into 4 lengths 0-5 µm, 5-10 µm, 10-20 µm, >20 µm. Two-way mixed design ANOVA with time as within-subject and morpholino treatment as between-subject factor yielded a significant interaction, $F(3,51)=3.165$ for branch density (*E*), p-value for the ANOVA is shown on the graph. Dunnett's post-hoc test was performed to find differences between the branch density over days within each morpholino treated group. Significant differences between Day 1 and Day 4 within the Ctrl-MO group are denoted as symbols on the graph (*E*). The analysis failed to yield significant differences within the p75-MO group. A two-way mixed design ANOVA for each bin was performed for axonal segment length and yielded a significant interaction, $F(3,51)=4.154$ for bin1 (0-5 µm) and $F(3,51)=5.073$ for bin2 (5-10 µm). To correct for the four ANOVA performed on related data, the p-values were calculated using Bonferroni's correction: $p=0.0416$ for bin1 and $p=0.0152$. Sidak's post-hoc test was used to compare differences between days within Ctrl-MO and p75-MO (significant p-values depicted as asterisks in G: for bin1 between Day1 and Day4; Day2 and Day4; for bin2 between Day2 and Day4 and *H*: for bin2 between Day2 and Day4, respectively). Ctrl-MO (n=8), p75-MO (n=11). Data are represented as mean±s.e.m. (*C*-*E*) and mean+s.e.m (*G*-*H*). * $p\leq0.05$, ** $p\leq0.01$. Scale bar: 20 µm, applies to all images.

A similar analysis was performed to examine whether there were any long-term differences between TrkB knockdown (TrkB-MO) and control (Ctrl-MO) axons (Figure 4). Consistent with the absence of effects of RGC TrkB knock down on axon branch dynamics, we were unable to identify any significant differences in branch number, branch

length or branch density between TrkB-MO and Ctrl-MO cells (Figure 4*C-E*). Furthermore, we did not observe significant interactions for the axonal segment analysis. The two-way ANOVA did indicate a significant time effect for the 0-5 μm bin and the 10-20 μm bin, which, in the absence of a significant interaction, suggests that the two conditions (Ctrl-MO and TrkB-MO) changed in parallel over time. Thus, taken together, our data suggest that p75NTR, but not TrkB, signaling in RGC axons is essential for normal exploratory branch growth in the developing retinotectal projection.

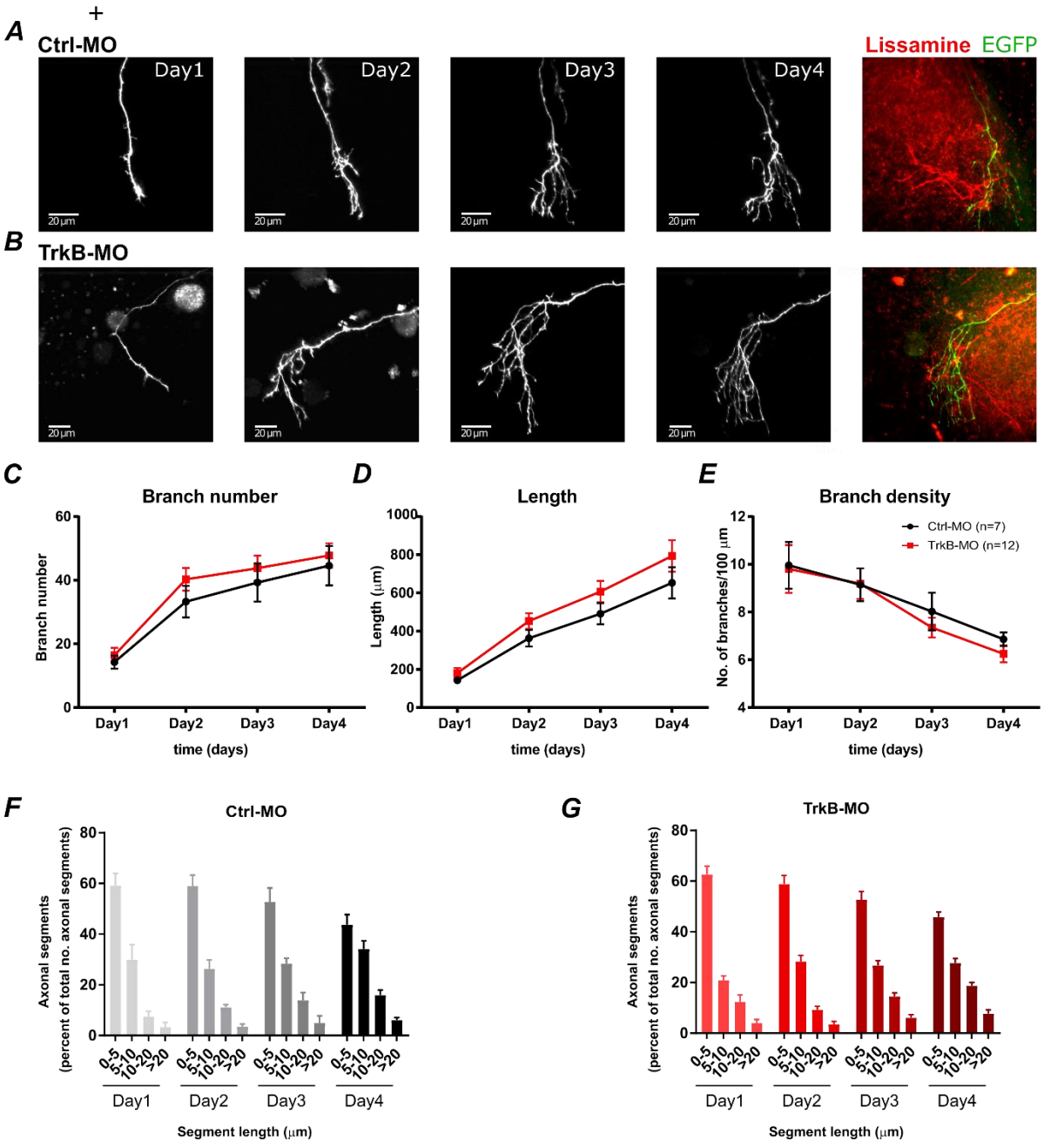
A
+
Ctrl-MO
Day1
Day2
Day3
Day4
Lissamine EGFP
20 μm
B
TrkB-MO
C
Branch number
Branch number
time (days)
D
Length
Length (μm)
time (days)
E
Branch density
No. of branches/100 μm
Ctrl-MO (n=7)
TrkB-MO (n=12)
time (days)
F
Ctrl-MO
Axonal segments
(percent of total no. axonal segments)
0-5
5-10
10-20
>20
Segment length (μm)
G
TrkB-MO

Figure 4. **RGC TrkB is dispensable for RGC axonal branch elaboration over days**

Example average intensity projections of images from RGC axons co-labeled with EGFP and lissamine from either Ctrl-MO (*A*) or TrkB-MO *(B*) over 4 days. To demonstrate the growth of single axon over 4 days, only the green channel image acquired at 910 nm is projected and the fluorescence in shown in greyscale. A merged average intensity projection of both the green and red channel acquired at 840 nm (*A-B*-right) shows the axon of interest surrounded by neighboring axons also filled with lissamine-tagged morpholino. Morphometric quantification of RGC axonal arbors: branch number (*C*), axonal length (*D*), branch density (*E*). Branch density is defined as the number of branches over 100 μm of axonal length. Two-way mixed design ANOVA with time as within-subject and morpholino treatment as between-subject factor did not yield a significant interaction. Axonal segment is defined as a segment between two branch points or between a branch point and a branch tip point. Analysis of the axonal segment length distribution over 4 days of axons filled with Ctrl-MO (*F*) and TrkB-MO (*G*). The axonal segment length was binned into 4 lengths 0-5 μm, 5-10 μm, 10-20 μm, >20 μm. A two-way mixed design ANOVA for each bin was performed and yielded a significant main effect for time, $F(3,51)=13.94$ for bin1 (0-5 μm) and $F(3,51)=4.442$ for bin3 (10-20 μm). To correct for the four ANOVA performed on related data, the p-values were calculated using Bonferroni's correction: $p<0.0004$ for bin1 (0-5 μm) and $p=0.03$ for bin3 (10-20 μm). Ctrl-MO (n=7), TrkB-MO (n=12). Data are represented as mean±s.e.m. (*C-E*) and mean+s.e.m (*F-G*). Scale bars:20 μm. The scale bars on the example images of Day 4 (greyscale) apply to the corresponding merged images.

9. Chapter 4: Roles of BDNF signaling, presynaptic p75NTR signaling and presynaptic TrkB signaling in neural activity correlation-dependent axonal branch dynamics

9.1. Overview, rationale and experimental approach

As described in Sections 6.2.3-6.2.4, BDNF can be released both through the constitutive and the regulated secretory pathways. In particular, BDNF is secreted in an activity-dependent manner. Some reports propose that BDNF could be translated on demand in the dendrites and released in the extracellular milieu as proBDNF (Yang et al., 2009; Orefice et al., 2016). Intriguingly, the stabilization of presynaptic clusters, which is in part mediated by BDNF, is likely downstream of NMDAR activation, suggesting that BDNF requires input co-activation (Hu et al., 2005). Furthermore, sustained and acute BDNF signaling have been shown to exert differential effects on neurite growth, with application of slowly increasing concentrations of BDNF resulting in sustained activation of TrkB and neurite branching, whereas acute application leads to transient activation of TrkB and neurite outgrowth (Ji et al., 2010; Guo et al., 2018). The aforementioned findings imply a dual mode of BDNF release, an acute activity-dependent and a more tonic, activity-independent BDNF secretion. To expand on our results in Chapter 3, we next address the involvement of BDNF signaling and specifically TrkB and p75NTR expressed on RGCs in the axonal response to patterned activity.

An experimental approach to study the role of neuronal activity in the structural remodeling of the developing visual system has previously been established in our laboratory (Munz et al., 2014). This approach utilizes single RGC axons that have ectopically grown to innervate the ipsilateral optic tectum. It is well described that unlike in mammals, in amphibians nearly all of the RGCs project to the contralateral optic tectum (Gaze, 1958). However, in about 40% of *Xenopus laevis* tadpoles, a small number of

ipsilaterally projecting RGC axons (typically < 3) are found (Munz et al., 2014). When a single axon projects to the ipsilateral optic tectum, it will be surrounded by axons whose somata are located in the contralateral retina of the animal (Figure 1*A*). This lone ipsilaterally projecting axon can be visually driven independently from its neighbors simply by flashing lights in the ipsilateral rather than contralateral eye of the animal (Figure 1*A*). Postsynaptic (tectal) neurons are driven preferentially by the contralateral eye due to the numerical superiority of the contralateral visual inputs. Alternatively, if flashes of light are synchronously presented to the two eyes (Figure 1*A*), the ipsilaterally projecting RGC axon effectively participates along with the contralateral eye inputs in driving postsynaptic neurons to fire action potentials. As described in Sections 6.1.2.4.6.-6.1.2.4.7, imaging the ipsilaterally projecting RGC axons, during synchronous/asynchronous visual stimulation paradigms has led to the conclusion that axonal branch growth follows a modified Hebbian rule: when the presynaptic and postsynaptic cell “fire together”, the axonal branches stabilize, and overall branch dynamic behaviors are downregulated. In contrast, during asynchronous stimulation when the pre- and postsynaptic cells “fire out of sync”, there is an increase in the growth and dynamics of axonal branches. In this chapter, we used this experimental approach to investigate the role of BDNF signaling, and more specifically signaling through presynaptic TrkB and p75NTR receptor in Hebbian stabilization of branch dynamics and in the asynchrony-induced promotion of axonal branch dynamics.

The main experimental paradigm, in which a single ipsilaterally projecting axon is imaged *in vivo* every 10 min for 1 h of darkness, 2 h of asynchronous binocular stimulation (0.5 Hz, 10 ms light flashes) and 2 h of synchronous binocular stimulation (0.5 Hz, 10 ms light flashes) will be referred to as dark/asynch/synch (DAS). Introducing a novel imaging chamber, as described in Chapter 2 (Figure 1), and the imaging of ipsilaterally projecting RGC axons co-electroporated with EGFP plasmid and lissamine-tagged control morpholino oligonucleotides (Ctrl-MO), did not alter the previously reported effects on axon branch additions of the DAS protocol. Similar to the observations of Munz and co-workers (2014) imaging ipsilaterally projecting EGFP-transfected cells, we observed that the rates of axonal branch addition increased during asynchronous stimulation and decreased during synchronous stimulation in Ctrl-MO axons (Figure 1*B*-*C*). However, we

were unable to reproduce Munz and colleagues' changes in branch elimination rates (Figure 1*D-E*). The reason for this disparity could be due to any of the numerous innovations introduced into the experimental design which were necessary to achieve the efficiency needed to carry out all the experiments reported below (e.g., electroporation of MO for targeted knockdown, new imaging chamber that improved animal survival rates, shorter baseline (darkness) imaging period that increased the number of completed experiments unimpeded by animal movement). For this chapter of the thesis, Ctrl-MO axons serve as the main control group for comparisons with animals in which various components of BDNF signaling have been manipulated.

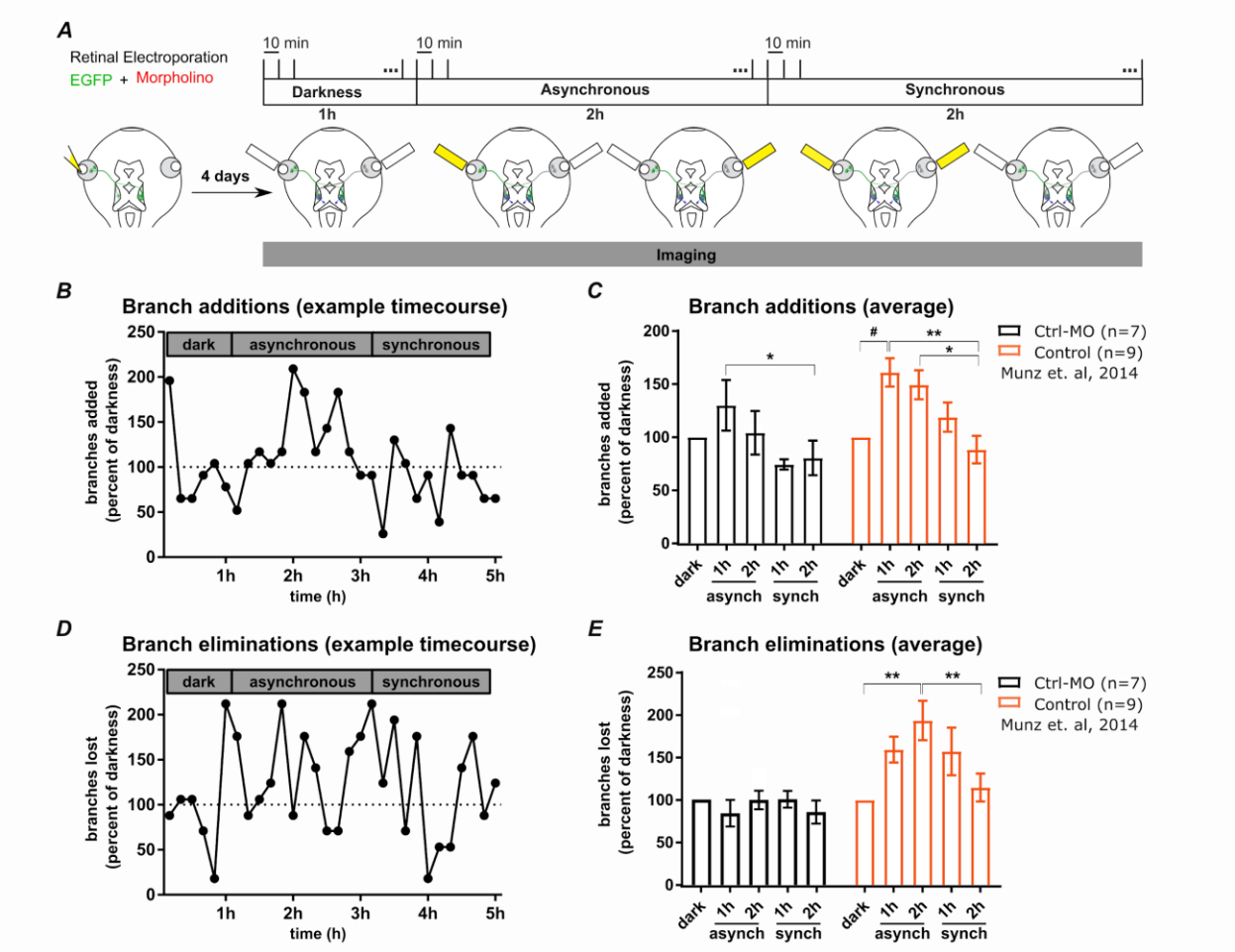

Figure 1. **Imaging protocol to study effect of correlated neural firing on axonal branch dynamics.**
(*A*) Experimental setup: Left - schematic of retinal co-electroporation of lissamine-tagged morpholino and EGFP and selection of animals with ipsilaterally projecting RGC axons co-labeled with lissamine and EGFP 3-4 days post-electroporation. Right - imaging paradigm as in (Munz et al., 2014): imaging of the labeled axons every 10 min for 1 or 1.5 h in darkness, 2h in asynchronous stimulation (alternating flashes of light between the two eyes), 2h in synchronous stimulation (simultaneous flashes of light in the two eyes). Example traces of branches additions (*B*) and branch eliminations (*D*), representing the number of branches added/10 min (*B*-*C*) or lost/10 min (*D*-*E*) normalized to the average number of branches added/10 min (*B*-*C*) or lost/10 min (*D*-*E*) during the whole darkness period. Average branch additions (*C*) and eliminations (*E*) for each hour of stimulation are displayed for ipsilaterally projecting RGC axons co-labeled with EGFP and lissamine (Ctrl-MO; n=7) acquired in the current study (black) and for ipsilaterally projecting RGC axons expressing only EGFP (n=9) in orange acquired by Munz et al., 2014. Robust regression and Outlier removal test (ROUT) at Q=2% was used to identify outliers in (*C*) and (*E*) led to removal of one cell in Ctrl-MO, resulting in n=7 for Ctrl-MO. Non-parametric version of one-way ANOVA (Friedman's test) was performed for branch additions: Ctrl-MO -- p=0.0075, Friedman's statistic=13.94, control from Munz et al., (2014) -- p=0.0007, Friedman's statistic=19.29; and for branch eliminations: Ctrl-MO -- n.s, Friedman's statistic=1.294, control from Munz et al., 2014 -- p=0.0005, Friedman's statistic=19.96. Dunn's post-hoc test was used to correct for multiple comparisons of the branch additions or eliminations between each hour of stimulation and p-values are displayed as symbols on the graphs. # $p \leq 0.1$, * $p \leq 0.05$, ** $p \leq 0.01$

9.2. Results

9.2.1. BDNF signaling is necessary for correlation-induced suppression of axonal branch addition and growth

We performed retinal electroporation with EGFP (without MO) and waited for 4 days to select animals with EGFP-expressing ipsilaterally projecting RGC axon and subjected these animals to ICV injection of TrkB-Fc, which serves as a soluble BDNF “sponge” to prevent endogenous signaling. We allowed 1 h for diffusion of the protein in the brain and then collected multiphoton z-series every 10 min for 1 h in darkness 1.5 h in asynchronous and 1.5 h in synchronous stimulation. We compared the dynamic morphometric data from the first hour of each stimulation period of the axons in animals injected with TrkB-Fc (TrkB-Fc axons) to the first hour of stimulation of the Ctrl-MO axons from Figure 1*B*-*E* (Figure 2).

While control axons show decreased rates of new branch addition in response to synchronous stimulation compared with asynchronous stimulation, axons in TrkB-Fc-injected animals, by contrast, showed a slight increase in the rate of branch additions during synchronous stimulation. This resulted in a significant statistical interaction for branch additions between Ctrl-MO and TrkB-Fc axons by two-way ANOVA (Figure 2*A*). Furthermore, the increase in branch addition rate is accompanied by a significant increase in branch elongation during synchronous stimulation in TrkB-Fc compared to Ctrl-MO (Figure 2*B*). Interestingly, we also found a significant increase in elongation during synchronous compared to asynchronous stimulation within the TrkB-Fc axons. We were unable to detect significant changes in rates of branch elimination (Figure 2*C*) or retraction (Figure 2*D*) between the two groups of axons, likely due to the increased variability in TrkB-Fc axons for those measures. Our data indicate that BDNF signaling in the retinotectal system is required for Hebbian stabilization of axonal branches, specifically for the suppression of new branch addition and elongation in response to correlated activity.

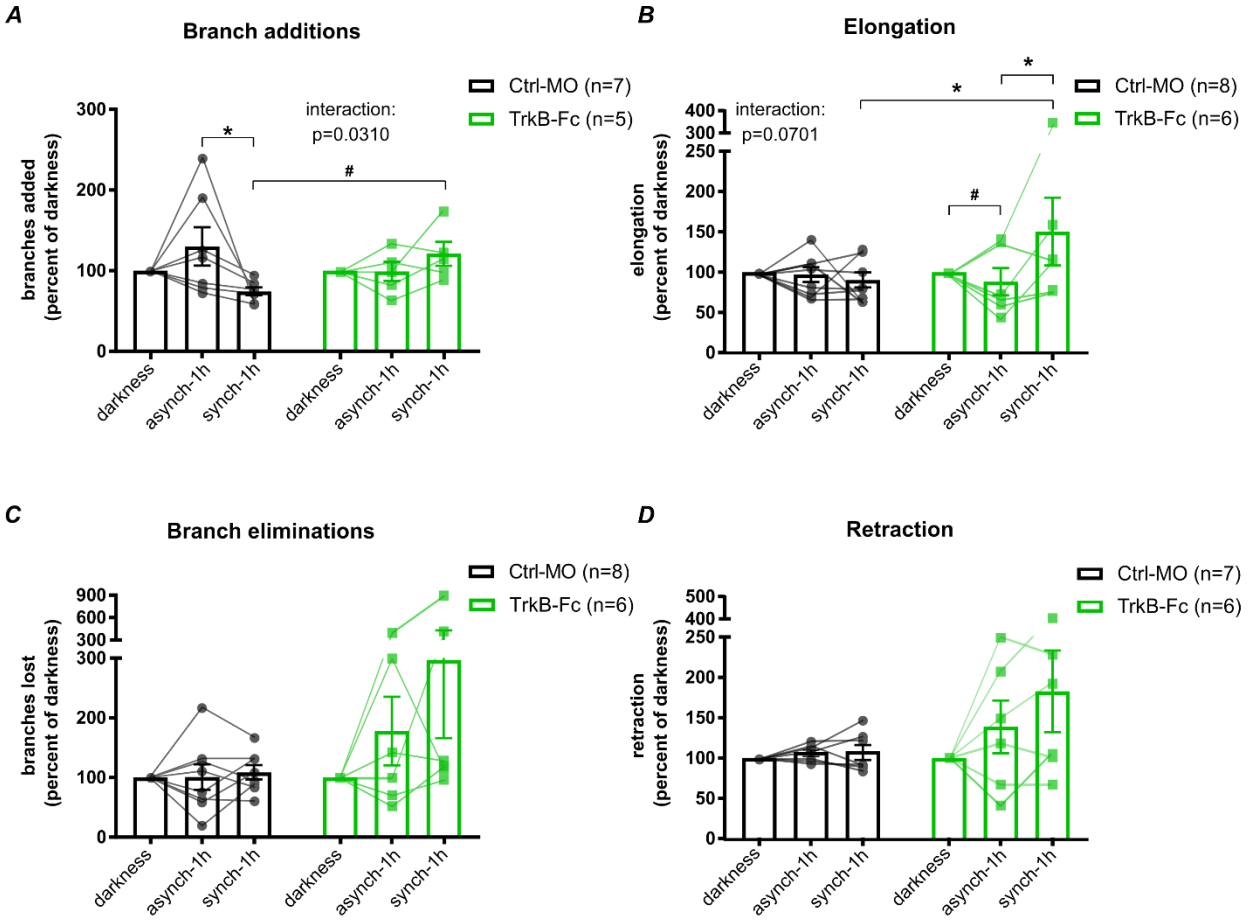
A
Branch additions
branches added
(percent of darkness)
300
200
100
0
*
#
interaction:
p=0.0310
Ctrl-MO (n=7)
TrkB-Fc (n=5)
darkness
asynch-1h
synch-1h
darkness
asynch-1h
synch-1h
B
Elongation
elongation
(percent of darkness)
400
300
250
200
150
100
50
0
*
*
#
interaction:
p=0.0701
Ctrl-MO (n=8)
TrkB-Fc (n=6)
darkness
asynch-1h
synch-1h
darkness
asynch-1h
synch-1h
C
Branch eliminations
branches lost
(percent of darkness)
900
600
300
300
200
100
0
Ctrl-MO (n=8)
TrkB-Fc (n=6)
darkness
asynch-1h
synch-1h
darkness
asynch-1h
synch-1h
D
Retraction
retraction
(percent of darkness)
500
400
250
200
150
100
50
0
Ctrl-MO (n=7)
TrkB-Fc (n=6)
darkness
asynch-1h
synch-1h
darkness
asynch-1h
synch-1h

Figure 2. **BDNF signaling is necessary for correlation-induced stabilization in axonal growth.**

Animals expressing EGFP in an ipsilaterally projecting RGC axon were subjected to ICV injection of 50 µg/mL TrkB-Fc at least 1 h prior to imaging and imaged using modified imaging paradigm: multiphoton z-series were obtained every 10 min for 1 h in darkness, 1.5 h in asynchronous stimulation and 1.5 h in synchronous stimulation. Branch additions (*A*) and eliminations (*C*), as well as elongation (*B*) and retraction (*D*) in the first hour of each stimulation period were compared to Ctrl-MO from figure 1. ROUT test at Q=2% was performed for each data set: for branch additions (*A*), one cell was identified as an outlier from each group (Ctrl-MO n=7, TrkB-Fc, n=5); for retraction (*D*) one cell was identified as an outlier from Ctrl-MO (n=7), but not for TrkB-Fc (n=6). No outliers were identified from either group for branch eliminations (*C*) and elongation (*B*), Ctrl-MO (n=8), TrkB-Fc (n=6). Branch additions and eliminations are defined as the number of branches added/10 min, normalized to the average number of branches added or lost for 10 min, respectively, for the whole darkness period. Elongation and retraction are defined as the positive change of length/10 min and the absolute value of the negative change in length/10 min normalized to the average elongation/10 min or retraction/10 min of the whole darkness period. Two-way ANOVA was performed and yielded significant interaction for branch additions (*A*), $p=0.0310$, $F(2,20)=4.155$ and a marginally significant interaction for elongation, $p=0.0701$, $F(2,24)=2.976$. Sidak's post-hoc test was performed to correct for multiple comparisons between the branch additions or elongation for each stimulation period and p-values are shown on the graphs as symbols. # $p \leq 0.1$, * $p \leq 0.05$

9.2.2. RGC p75NTR is required for the differential effects on axonal branch additions of asynchronous and synchronous firing of an axon with its neighboring input.

Four days after retinal co-electroporation of lissamine-tagged morpholinos (Ctrl-MO, TrkB-MO, or p75-MO), we selected animals in which a single or a couple of ipsilaterally projecting RGC axons were labeled both with EGFP and lissamine. We then performed multiphoton *in vivo* imaging of the selected axons using the DAS protocol illustrated in Figure 1*A.* We found that suppression of p75NTR expression in ipsilaterally projecting RGC axons eliminated the significant difference in branch addition rates that we observed between asynchronous and synchronous stimulation in Ctrl-MO axons (Figure 3A). TrkB knockdown, on the other hand, did not prevent the axon from responding differentially to the different stimulation conditions, suggesting its role in RGCs is less critical than p75NTR for regulating activity-dependent axonal branch additions. The effects of p75NTR knockdown could reflect either a lack of asynchrony-induced branch additions or an impairment in the suppression of branch additions during synchronous stimulation. Considering our results from Chapter 3, it is very likely that p75NTR is required for asynchrony-induced branch addition.

9.2.3. RGC TrkB signaling suppresses activity-induced branch elimination

Interestingly, we observed that there is a marginally significant increase in branch elimination by the second hour of asynchronous stimulation in TrkB-MO axons, which does not decline during synchronous stimulation (Figure 3*B*). Our data suggest that RGC TrkB may act as a general activity-driven brake on axonal branch elimination.

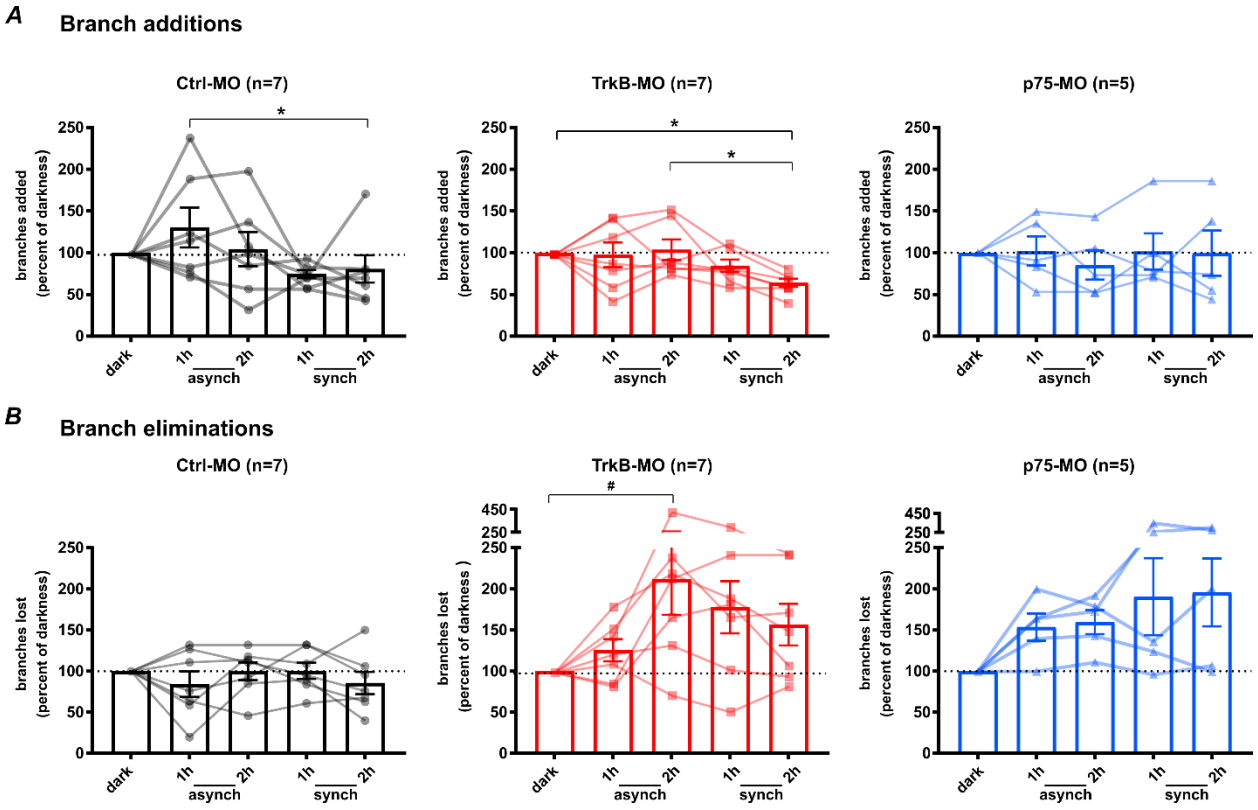
A
Branch additions
Ctrl-MO (n=7)
TrkB-MO (n=7)
p75-MO (n=5)
branches added
(percent of darkness)
dark
1h
2h
asynch
synch
B
Branch eliminations
branches lost
(percent of darkness)
#

Figure 3. **Presynaptic p75NTR but not TrkB signaling is required for synchrony-induced axonal branch stabilization.**

Ipsilaterally projecting RGC axons co-filled with lissamine-tagged morpholino and EGFP were imaged using the imaging paradigm from Figure. 1*A*. Branch additions (*A*) and eliminations (*B*) are defined as the number of branches added/10 min or lost/10 min normalized to the average number of branches added/10 min or lost/10 min during the whole darkness period, respectively. The data are averaged over each hour of stimulation. ROUT test at Q=2% was performed for each data set and one cell was identified as an outlier and removed for both branch addition and eliminations from the Ctrl-MO group, n=7. No outliers were identified in any of the other groups, TrkB-MO (n=7), p75-MO (n=5). Non-parametric version of one-way ANOVA (Friedman's test) was performed for branch additions: Ctrl-MO -- p=0.0075, Friedman's statistic=13.94, TrkB-MO -- p=0.0140, Friedman's statistic=12.5; p75-MO, n.s., Friedman's statistic=1.333 and for branch eliminations: Ctrl-MO – n.s., Friedman's statistic=1.294, TrkB-MO -- p=0.0718, Friedman's statistic=8.604, p75-MO, n.s., Friedman's statistic=6.898. Dunn's post-hoc test was used to correct for multiple comparisons between the branch additions and eliminations within each hour of stimulation and p-values are displayed as symbols on the graphs. # $p \leq 0.1$, * $p \leq 0.05$

10. Chapter 5: Discussion

There has been an effort to identify molecular and cellular mechanisms underlying activity-dependent circuit refinement in the developing brain over several decades. Although much progress has been made in revealing molecular players, a lot of the manipulations relied on systemic pharmacological blockade which did not provide much detail on the sites of molecular communication between the projecting and target neurons in a refining neural circuit. BDNF is one of the molecular candidates proposed to serve as a retrograde or autocrine signal resulting in stabilization of axonal arbors and synapses, but its exact role in these processes remains ill-defined (Cohen-Cory and Fraser, 1995; Hu et al., 2005; Lindskog et al., 2010; Je et al., 2012; Harward et al., 2016; Choo et al., 2017, Niculescu et al., 2018).

10.1. RGC p75NTR promotes exploratory axonal branch dynamism

In the *Xenopus laevis* retinotectal projection a role for BDNF in axon arbor elaboration has been clearly established. However, whether BDNF acts directly on the axon to exert its functions remains elusive. BDNF signaling through p75NTR and TrkB receptors is complex as p75NTR interacts with other receptors and its presence or absence affects TrkB's affinity to BDNF. In this study, we attempted to discriminate between the functions of the two receptors on the experience-dependent modulation of axon arbor morphology by specifically knocking them down in the projection neurons (RGC) and not the target neurons (tectal cells). We found that in conditions of complete darkness p75NTR expressed on the RGC is required for normal axonal branch dynamism, both in terms of initiating additions of new branches and elongation of pre-existing branches, eliminating branches and retraction of pre-existing branches. High rates of axonal branch additions and eliminations are consistent with an exploratory behavior of the RGC, while in search of a "correct" postsynaptic partner, which, in the context of retinotopic map refinement would be a tectal neuron that receives inputs that are highly correlated with this axon (Munz et al., 2014). Such increased dynamism has been shown to be associated with a state of weak synaptic strengths of the existing

synapses with “incorrect” (i.e., uncorrelated) postsynaptic neuronal partners. Our proposition that p75NTR expressed on the RGC is required for exploratory behavior agrees with reports that proBDNF signaling through p75NTR promotes LTD both in the developing visual system in *Xenopus laevis* tadpoles and in the developing hippocampus (Schwartz et al., 2011; Winnubst et al., 2015). Previous studies have suggested that proBDNF signaling through p75NTR may lead to activation of RhoA and filopodial retraction (Sun et al., 2012). Regulation of RhoA activity downstream of p75NTR is a plausible mechanism that could underlie at least in part the function of the receptor as promoter of axonal exploration.

10.2. RGC TrkB is dispensable for basal axonal branch dynamics

Intriguingly, knockdown of TrkB from RGC failed to induce any changes in axonal branch dynamics in conditions of complete darkness. This result is somewhat surprising considering the widely accepted model of BDNF action through TrkB to induce synaptic stabilization and strengthening which in turn are associated with stabilization of axonal arbor dynamics (Alsina et al., 2001; Du and Poo, 2004; Hu et al., 2005; Ruthazer et al., 2006; Schwartz et al., 2011; Van Horn et al., 2017). However, in those experiments, systemic application BDNF or inhibitor k252a was used to block TrkB, which might affect postsynaptic TrkB and thus impair the signaling of an alternate retrograde signal to stabilize axonal branches. Moreover, k252a has been shown to exhibit relatively broad inhibitory action, including on PKC, which is crucial for synaptic plasticity (Kase et al., 1987; Ramakers et al., 1997). One study in *Xenopus laevis* tadpoles described that presynaptically expressed TrkB.T1 leads to increased dynamics of axonal branches over 2 hours (Marshak et al., 2007). There are a few important experimental differences between our findings and the results that Marshak and colleagues described. Firstly, overexpression of TrkB.T1 functions as a more localized “molecular sponge” for BDNF compared to TrkB-Fc or anti-BDNF. TrkB.T1 overexpression will then impact both p75NTR and TrkB signaling, especially in the case of presynaptic release of BDNF. In our experiments, however, we went on to specifically target one or the other receptor. Secondly, as described above (Section 6.2.9.1.2) BDNF-dependent TrkB.T1 activation

results in RhoA inhibition which might lead to profound effects on axonal morphology such as increased rates of elongation (Yamashita et al., 1999). Thirdly, Marshak and colleagues revealed a cell-autonomous mechanism as they relied on TrkB.T1 expression in single RGC axons. On the other hand, the morpholinos we electroporated are small oligos which get into multiple RGCs with high efficiency, leading to knockdown in a large number of RGCs. This difference is important as sequestering of BDNF, or TrkB blockade in a single RGC, might place it at a competitive disadvantage with its neighbors. Fourthly, our imaging was performed using multiphoton imaging with infrared excitation light that is invisible to the animals, allowing us to assess the structural changes of RGC in darkness, whereas Marshak and colleagues used confocal microscopy, which provides inadvertent intense visual stimulation. Since BDNF release has an activity-dependent mode, the imaging conditions might have led to significant changes in the observed dynamics. Finally, differences in outcomes could arise from the slight differences in the timecourses of imaging between the two studies. We assed branch dynamics every 10 min over the course of an hour, whereas the other groups examined branch dynamics every 2 h over 6 h.

Our results on axonal branch dynamics suggest a mechanism in which at least during darkness, when BDNF release may be shifted towards a more constitutive rather than activity-dependent mode, RGC p75NTR is required for exploratory dynamism, which includes branch addition and elimination, as well as elongation and retraction. RGC TrkB, however, is not required for any aspect of axonal branch dynamics that we measured. These findings in the context of the existing knowledge of BDNF signaling suggest that the well-established roles of BDNF in synaptic strengthening and axon branch stabilization in the retinotectal projection are most likely exerted through activating postsynaptic TrkB rather than axonal TrkB. In this scenario, activation of TrkB, in turn, would lead to generation of another retrograde signal instructing synaptic strengthening and branch stabilization.

10.3. RGC p75NTR but not TrkB contributes to long-term axonal arbor elaboration

We were further interested whether effects of p75NTR knockdown on RGC axonal branch dynamics persisted over long periods of time or there is an alternative compensatory mechanism that comes into play later in development. Furthermore, as we failed to observe any changes on branch dynamics of RGC TrkB knockdown axons over a 1 h period, we asked whether we could detect any long-term effects of this manipulation, which might reflect a specific period of retinotectal refinement sensitive to RGC TrkB signaling. Notably, in these experiments, the animals were imaged once a day for about 20 min at a time and were exposed to their regular light/dark cycle during the intervening time. Therefore, with these experiments, we are not simply investigating the basal effects of TrkB and p75NTR knockdown in conditions of darkness. Our data indicate that RGC p75NTR helps mediate the normal decrease in axonal branch density over a 4-day period, which in this case started three days after morpholino electroporation. This decrease in axonal branch density could be indicative of a decrease in branch number or an increase in the lengths of each branch segment. It is clear that the RGC axons we imaged add more branches over days (Chapter 3, Figure 3 and Figure 4). Therefore, the decrease in branch density must reflect the elongation of branch segments. Our analysis of segment length suggests that the difference between p75NTR knockdown and control axons comes mainly because the shortest segments fail to elongate over days. A recent study showed that precocious synapse maturation in animals treated with the NMDAR co-agonist D-serine correlated with simpler and shorter arbors of RGC axons (Van Horn et al., 2017). One could imagine that the RGC axon puts a break on its exploratory growth in search of postsynaptic partners once most or all of its synapses with tectal neurons have gone through maturation. Consistently, the p75NTR knockdown axonal branches fail to elongate their shortest branches over days, which might be indicative of more mature synapses compared to control axons.

In line with the lack of an effect of TrkB knockdown in RGCs on axonal branch dynamics, we failed to detect any changes in axon arbor elaboration over days.

Importantly, other groups have shown that the TrkB-MO used in this study results in a decrease in *Xenopus* TrkB protein levels (Du and Poo, 2004; Je et al., 2012) and we were able to confirm this by showing a decrease in the level of BDNF-induced TrkB activation (Chapter 3, Figure 1), suggesting that the lack of both short-term and long-term effects of TrkB knockdown in RGCs is not due to inefficacy of the knockdown.

As described in in Section 6.2, TrkB is a neurotrophin receptor, that can bind to BDNF, NT-3 and NT-4. On the other hand, p75NTR forms receptor complexes with sortilin, NogoR, and LINGO-1, and therefore the activation of any of those receptors by their specific ligands can modulate p75NTR activity. Detailed analysis of plausible p75NTR ligands would be required to make a conclusion on which one, if any, promotes axonal exploratory elaboration. However, BDNF, and in particular its propeptide and precursor proBDNF are excellent candidates, as they have been shown to act through p75NTR to facilitate LTD, axonal retraction and a decrease in spine density (Section 6.2.10; Schwartz et al., 2011; Je et al., 2012; Guo et al., 2016).

To summarize, the findings described in Chapter 3 indicate that p75NTR expressed on the RGC is an important player in exploratory dynamism in basal conditions without visual stimulation, promoting increased branch addition, elimination, elongation and retraction. This function of p75NTR translates into elongation of the shortest filopodia-like branches, which likely helps RGC axons to contact additional postsynaptic partners.

10.4. BDNF signaling is required for correlation-induced suppression of branch addition and elongation

In Chapter 4, we investigated whether specific components of BDNF signaling underlie any of the morphological outcomes of patterned activity on RGC axon arbor formation. As described in Sections 6.1.2.4.6-6.1.2.4.5.7, asynchronous firing of an RGC with its neighboring inputs induces an increase in axonal dynamism, both branch additions and eliminations (i.e., Stentian mechanisms), whereas synchronous firing of an RGC with its neighboring axons results in suppression of new axonal branch addition and elimination (i.e., Hebbian mechanisms). Using a novel imaging setup, we were able to

reproduce these previously obtained results in terms of branch additions, even in ipsilaterally projecting axons electroporated with Ctrl-MO. The branch elimination measurements, which differed from prior reported data might be more sensitive to the changes introduced to the protocol, or to the tracing of the axons, which was performed by different individuals and thus it might require greater number of imaged cells to reproduce the effect.

We also investigated whether sequestering available endogenous BDNF by ICV injection of TrkB-Fc specifically affects the Stentian or Hebbian mechanisms mentioned above. Our data indicated that sequestering of BDNF likely affects Hebbian mechanisms to a greater extent. It appears that BDNF signaling is required for synchrony-induced suppression of axonal branch addition and elongation. The effect on elongation is likely more complex, as it seems that blocking BDNF signaling may result in reduced elongation during asynchronous conditions (Chapter 4, Figure 2). This experiment by itself does not address whether BDNF acts pre- or postsynaptically but implicates BDNF as a ligand triggering a molecular mechanism that suppresses new branch initiation and further growth of all branches. This experiment is in line with a previously described study in *Xenopus laevis* relying on TrkB.T1 overexpression in RGCs, which showed that sequestering of BDNF impairs the stabilization of axonal branches and the maturation of synapses, and promotes addition of new branches (Marshak et al., 2007). However, our data suggest that this mechanism is specific to the case when an axon is firing in synchrony with its neighbors. Previous studies have shown that the suppression of branch addition is induced by NMDAR activation, likely on the postsynaptic neuron (Zou and Cline, 1996; Rajan et al., 1999; Munz et al., 2014). Thus, it is possible that postsynaptic NMDAR activation, directly or via another factor, mobilizes BDNF signaling. Moreover, a separate mechanism involving BDNF signaling might be in play to induce exploratory elongation during asynchronous firing. As blockade of NMDARs does not prevent activity-dependent exploratory branch dynamics, this latter mechanism likely involves NMDAR-independent BDNF signaling.

10.5. RGC p75NTR is required for the differential effect of Stentian and Hebbian mechanisms on axonal branch addition

To parse out activity-dependent BDNF signaling through its two receptors p75NTR and TrkB, we used the knockdown strategy described in Chapter 3 but combined it with the DAS stimulation paradigm. Knocking down p75NTR on RGC axons abrogated the difference in rates of branch addition between conditions of asynchronous and synchronous firing (Chapter 4, Figure 3). The difference involves asynchrony-induced enhancement and synchrony-induced suppression of newly added branches. Considering that p75NTR has been implicated in facilitating LTD and that asynchronous stimulation was found to induce a marked decrease in synaptic strength, it is reasonable to propose that p75NTR may be required for “Stentian” branch addition, which occurs during asynchronous stimulation (Schwartz et al., 2011; Munz et al., 2014). This effect was only eliminated in p75NTR knockdown axons, but not TrkB knockdown axons. As in Chapter 3, it is plausible that knocking down the receptors in the RGC somato-dendritic compartment, rather than at the axon terminals themselves could account for our results. However, this is less likely to explain the findings presented in Chapter 4, as the different axonal branch behaviors were induced in response to changes in the correlation of firing between the ipsilaterally projecting axon and its neighbors. This is a non-cell-autonomous effect that requires input from both eyes, but the morpholino is only present in the ipsilateral eye. Evidence that p75NTR is expressed mostly on axonal terminals in other systems also supports the notion that activation of presynaptic p75NTR can promote axonal branch addition (Dougherty and Milner, 1999).

10.6. RGC TrkB signaling suppresses activity-induced branch elimination

Intriguingly, we observed that RGC knockdown of TrkB resulted in an increase in branch eliminations during asynchronous stimulation which seemed to stay high during synchronous stimulation. Thus, RGC firing driven by this specific stimulation paradigm may recruit axonal TrkB to suppress axonal branch elimination, whereas in darkness this mechanism is not activated. It is plausible that activity may be required for a fast burst of

BDNF release leading to acute activation of TrkB as described by (Ji et al., 2010), which differs from a sustained mode of TrkB activation related to constitutive BDNF secretion in darkness. Another possibility could be that activity is required for the conversion of proBDNF to mature BDNF, which then could act through TrkB (proposed by Je et al., 2012) to put a break on branch elimination. It is also possible that activity is required for a non-ligand activation of TrkB, as revealed by Huang et al. (2008). An alternative explanation could be that compared to the experiments in Chapter 3, where TrkB was knocked down in a large number of RGC, in Chapter 4, only one or a couple of ipsilaterally projecting axons were electroporated with TrkB-MO, surrounded by a multitude of non-electroporated axons. Since BDNF has a pro-survival role in the retina in *Xenopus laevis* (Cohen-Cory et al., 1996), the axons we imaged might be at a competitive disadvantage to their neighbors. This could explain why we observed an increase in axonal branch elimination uncoupled from changes in axonal branch additions. Finally, it is worth mentioning that the described role of TrkB might be due to activation by not only BDNF, but also by NT-3 or NT-4. Exogenous NT-3 application has been shown to lead to an increase in additions and retractions of short filopodia-like RGC axonal branches in *Xenopus laevis* (Cohen-Cory and Fraser, 1995). Exogenous NT-4 application results in a slight increase in additions of short filopodia-like branches. However, it does not seem to have any effect on light-evoked responses in tectal neurons measured with whole-cell patch clamp recordings. It seems unlikely then that the knockdown of its receptor will produce the same effect as application of NT-3 itself. Unlike BDNF, both NT-3 and NT-4 seem also inert in altering RGC dendrite morphology and just affect the somatic size (Lom and Cohen-Cory, 1999).

To summarize, our first finding in Chapter 4 suggests that BDNF signaling is crucial for Hebbian suppression of branch addition. Considering the fact that knockdown of neither receptor in RGCs phenocopied the main effects of TrkB-Fc application, this synchrony-induced role of BDNF is likely via activation of one of its receptors on the postsynaptic site. Since it is a synchrony-induced effect, it is possible that BDNF signaling is downstream of NMDAR activation in this case. Furthermore, because BDNF-dependent TrkB activation has been shown to promote LTP in the retinotectal system (Du et al., 2009; Schwartz et al., 2011), we propose that the BDNF-dependent Hebbian

suppression of branch addition takes place through activation of postsynaptic TrkB. Sequestering BDNF leads to a decrease in RGC axon elongation during asynchronous stimulation, which may be associated with the role of presynaptic p75NTR described in Chapter 3. The second finding in Chapter 4 which is consistent with the observations in Chapter 3 showing that p75NTR on RGCs promotes axonal branch dynamism, is that possible presynaptic p75NTR signaling is required for the increased exploratory branch additions. Thirdly, presynaptic TrkB signaling participates in suppression of branch elimination under any conditions of neuronal activity regardless of whether it is correlated with neighboring inputs or not.

10.7. Caveats and limitations

10.7.1. Cell-type specificity and subcellular localization of the receptor knockdown

The approach we chose relies on retinal electroporation, which allows for distinguishing the roles of TrkB and p75NTR on RGC and tectal neurons but comes with several drawbacks. Firstly, we are not able to target the knockdown exclusively to the RGC, but any cell in the retina could potentially be randomly electroporated with morpholino. This might affect the retinal circuit locally and lead to alterations in the processing or relaying of visual stimuli to the RGCs and ultimately changing what is passed to the tectal neurons. The lack of control over the cell type specificity of the knockdown should be considered particularly in the interpretation of the results in Chapter 4. Furthermore, within the RGC the knockdown affects both RGC dendrites, soma and axons. It is thus very hard to attribute the observed effects specifically on axonal receptors. It is worth mentioning however, that exogenous BDNF application in the retina does not induce any changes of visually-evoked postsynaptic currents in tectal neurons or any changes in RGC axon arbors (Du and Poo, 2004; Lom et al., 2002). Development of reliable subcellular protein targeting will be crucial to address more rigorously the subcellular localization of p75NTR and TrkB signaling on the RGC.

10.7.2. Long-term developmental changes introduced by the knockdown

We electroporated the morpholino and reared the animals for 3-4 days until imaging. Specifically, in the experiments in which we imaged the RGC over the course of 4 days, it is possible that knockdown of TrkB or p75NTR might have altered the connectivity within the retinal circuit and the observed findings were not due to the direct functions of the receptors themselves. Exogenously applied BDNF has been reported to induce activation of CREB and increase of immediate early genes such as *Arc* (Zhou et al., 2011). It is possible then that our observations are due to an executed genetic program altering the signaling of a myriad of molecular players which could result in the revealed morphological changes. Further rescue experiments in which the receptor of interest is subsequently reintroduced in the RGC are required in order to fully address this caveat.

10.7.3. ICV injections of TrkB-Fc

The administration of TrkB-Fc was performed using ICV injections. Although this is an accepted method when using *Xenopus laevis* as a model organism, it poses a few limitations. It is virtually impossible to estimate the final concentration of the injected pharmacological agent. Precise calculation of the ventricular volume of each animal depends on its specific anatomical properties and it is therefore challenging to estimate the final dilution of the injected drug, and in particular the concentration of active reagent reaching the neurons of interest after diffusion.

Moreover, ICV injection is an invasive procedure which could result in an inflammatory response, likely through microglial activation. It has been reported that in the mouse cortex the turnover rate of dendritic spines was significantly affected depending on whether experiments were done using an open cranial window or thinned-skull preparation (Xu et al., 2007). The greater dynamics of dendritic spines in the open cranial window setup were associated with larger numbers of activated microglia. Data from our group suggest that inflammation may similarly induce changes in RGC axonal branch dynamics (Farooqi, 2016; Solek, Farooqi, Brake, Ruthazer, 2017).

10.7.4. Ipsilaterally projecting RGC axon as a model of the regular projection

As mentioned earlier, amphibians such as the albino *Xenopus laevi*s tadpole provide an excellent animal model to image the developing neural circuit *in vivo*. Their translucency allows for a natural “window” in the brain. However, this same advantage turns into disadvantage when it comes to manipulation of the neural activity in the visual system. Classical optogenetic manipulations using channelrhodopsins, halorhodopsin or archaerhodopsin prove challenging as their activation relies on intense light stimulation. The wavelengths of the light used to activate these channels lie within the visual spectrum, making the use of optogenetics to create specific patterns of activity within the retinotectal system fruitless. Therefore, our lab has utilized the ectopic ipsilaterally projecting RGC to study the effects of patterned activity on circuit refinement. Those RGC are likely not an inherently genetically distinct group of RGC, since they are present in only about 40% of the animals (Munz et al., 2014). However, if the animals are not exposed to a particular visually manipulated environment but are reared in a regular light/dark cycle, the ipsilaterally projecting RGC axons are being exposed to a nearly permanent asynchronous stimulation, as the two eyes of the tadpole always see a different part of the visual field. The regular contralateral projection likely experiences both asynchronous and synchronous firing with its neighbors as it is refining its synapses with tectal neurons. It is therefore possible that this extreme asynchrony that the ipsilaterally projecting RGC neuron lives in, over time results in alterations in transcription programs or connectivity. We therefore cannot be certain that ipsilaterally projecting RGC axons have the same molecular properties as the regular projection. However, our p75NTR data in contralaterally projecting RGC are line with the findings for ipsilaterally projecting RGC.

10.7.5. Semi-automatic axonal tracing

In this study, we used two different software packages to trace the axons. For dynamic imaging, Dynamo developed and provided to us by the group of Dr. Kurt Haas allows for alignment of traces between timepoints. The tracing of the first timepoint is done manually and further manual adjustments are required for the consecutive

timepoints. Imaris, the commercial software product used to trace the daily imaging data has an automatic tracing feature. However, it fails to perfectly trace at the branch points, making it a semi-automatic feature which requires the user to adjust the automatically traced arbor. Both of these software packages rely on the human user to make a decision whether a protrusion of the axon is a branch or not. Manual tracing has been the standard way of quantifying structural imaging data in the field. Although in this study all the axons were traced blind to the experimental design, it is plausible that the subjective nature of the procedure introduced a substantial error influencing the obtained results. The significant advances in computer vision brought by machine learning algorithms will allow for training of a neural network with large number of tracings generated by many human users and hopefully reduce the subjectivity of this quantification procedure in the future.

10.8. Proposed model

Considering the described limitations of the experiments we performed, here we would like to propose a model (Figure 1) encompassing our findings in the context of the existing literature for molecular mechanisms underlying patterned neuronal activity-induced structural remodeling during neural circuit refinement. Many of the components of this model require further investigation to be fully understood.

Neural activity is required to activate possibly presynaptic TrkB to put a brake on axonal branch elimination. NMDAR activation, likely on the postsynaptic neuron, results in either release of mature BDNF, or cleavage (by MMP or tPA) of proBDNF to activate TrkB receptor on the postsynaptic cell. BDNF secretion as either proBDNF or mBDNF in this model could take place in presynaptic, postsynaptic or glial cells. TrkB signaling then leads to secretion or activation of a retrograde messenger (likely more than one specific molecule) which suppresses exploratory branch addition. A default mode of an exploratory branch dynamism exists in darkness. If an axon fires asynchronously with its neighbors, it requires presynaptic p75NTR for an increase in exploratory branch addition in order to find a “proper” postsynaptic partner. Whether p75NTR induces branch addition in a ligand dependent manner, and what the exact ligand is, is still elusive. However, BDNF signaling may now be implicated in asynchrony induced axonal arbor elongation.

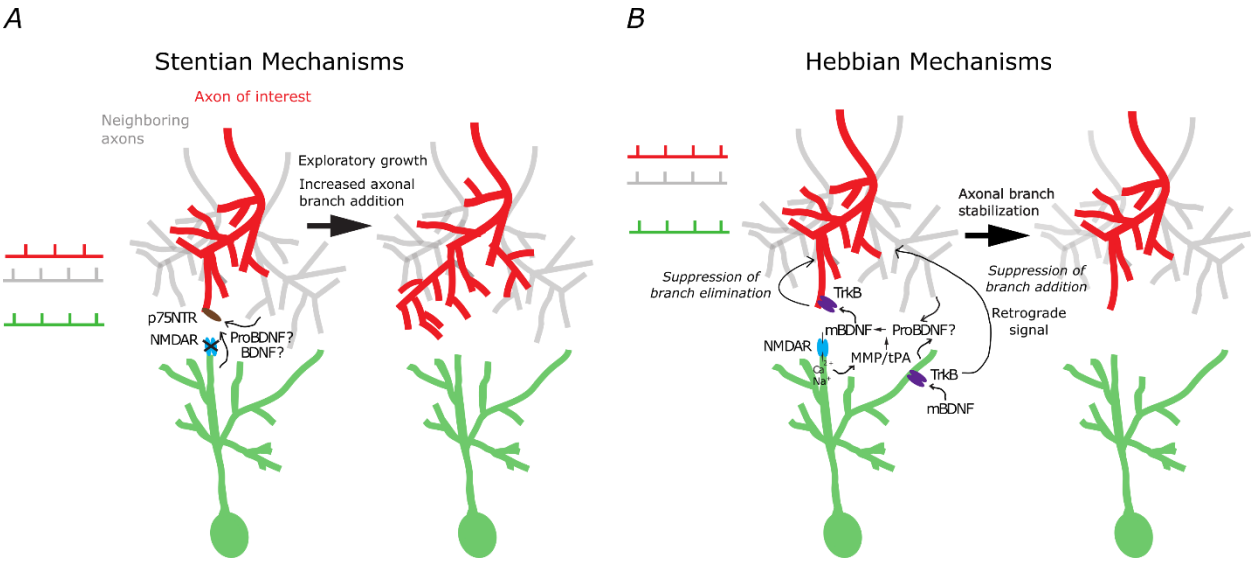

Figure 1. **Proposed model for molecular signaling in Stentian and Hebbian mechanisms in neural circuit refinement**

11. Contributions to Original Knowledge

Our study provides side-by-side comparison between the roles of the two BDNF receptors TrkB and p75NTR on RGC in structural remodeling in the developing retinotectal projection *in vivo.* To our knowledge this is the first time knockdown of the receptors in RGC were used to study short-term RGC axon dynamics in live animals. Although TrkB systemic blockade was previously described to induce synaptic strengthening in *Xenopus laevis* tadpoles, according to our findings, it is more likely that this effect together with the associated stabilization of axonal branches is caused by postsynaptic tectal TrkB, than presynaptic TrkB. We described a novel role of p75NTR in exploratory branch dynamism.

To the best of our knowledge, this is the first attempt to dissect the molecular players underlying patterned activity-induced changes in axonal growth dynamics *in vivo*. Neuronal activity has previously been implicated in BDNF signaling. However, this was done with systemic pharmacological blockade of NMDAR or firing of action of potentials, which proved to have limitations when studying the instructive functions of neuronal activity in the developing neural circuits. Here, we were able to reveal distinct roles of BDNF signaling in synchrony-induced suppression of branch addition and in asynchrony-induced exploratory elongation. Furthermore, we found that RGC TrkB signaling may be activated by any neuronal activity regardless of precise timing to decrease axonal branch eliminations overall.

12. Concluding remarks

"Many cognitive psychologists see the brain as a computer. But every single brain is absolutely individual, both in its development and in the way it encounters the world"

Gerald Edelman, Nobel Prize Laureate
(Interview in Discover Magazine, 2009)

In the history of investigating the mechanisms of brain development, there used to be two opposing hypotheses: one, that all of the mechanisms required for building a brain are encoded in an inherited genetic program; and the other, that brain development depends solely on the specific experience the animal has in its environment. It has become apparent that there is a complex interplay between both genetic and environmental factors which govern how to build the connections between the neurons in the developing brain. It is this very interplay between the specific genetic program we inherit from our parents and the particular environment we live in that makes our brains unique. Consistently, research in recent years has demonstrated that developmental disorders such as autism spectrum disorder and schizophrenia have some genetic components but often also depend on environmental factors.

In this study, we were interested in how the environment impacts neuronal connectivity. In particular, we investigated what molecular signals the neurons in the developing brain use to communicate between each other the experience-evoked patterns of neuronal activity. Although BDNF has previously been implicated in activity-dependent circuit refinement, we provided details on the specific patterns of neuronal activity required to activate particular aspects of BDNF signaling through its receptors TrkB and p75NTR. Furthermore, we gained some insight into the pre- vs. post-synaptic functions of those receptors. Understanding the molecular mechanisms underlying normal experience-dependent development in such detail is crucial for explaining the pathological alterations occurring in developmental disorders.

13. References

Ackman JB, Burbridge TJ, Crair MC (2012) Retinal waves coordinate patterned activity throughout the developing visual system. Nature 490:219–225.

Ackman JB, Crair MC (2014) Role of emergent neural activity in visual map development. Curr Opin Neurobiol 24:166–175.

Adachi N, Kohara K, Tsumoto T (2005) Difference in trafficking of brain-derived neurotrophic factor between axons and dendrites of cortical neurons, revealed by live-cell imaging. BMC Neurosci 6:42.

Aid T, Kazantseva A, Piirsoo M, Palm K, Timmusk T (2007) Mouse and rat BDNF gene structure and expression revisited. J Neurosci Res 85:525–535.

Alderson RF, Curtis R, Alterman AL, Lindsay RM, DiStefano PS (2000) Truncated TrkB mediates the endocytosis and release of BDNF and neurotrophin-4/5 by rat astrocytes and schwann cells in vitro. Brain Res 871:210–222.

Alsina B, Vu T, Cohen-Cory S (2001) Visualizing synapse formation in arborizing optic axons in vivo: dynamics and modulation by BDNF. Nat Neurosci 4:1093–1101.

Altar CA, Cai N, Bliven T, Juhasz M, Conner JM, Acheson AL, Lindsay RM, Wiegand SJ (1997) Anterograde transport of brain-derived neurotrophic factor and its role in the brain. Nature 389:856–860.

Amaral MD, Pozzo-Miller L (2007) TRPC3 channels are necessary for brain-derived neurotrophic factor to activate a nonselective cationic current and to induce dendritic spine formation. J Neurosci 27:5179–5189.

Ambigapathy G, Zheng Z, Keifer J (2015) Regulation of BDNF chromatin status and promoter accessibility in a neural correlate of associative learning. Epigenetics 10:981–993.

Anastasia A, Deinhardt K, Chao MV, Will NE, Irmady K, Lee FS, Hempstead BL, Bracken C (2013) Val66Met polymorphism of BDNF alters prodomain structure to induce neuronal growth cone retraction. Nat Commun 4:2490.

Andreska T, Aufmkolk S, Sauer M, Blum R (2014) High abundance of BDNF within glutamatergic presynapses of cultured hippocampal neurons. Front Cell Neurosci 8:107.

Andrés ME, Burger C, Peral-Rubio MJ, Battaglioli E, Anderson ME, Grimes J, Dallman J, Ballas N, Mandel G (1999) CoREST: a functional corepressor required for regulation of neural-specific gene expression. Proc Natl Acad Sci U S A 96:9873–9878.

An JJ, Gharami K, Liao G-Y, Woo NH, Lau AG, Vanevski F, Torre ER, Jones KR, Feng Y, Lu B, Xu B (2008) Distinct role of long 3' UTR BDNF mRNA in spine morphology and synaptic plasticity in hippocampal neurons. Cell 134:175–187.

Arakawa T, Haniu M, Narhi LO, Miller JA, Talvenheimo J, Philo JS, Chute HT, Matheson C, Carnahan J, Louis JC (1994) Formation of heterodimers from three neurotrophins, nerve growth factor, neurotrophin-3, and brain-derived neurotrophic factor. J Biol Chem 269:27833–27839.

Arimura N, Kimura T, Nakamuta S, Taya S, Funahashi Y, Hattori A, Shimada A, Ménager C, Kawabata S, Fujii K, Iwamatsu A, Segal RA, Fukuda M, Kaibuchi K (2009) Anterograde transport of TrkB in axons is mediated by direct interaction with Slp1 and Rab27. Dev Cell 16:675–686.

Arroyo DA, Feller MB (2016) Spatiotemporal Features of Retinal Waves Instruct the Wiring of the Visual Circuitry. Front Neural Circuits 10:54.

Attardi DG, Sperry RW (1963) Preferential selection of central pathways by regenerating optic fibers. Exp Neurol 7:46–64.

Auer TO, Xiao T, Bercier V, Gebhardt C, Duroure K, Concordet J-P, Wyart C, Suster M, Kawakami K, Wittbrodt J, Baier H, Del Bene F (2015) Deletion of a kinesin I motor unmasks a mechanism of homeostatic branching control by neurotrophin-3. Elife 4: e05061.

Autry AE, Adachi M, Nosyreva E, Na ES, Los MF, Cheng P-F, Kavalali ET, Monteggia LM (2011) NMDA receptor blockade at rest triggers rapid behavioural antidepressant responses. Nature 475:91–95.

Baho E, Chattopadhyaya B, Lavertu-Jolin M, Mazziotti R, Awad PN, Chehrazi P, Groleau M, Jahannault-Talignani C, Vaucher E, Ango F, Pizzorusso T, Baroncelli L, Di Cristo G (2019) p75 Neurotrophin Receptor Activation Regulates the Timing of the Maturation of Cortical Parvalbumin Interneuron Connectivity and Promotes Juvenile-like Plasticity in Adult Visual Cortex. J Neurosci 39:4489–4510.

Baldwin AN, Shooter EM (1995) Zone mapping of the binding domain of the rat low affinity nerve growth factor receptor by the introduction of novel N-glycosylation sites. J Biol Chem 270:4594–4602.

Balkowiec A, Katz DM (2000) Activity-Dependent Release of Endogenous Brain-Derived Neurotrophic Factor from Primary Sensory Neurons Detected by ELISA In Situ. J Neurosci 20:7417–7423.

Balkowiec A, Katz DM (2002) Cellular mechanisms regulating activity-dependent release of native brain-derived neurotrophic factor from hippocampal neurons. J Neurosci 22:10399–10407.

Bamji SX, Majdan M, Pozniak CD, Belliveau DJ, Aloyz R, Kohn J, Causing CG, Miller

FD (1998) The p75 neurotrophin receptor mediates neuronal apoptosis and is essential for naturally occurring sympathetic neuron death. J Cell Biol 140:911–923.

Banerjee A, Larsen RS, Philpot BD, Paulsen O (2016) Roles of Presynaptic NMDA Receptors in Neurotransmission and Plasticity. Trends Neurosci 39:26–39.

Banfield MJ, Naylor RL, Robertson AG, Allen SJ, Dawbarn D, Brady RL (2001) Specificity in Trk receptor:neurotrophin interactions: the crystal structure of TrkB-d5 in complex with neurotrophin-4/5. Structure 9:1191–1199.

Bansal A, Singer JH, Hwang BJ, Xu W (2000) Mice lacking specific nicotinic acetylcholine receptor subunits exhibit dramatically altered spontaneous activity patterns and reveal a limited role for retinal waves in forming ON and OFF circuits in the inner retina. J Neurosci 20:7672-7681.

Baquet ZC, Gorski JA, Jones KR (2004) Early striatal dendrite deficits followed by neuron loss with advanced age in the absence of anterograde cortical brain-derived neurotrophic factor. J Neurosci 24:4250–4258.

Barde YA, Edgar D, Thoenen H (1982) Purification of a new neurotrophic factor from mammalian brain. EMBO J 1:549–553.

Barker PA (2009) Whither proBDNF? Nat Neurosci 12:105–106.

Barnes P, Thomas KL (2008) Proteolysis of proBDNF is a key regulator in the formation of memory. PLoS One 3: e3248.

Bazzini AA, Lee MT, Giraldez AJ (2012) Ribosome profiling shows that miR-430 reduces translation before causing mRNA decay in zebrafish. Science 336:233–237.

Beattie MS, Harrington AW, Lee R, Kim JY, Boyce SL, Longo FM, Bresnahan JC, Hempstead BL, Yoon SO (2002) ProNGF induces p75-mediated death of oligodendrocytes following spinal cord injury. Neuron 36:375–386.

Benito-Gutiérrez E, Garcia-Fernàndez J, Comella JX (2006) Origin and evolution of the Trk family of neurotrophic receptors. Mol Cell Neurosci 31:179–192.

Benjumeda I, Escalante A, Law C, Morales D, Chauvin G, Muça G, Coca Y, Márquez J, López-Bendito G, Kania A, Martínez L, Herrera E (2013) Uncoupling of EphA/ephrinA signaling and spontaneous activity in neural circuit wiring. J Neurosci 33:18208–18218.

Berardi N, Pizzorusso T, Ratto GM, Maffei L (2003) Molecular basis of plasticity in the visual cortex. Trends Neurosci 26:369–378.

Berkemeier LR, Winslow JW, Kaplan DR, Nikolics K, Goeddel DV, Rosenthal A (1991)

Neurotrophin-5: a novel neurotrophic factor that activates trk and trkB. Neuron 7:857–866.

Bertrand T (2017) Crystal Structures of Neurotrophin Receptors Kinase Domain. Vitam Horm 104:1–18.

Besse F, Ephrussi A (2008) Translational control of localized mRNAs: restricting protein synthesis in space and time. Nat Rev Mol Cell Biol 9:971–980.

Bibel M, Hoppe E, Barde YA (1999) Biochemical and functional interactions between the neurotrophin receptors trk and p75NTR. EMBO J 18:616–622.

Bienenstock EL, Cooper LN, Munro PW (1982) Theory for the development of neuron selectivity: orientation specificity and binocular interaction in visual cortex. J Neurosci 2:32–48.

Biffo S, Offenhäuser N, Carter BD, Barde YA (1995) Selective binding and internalisation by truncated receptors restrict the availability of BDNF during development. Development 121:2461–2470.

Boeshore KL, Luckey CN, Zigmond RE, Large TH (1999) TrkB isoforms with distinct neurotrophin specificities are expressed in predominantly nonoverlapping populations of avian dorsal root ganglion neurons. J Neurosci 19:4739–4747.

Bonhoeffer F, Huf J (1980) Recognition of cell types by axonal growth cones in vitro. Nature 288:162–164.

Bothwell M (1995) Functional interactions of neurotrophins and neurotrophin receptors. Annu Rev Neurosci 18:223–253.

Bothwell M (2006) Evolution of the neurotrophin signaling system in invertebrates. Brain Behav Evol 68:124–132.

Bothwell M (2014) NGF, BDNF, NT3, and NT4. In: Neurotrophic Factors (Lewin GR, Carter BD, eds), pp 3–15. Berlin, Heidelberg: Springer Berlin Heidelberg.

Bothwell MA, Shooter EM (1977) Dissociation equilibrium constant of beta nerve growth factor. J Biol Chem 252:8532–8536.

Bredy TW, Wu H, Crego C, Zellhoefer J, Sun YE, Barad M (2007) Histone modifications around individual BDNF gene promoters in prefrontal cortex are associated with extinction of conditioned fear. Learn Mem 14:268–276.

Brennan C, Monschau B, Lindberg R, Guthrie B, Drescher U, Bonhoeffer F, Holder N (1997) Two Eph receptor tyrosine kinase ligands control axon growth and may be involved in the creation of the retinotectal map in the zebrafish. Development 124:655–664.

Brigadski T, Hartmann M, Lessmann V (2005) Differential vesicular targeting and time course of synaptic secretion of the mammalian neurotrophins. J Neurosci 25:7601–7614.

Bronfman FC, Fainzilber M (2004) Multi-tasking by the p75 neurotrophin receptor: sortilin things out? EMBO Rep 5:867–871.

Bucci C, Alifano P, Cogli L (2014) The role of rab proteins in neuronal cells and in the trafficking of neurotrophin receptors. Membranes 4:642–677.

Burbridge TJ, Xu H-P, Ackman JB, Ge X, Zhang Y, Ye M-J, Zhou ZJ, Xu J, Contractor A, Crair MC (2014) Visual circuit development requires patterned activity mediated by retinal acetylcholine receptors. Neuron 84:1049–1064.

Burrill JD, Easter SS Jr (1994) Development of the retinofugal projections in the embryonic and larval zebrafish (Brachydanio rerio). J Comp Neurol 346:583–600.

Butowt R, von Bartheld CS (2007) Conventional kinesin-I motors participate in the anterograde axonal transport of neurotrophins in the visual system. J Neurosci Res 85:2546–2556.

Cabelli RJ, Shelton DL, Segal RA, Shatz CJ (1997) Blockade of endogenous ligands of trkB inhibits formation of ocular dominance columns. Neuron 19:63–76.

Carim-Todd L, Bath KG, Fulgenzi G, Yanpallewar S, Jing D, Barrick CA, Becker J, Buckley H, Dorsey SG, Lee FS, Tessarollo L (2009) Endogenous truncated TrkB.T1 receptor regulates neuronal complexity and TrkB kinase receptor function in vivo. J Neurosci 29:678–685.

Carrasco MM, Razak KA, Pallas SL (2005) Visual experience is necessary for maintenance but not development of receptive fields in superior colliculus. J Neurophysiol 94:1962–1970.

Cattaneo A, Cattane N, Begni V, Pariante CM, Riva MA (2016) The human BDNF gene: peripheral gene expression and protein levels as biomarkers for psychiatric disorders. Transl Psychiatry 6:e958.

Causing CG, Gloster A, Aloyz R, Bamji SX, Chang E, Fawcett J, Kuchel G, Miller FD (1997) Synaptic innervation density is regulated by neuron-derived BDNF. Neuron 18:257–267.

Ceni C, Kommaddi RP, Thomas R, Vereker E, Liu X, McPherson PS, Ritter B, Barker PA (2010) The p75NTR intracellular domain generated by neurotrophin-induced receptor cleavage potentiates Trk signaling. J Cell Sci 123:2299–2307.

Ceni C, Unsain N, Zeinieh MP, Barker PA (2014) Neurotrophins in the Regulation of Cellular Survival and Death. In: Neurotrophic Factors (Lewin GR, Carter BD, eds), pp 193–221. Berlin, Heidelberg: Springer Berlin Heidelberg.

Chandrasekaran AR, Plas DT, Gonzalez E, Crair MC (2005) Evidence for an instructive role of retinal activity in retinotopic map refinement in the superior colliculus of the mouse. J Neurosci 25:6929–6938.

Chang J, Zhang B, Heath H, Galjart N, Wang X, Milbrandt J (2010) Nicotinamide adenine dinucleotide (NAD)-regulated DNA methylation alters CCCTC-binding factor (CTCF)/cohesin binding and transcription at the BDNF locus. Proc Natl Acad Sci U S A 107:21836–21841.

Chao MV (1994) The p75 neurotrophin receptor. J Neurobiol 25:1373–1385.

Chao MV, Bothwell MA, Ross AH, Koprowski H, Lanahan AA, Buck CR, Sehgal A (1986) Gene transfer and molecular cloning of the human NGF receptor. Science 232:518–521.

Chao MV, Hempstead BL (1995) p75 and Trk: a two-receptor system. Trends Neurosci 18:321–326.

Chapman BS (1995) A region of the 75 kDa neurotrophin receptor homologous to the death domains of TNFR-I and Fas. FEBS Lett 374:216–220.

Chen A, Xiong L-J, Tong Y, Mao M (2013) Neuroprotective effect of brain-derived neurotrophic factor mediated by autophagy through the PI3K/Akt/mTOR pathway. Mol Med Rep 8:1011–1016.

Chen H, Weber AJ (2001) BDNF enhances retinal ganglion cell survival in cats with optic nerve damage. Invest Ophthalmol Vis Sci 42:966–974.

Chen SX, Tari PK, She K, Haas K (2010) Neurexin-neuroligin cell adhesion complexes contribute to synaptotropic dendritogenesis via growth stabilization mechanisms in vivo. Neuron 67:967–983.

Chen Z-Y, Ieraci A, Teng H, Dall H, Meng C-X, Herrera DG, Nykjaer A, Hempstead BL, Lee FS (2005) Sortilin controls intracellular sorting of brain-derived neurotrophic factor to the regulated secretory pathway. J Neurosci 25:6156–6166.

Chen Z-Y, Patel PD, Sant G, Meng C-X, Teng KK, Hempstead BL, Lee FS (2004) Variant brain-derived neurotrophic factor (BDNF) (Met66) alters the intracellular trafficking and activity-dependent secretion of wild-type BDNF in neurosecretory cells and cortical neurons. J Neurosci 24:4401–4411.

Cherry M, Williams DH (2004) Recent Kinase and Kinase Inhibitor X-ray Structures: Mechanisms of Inhibition and Selectivity Insights. Curr Med Chem 11:663–673.

Chiaruttini C, Sonego M, Baj G, Simonato M, Tongiorgi E (2008) BDNF mRNA splice variants display activity-dependent targeting to distinct hippocampal laminae. Mol Cell Neurosci 37:11–19.

Chklovskii DB, Mel BW, Svoboda K (2004) Cortical rewiring and information storage. Nature 431:782–788.

Choo M, Miyazaki T, Yamazaki M, Kawamura M, Nakazawa T, Zhang J, Tanimura A, Uesaka N, Watanabe M, Sakimura K, Kano M (2017) Retrograde BDNF to TrkB signaling promotes synapse elimination in the developing cerebellum. Nat Commun 8:195.

Chuang HH, Prescott ED, Kong H, Shields S, Jordt SE, Basbaum AI, Chao MV, Julius D (2001) Bradykinin and nerve growth factor release the capsaicin receptor from PtdIns(4,5)P2-mediated inhibition. Nature 411:957–962.

Cline H, Haas K (2008) The regulation of dendritic arbor development and plasticity by glutamatergic synaptic input: a review of the synaptotrophic hypothesis. J Physiol 586:1509–1517.

Cline HT, Constantine-Paton M (1989) NMDA receptor antagonists disrupt the retinotectal topographic map. Neuron 3:413–426.

Cline HT, Constantine-Paton M (1990) NMDA receptor agonist and antagonists alter retinal ganglion cell arbor structure in the developing frog retinotectal projection. J Neurosci 10:1197–1216.

Cline HT, Debski EA, Constantine-Paton M (1987) N-methyl-D-aspartate receptor antagonist desegregates eye-specific stripes. Proc Natl Acad Sci U S A 84:4342–4345.

Cohen-Cory S (1999) BDNF modulates, but does not mediate, activity-dependent branching and remodeling of optic axon arbors in vivo. J Neurosci 19:9996–10003.

Cohen-Cory S, Escandón E, Fraser SE (1996) The cellular patterns of BDNF and trkB expression suggest multiple roles for BDNF during Xenopus visual system development. Dev Biol 179:102–115.

Cohen-Cory S, Fraser SE (1995) Effects of brain-derived neurotrophic factor on optic axon branching and remodelling in vivo. Nature 378:192–196.

Cohen S, Levi-Montalcini R (1956) A NERVE GROWTH-STIMULATING FACTOR ISOLATED FROM SNAKE VENOM. Proc Natl Acad Sci U S A 42:571–574.

Cohen S, Levi-Montalcini R, Hamburger V (1954) A NERVE GROWTH-STIMULATING FACTOR ISOLATED FROM SARCOM AS 37 AND 180. Proc Natl Acad Sci U S A 40:1014–1018.

Constantine-Paton M, Law MI (1978) Eye-specific termination bands in tecta of three-eyed frogs. Science 202:639–641.

Corlew R, Brasier DJ, Feldman DE, Philpot BD (2008) Presynaptic NMDA receptors:

newly appreciated roles in cortical synaptic function and plasticity. Neuroscientist 14:609–625.

Coupé P, Munz M, Manjón JV, Ruthazer ES, Collins DL (2012) A CANDLE for a deeper in vivo insight. Med Image Anal 16:849–864.

Dean C, Liu H, Dunning FM, Chang PY, Jackson MB, Chapman ER (2009) Synaptotagmin-IV modulates synaptic function and long-term potentiation by regulating BDNF release. Nat Neurosci 12:767–776.

Dechant G, Biffo S, Okazawa H, Kolbeck R, Pottgiesser J, Barde YA (1993) Expression and binding characteristics of the BDNF receptor chick trkB. Development 119:545–558.

Deinhardt K, Chao MV (2014) Trk receptors. Handb Exp Pharmacol 220:103–119.

Demas JA, Payne H, Cline HT (2012) Vision drives correlated activity without patterned spontaneous activity in developing Xenopus retina. Dev Neurobiol 72:537–546.

Dempsey PW, Doyle SE, He JQ, Cheng G (2003) The signaling adaptors and pathways activated by TNF superfamily. Cytokine Growth Factor Rev 14:193–209.

Dhande OS, Hua EW, Guh E, Yeh J, Bhatt S, Zhang Y, Ruthazer ES, Feller MB, Crair MC (2011) Development of single retinofugal axon arbors in normal and β2 knock-out mice. J Neurosci 31:3384–3399.

Di Cristo G, Wu C, Chattopadhyaya B, Ango F, Knott G, Welker E, Svoboda K, Huang ZJ (2004) Subcellular domain-restricted GABAergic innervation in primary visual cortex in the absence of sensory and thalamic inputs. Nat Neurosci 7:1184–1186.

Dieni S, Matsumoto T, Dekkers M, Rauskolb S, Ionescu MS, Deogracias R, Gundelfinger ED, Kojima M, Nestel S, Frotscher M, Barde Y-A (2012) BDNF and its pro-peptide are stored in presynaptic dense core vesicles in brain neurons. J Cell Biol 196:775–788.

Dingwell KS, Holt CE, Harris WA (2000) The multiple decisions made by growth cones of RGCs as they navigate from the retina to the tectum in Xenopus embryos. J Neurobiol 44:246–259.

Di Polo A, Aigner LJ, Dunn RJ, Bray GM, Aguayo AJ (1998) Prolonged delivery of brain-derived neurotrophic factor by adenovirus-infected Müller cells temporarily rescues injured retinal ganglion cells. Proc Natl Acad Sci U S A 95:3978–3983.

DiStefano PS, Chelsea DM, Schick CM, McKelvy JF (1993) Involvement of a metalloprotease in low-affinity nerve growth factor receptor truncation: inhibition of truncation in vitro and in vivo. J Neurosci 13:2405–2414.

Djuranovic S, Nahvi A, Green R (2012) miRNA-mediated gene silencing by translational

repression followed by mRNA deadenylation and decay. Science 336:237–240.

Dong W, Aizenman CD (2012) A competition-based mechanism mediates developmental refinement of tectal neuron receptive fields. J Neurosci 32:16872–16879.

Dong W, Lee RH, Xu H, Yang S, Pratt KG, Cao V, Song Y-K, Nurmikko A, Aizenman CD (2009) Visual avoidance in Xenopus tadpoles is correlated with the maturation of visual responses in the optic tectum. J Neurophysiol 101:803–815.

Dougherty KD, Milner TA (1999) p75NTR immunoreactivity in the rat dentate gyrus is mostly within presynaptic profiles but is also found in some astrocytic and postsynaptic profiles. J Comp Neurol 407:77–91.

Dräger UC, Olsen JF (1980) Origins of crossed and uncrossed retinal projections in pigmented and albino mice. J Comp Neurol 191:383–412.

Drake CT, Milner TA, Patterson SL (1999) Ultrastructural localization of full-length trkB immunoreactivity in rat hippocampus suggests multiple roles in modulating activity-dependent synaptic plasticity. J Neurosci 19:8009–8026.

Drescher U, Bonhoeffer F, Müller BK (1997) The Eph family in retinal axon guidance. Curr Opin Neurobiol 7:75–80.

Drescher U, Kremoser C, Handwerker C, Löschinger J, Noda M, Bonhoeffer F (1995) In vitro guidance of retinal ganglion cell axons by RAGS, a 25 kDa tectal protein related to ligands for Eph receptor tyrosine kinases. Cell 82:359–370.

Du J-L, Poo M-M (2004) Rapid BDNF-induced retrograde synaptic modification in a developing retinotectal system. Nature 429:878–883.

Du J-L, Wei H-P, Wang Z-R, Wong ST, Poo M-M (2009) Long-range retrograde spread of LTP and LTD from optic tectum to retina. Proceedings of the National Academy of Sciences 106:18890–18896.

Easter SS Jr, Taylor JS (1989) The development of the Xenopus retinofugal pathway: optic fibers join a pre-existing tract. Development 107:553–573.

Edelmann E, Cepeda-Prado E, Franck M, Lichtenecker P, Brigadski T, Leßmann V (2015) Theta Burst Firing Recruits BDNF Release and Signaling in Postsynaptic CA1 Neurons in Spike-Timing-Dependent LTP. Neuron 86:1041–1054.

Egan MF, Kojima M, Callicott JH, Goldberg TE, Kolachana BS, Bertolino A, Zaitsev E, Gold B, Goldman D, Dean M, Lu B, Weinberger DR (2003) The BDNF val66met polymorphism affects activity-dependent secretion of BDNF and human memory and hippocampal function. Cell 112:257–269.

Egea J, Klein R (2007) Bidirectional Eph-ephrin signaling during axon guidance. Trends

in Cell Biology 17:230–238.

Farooqi NAI (2016) Early in lammation dysregulates neural circuit formation in vivo via microglial activation and Interleukin 1β. Available at: http://digitool.library.mcgill.ca/webclient/DeliveryManager?pid=145465&custom_att_2=direct.

Fawcett JP, Aloyz R, McLean JH, Pareek S, Miller FD, McPherson PS, Murphy RA (1997) Detection of brain-derived neurotrophic factor in a vesicular fraction of brain synaptosomes. J Biol Chem 272:8837–8840.

Feinstein DL, Larhammar D (1990) Identification of a conserved protein motif in a group of growth factor receptors. FEBS Lett 272:7–11.

Feldheim DA, Kim YI, Bergemann AD, Frisén J, Barbacid M, Flanagan JG (2000) Genetic analysis of ephrin-A2 and ephrin-A5 shows their requirement in multiple aspects of retinocollicular mapping. Neuron 25:563–574.

Feldheim DA, O'Leary DDM (2010) Visual map development: bidirectional signaling, bifunctional guidance molecules, and competition. Cold Spring Harbor perspectives in biology 2 Available at: http://cshperspectives.cshlp.org/content/2/11/a001768.long.

Felleman DJ, Van Essen DC (1991) Distributed hierarchical processing in the primate cerebral cortex. Cereb Cortex 1:1–47.

Feller MB, Wellis DP, Stellwagen D, Werblin FS, Shatz CJ (1996) Requirement for cholinergic synaptic transmission in the propagation of spontaneous retinal waves. Science 272:1182–1187.

Feng D, Kim T, Ozkan E, Light M, Torkin R, Teng KK, Hempstead BL, Garcia KC (2010) Molecular and structural insight into proNGF engagement of p75NTR and sortilin. J Mol Biol 396:967–984.

Fenner BM (2012) Truncated TrkB: beyond a dominant negative receptor. Cytokine Growth Factor Rev 23:15–24.

Figurov A, Pozzo-Miller LD, Olafsson P, Wang T, Lu B (1996) Regulation of synaptic responses to high-frequency stimulation and LTP by neurotrophins in the hippocampus. Nature 381:706–709.

Frade JM, Barde YA (1999) Genetic evidence for cell death mediated by nerve growth factor and the neurotrophin receptor p75 in the developing mouse retina and spinal cord. Development 126:683–690.

Gahtan E, Tanger P, Baier H (2005) Visual prey capture in larval zebrafish is controlled by identified reticulospinal neurons downstream of the tectum. J Neurosci 25:9294–9303.

Garner AS, Menegay HJ, Boeshore KL, Xie XY, Voci JM, Johnson JE, Large TH (1996) Expression of TrkB receptor isoforms in the developing avian visual system. J Neurosci 16:1740–1752.

Gärtner A, Staiger V (2002) Neurotrophin secretion from hippocampal neurons evoked by long-term-potentiation-inducing electrical stimulation patterns. Proc Natl Acad Sci U S A 99:6386–6391.

Gaze RM (1958) THE REPRESENTATION OF THE RETINA ON THE OPTIC LOBE OF THE FROG. Exp Physiol 43:209–214.

Gehler S, Gallo G, Veien E, Letourneau PC (2004) p75 neurotrophin receptor signaling regulates growth cone filopodial dynamics through modulating RhoA activity. J Neurosci 24:4363–4372.

Gene Tools. Custom Morpholinos, Controls and End Modifications. Gene Tools, LLC Available at: http://www.gene-tools.com/custom_morpholinos_controls_endmodifications [Accessed July 19, 2018a].

Gharami K, Das S (2014) BDNF local translation in viable synaptosomes: implication in spine maturation. Neurochem Int 69:28–34.

Gianfranceschi L, Siciliano R, Walls J, Morales B, Kirkwood A, Huang ZJ, Tonegawa S, Maffei L (2003) Visual cortex is rescued from the effects of dark rearing by overexpression of BDNF. Proc Natl Acad Sci U S A 100:12486–12491.

Giehl KM, Schütte A, Mestres P, Yan Q (1998) The survival-promoting effect of glial cell line-derived neurotrophic factor on axotomized corticospinal neurons in vivo is mediated by an endogenous brain-derived neurotrophic factor mechanism. J Neurosci 18:7351–7360.

Gnuegge L, Schmid S, Neuhauss SC (2001) Analysis of the activity-deprived zebrafish mutant macho reveals an essential requirement of neuronal activity for the development of a fine-grained visuotopic map. J Neurosci 21:3542–3548.

Godement P, Salaün J, Imbert M (1984) Prenatal and postnatal development of retinogeniculate and retinocollicular projections in the mouse. J Comp Neurol 230:552–575.

Goldschmidt-Clermont PJ, Kim JW, Machesky LM, Rhee SG, Pollard TD (1991) Regulation of phospholipase C-gamma 1 by profilin and tyrosine phosphorylation. Science 251:1231–1233.

Gong Y, Cao P, Yu H-J, Jiang T (2008) Crystal structure of the neurotrophin-3 and p75NTR symmetrical complex. Nature 454:789–793.

Goodman LJ, Valverde J, Lim F, Geschwind MD, Federoff HJ, Geller AI, Hefti F (1996)

Regulated release and polarized localization of brain-derived neurotrophic factor in hippocampal neurons. Mol Cell Neurosci 7:222–238.

Gorski JA, Zeiler SR, Tamowski S, Jones KR (2003) Brain-derived neurotrophic factor is required for the maintenance of cortical dendrites. J Neurosci 23:6856–6865.

Gosse NJ, Nevin LM, Baier H (2008) Retinotopic order in the absence of axon competition. Nature 452:892–895.

Götz R, Köster R, Winkler C, Raulf F, Lottspeich F, Schartl M, Thoenen H (1994) Neurotrophin-6 is a new member of the nerve growth factor family. Nature 372:266–269.

Graf JD, Kobel HR (1991) Genetics of Xenopus laevis. Methods Cell Biol 36:19–34.

Greer EL, Shi Y (2012) Histone methylation: a dynamic mark in health, disease and inheritance. Nat Rev Genet 13:343–357.

Grimes ML, Zhou J, Beattie EC, Yuen EC, Hall DE, Valletta JS, Topp KS, LaVail JH, Bunnett NW, Mobley WC (1996) Endocytosis of activated TrkA: evidence that nerve growth factor induces formation of signaling endosomes. J Neurosci 16:7950–7964.

Grob PM, Berlot CH, Bothwell MA (1983) Affinity labeling and partial purification of nerve growth factor receptors from rat pheochromocytoma and human melanoma cells. Proc Natl Acad Sci U S A 80:6819–6823.

Grob PM, Ross AH, Koprowski H, Bothwell M (1985) Characterization of the human melanoma nerve growth factor receptor. J Biol Chem 260:8044–8049.

Guan J-S, Haggarty SJ, Giacometti E, Dannenberg J-H, Joseph N, Gao J, Nieland TJF, Zhou Y, Wang X, Mazitschek R, Bradner JE, DePinho RA, Jaenisch R, Tsai L-H (2009) HDAC2 negatively regulates memory formation and synaptic plasticity. Nature 459:55–60.

Guo H, Ingolia NT, Weissman JS, Bartel DP (2010) Mammalian microRNAs predominantly act to decrease target mRNA levels. Nature 466:835–840.

Guo J, Ji Y, Ding Y, Jiang W, Sun Y, Lu B, Nagappan G (2016) BDNF pro-peptide regulates dendritic spines via caspase-3. Cell Death Dis 7:e2264.

Guo W, Nagappan G, Lu B (2018) Differential effects of transient and sustained activation of BDNF-TrkB signaling. Dev Neurobiol 78:647–659.

Haas K, Li J, Cline HT (2006) AMPA receptors regulate experience-dependent dendritic arbor growth in vivo. Proc Natl Acad Sci U S A 103:12127–12131.

Häcker H, Tseng P-H, Karin M (2011) Expanding TRAF function: TRAF3 as a tri-faced

immune regulator. Nat Rev Immunol 11:457–468.

Ha H, Han D, Choi Y (2009) TRAF-mediated TNFR-family signaling. Curr Protoc Immunol Chapter 11:Unit11.9D.

Hahm JO, Cramer KS, Sur M (1999) Pattern formation by retinal afferents in the ferret lateral geniculate nucleus: developmental segregation and the role of N-methyl-D-aspartate receptors. J Comp Neurol 411:327–345.

Hallböök F, Ibáñez CF, Persson H (1991) Evolutionary studies of the nerve growth factor family reveal a novel member abundantly expressed in Xenopus ovary. Neuron 6:845–858.

Hallböök F, Wilson K, Thorndyke M, Olinski RP (2006) Formation and evolution of the chordate neurotrophin and Trk receptor genes. Brain Behav Evol 68:133–144.

Hamburger V (1934) The effects of wing bud extirpation on the development of the central nervous system in chick embryos. J Exp Zool 68:449–494.

Hamburger V (1939) Motor and Sensory Hyperplasia following Limb-Bud Transplantations in Chick Embryos. Physiol Zool 12:268–284.

Hanson PI, Schulman H (1992) Neuronal Ca2+/calmodulin-dependent protein kinases. Annu Rev Biochem 61:559–601.

Harris WA (1984) Axonal pathfinding in the absence of normal pathways and impulse activity. J Neurosci 4:1153–1162.

Hartmann M, Heumann R, Lessmann V (2001) Synaptic secretion of BDNF after high-frequency stimulation of glutamatergic synapses. EMBO J 20:5887–5897.

Harward SC, Hedrick NG, Hall CE, Parra-Bueno P, Milner TA, Pan E, Laviv T, Hempstead BL, Yasuda R, McNamara JO (2016) Autocrine BDNF–TrkB signalling within a single dendritic spine. Nature 538:99.

Haubensak W, Narz F, Heumann R, Lessmann V (1998) BDNF-GFP containing secretory granules are localized in the vicinity of synaptic junctions of cultured cortical neurons. J Cell Sci 111 (Pt 11):1483–1493.

Hebb DO (1949) The Organization of Behavior:A Neuropsychological Theory. New York: John Wiley.

Hellman A, Chess A (2007) Gene body-specific methylation on the active X chromosome. Science 315:1141–1143.

Hempstead BL (2014) Deciphering Proneurotrophin Actions. In: Neurotrophic Factors (Lewin GR, Carter BD, eds), pp 17–32. Berlin, Heidelberg: Springer Berlin Heidelberg.

He X-L, Garcia KC (2004) Structure of nerve growth factor complexed with the shared neurotrophin receptor p75. Science 304:870–875.

Hibbert AP, Kramer BMR, Miller FD, Kaplan DR (2006) The localization, trafficking and retrograde transport of BDNF bound to p75NTR in sympathetic neurons. Mol Cell Neurosci 32:387–402.

Higenell V, Han SM, Feldheim DA, Scalia F, Ruthazer ES (2012) Expression patterns of Ephs and ephrins throughout retinotectal development in Xenopus laevis. Dev Neurobiol 72:547–563.

Hindges R, McLaughlin T, Genoud N, Henkemeyer M, O'Leary DDM (2002) EphB forward signaling controls directional branch extension and arborization required for dorsal-ventral retinotopic mapping. Neuron 35:475–487.

Hiramoto M, Cline HT (2014) Optic flow instructs retinotopic map formation through a spatial to temporal to spatial transformation of visual information. Proc Natl Acad Sci U S A 111:E5105–E5113.

Hofer M, Pagliusi SR, Hohn A, Leibrock J, Barde YA (1990) Regional distribution of brain-derived neurotrophic factor mRNA in the adult mouse brain. EMBO J 9:2459–2464.

Hohn A, Leibrock J, Bailey K, Barde YA (1990) Identification and characterization of a novel member of the nerve growth factor/brain-derived neurotrophic factor family. Nature 344:339–341.

Holt CE, Harris WA (1983) Order in the initial retinotectal map in Xenopus: a new technique for labelling growing nerve fibres. Nature 301:150–152.

Hong EJ, McCord AE, Greenberg ME (2008) A biological function for the neuronal activity-dependent component of Bdnf transcription in the development of cortical inhibition. Neuron 60:610–624.

Hornberger MR, Dütting D, Ciossek T, Yamada T, Handwerker C, Lang S, Weth F, Huf J, Wessel R, Logan C, Tanaka H, Drescher U (1999) Modulation of EphA receptor function by coexpressed ephrinA ligands on retinal ganglion cell axons. Neuron 22:731–742.

Hua JY, Smear MC, Baier H, Smith SJ (2005) Regulation of axon growth in vivo by activity-based competition. Nature 434:1022–1026.

Huang EJ, Reichardt LF (2001) Neurotrophins: roles in neuronal development and function. Annu Rev Neurosci 24:677–736.

Huang EJ, Reichardt LF (2003) Trk receptors: roles in neuronal signal transduction. Annu Rev Biochem 72:609–642.

Huang L, Pallas SL (2001) NMDA antagonists in the superior colliculus prevent developmental plasticity but not visual transmission or map compression. J Neurophysiol 86:1179–1194.

Huang S-H, Duan S, Sun T, Wang J, Zhao L, Geng Z, Yan J, Sun H-J, Chen Z-Y (2011) JIP3 mediates TrkB axonal anterograde transport and enhances BDNF signaling by directly bridging TrkB with kinesin-1. J Neurosci 31:10602–10614.

Huang S-H, Wang J, Sui W-H, Chen B, Zhang X-Y, Yan J, Geng Z, Chen Z-Y (2013) BDNF-dependent recycling facilitates TrkB translocation to postsynaptic density during LTP via a Rab11-dependent pathway. J Neurosci 33:9214–9230.

Huang Y, Myers SJ, Dingledine R (1999a) Transcriptional repression by REST: recruitment of Sin3A and histone deacetylase to neuronal genes. Nat Neurosci 2:867–872.

Huang YZ, Pan E, Xiong Z-Q, McNamara JO (2008) Zinc-mediated transactivation of TrkB potentiates the hippocampal mossy fiber-CA3 pyramid synapse. Neuron 57:546–558.

Huang ZJ, Kirkwood A, Pizzorusso T, Porciatti V, Morales B, Bear MF, Maffei L, Tonegawa S (1999b) BDNF regulates the maturation of inhibition and the critical period of plasticity in mouse visual cortex. Cell 98:739–755.

Hubbard SR, Wei L, Ellis L, Hendrickson WA (1994) Crystal structure of the tyrosine kinase domain of the human insulin receptor. Nature 372:746–754.

Hu B, Nikolakopoulou AM, Cohen-Cory S (2005) BDNF stabilizes synapses and maintains the structural complexity of optic axons in vivo. Development 132:4285–4298.

Hutson LD, Bothwell M (2001) Expression and function of Xenopus laevis p75NTR suggest evolution of developmental regulatory mechanisms. J Neurobiol 49:79–98.

Huynh G, Heinrich G (2001) Brain-derived neurotrophic factor gene organization and transcription in the zebrafish embryo. Int J Dev Neurosci 19:663–673.

Ibáñez CF (1995) Neurotrophic factors: from structure-function studies to designing effective therapeutics. Trends Biotechnol 13:217–227.

Ibáñez CF, Ebendal T, Persson H (1991) Chimeric molecules with multiple neurotrophic activities reveal structural elements determining the specificities of NGF and BDNF. EMBO J 10:2105–2110.

Irvine RF, Letcher AJ, Heslop JP, Berridge MJ (1986) The inositol tris/tetrakisphosphate pathway--demonstration of Ins(1,4,5)P3 3-kinase activity in animal tissues. Nature 320:631–634.

Je HS, Yang F, Ji Y, Nagappan G, Hempstead BL, Lu B (2012) Role of pro-brain-derived neurotrophic factor (proBDNF) to mature BDNF conversion in activity-dependent competition at developing neuromuscular synapses. Proc Natl Acad Sci U S A 109:15924–15929.

Je HS, Yang F, Ji Y, Potluri S, Fu X-Q, Luo Z-G, Nagappan G, Chan JP, Hempstead B, Son Y-J, Lu B (2013) ProBDNF and mature BDNF as punishment and reward signals for synapse elimination at mouse neuromuscular junctions. J Neurosci 33:9957–9962.

Jiang X, Tian F, Du Y, Copeland NG, Jenkins NA, Tessarollo L, Wu X, Pan H, Hu X-Z, Xu K, Kenney H, Egan SE, Turley H, Harris AL, Marini AM, Lipsky RH (2008) BHLHB2 controls Bdnf promoter 4 activity and neuronal excitability. J Neurosci 28:1118–1130.

Ji Y, Lu Y, Yang F, Shen W, Tang TT-T, Feng L, Duan S, Lu B (2010) Acute and gradual increases in BDNF concentration elicit distinct signaling and functions in neurons. Nat Neurosci 13:302–309.

Johnson EM Jr, Taniuchi M, Clark HB, Springer JE, Koh S, Tayrien MW, Loy R (1987) Demonstration of the retrograde transport of nerve growth factor receptor in the peripheral and central nervous system. J Neurosci 7:923–929.

Jungbluth S, Bailey K, Barde YA (1994) Purification and characterisation of a brain-derived neurotrophic factor/neurotrophin-3 (BDNF/NT-3) heterodimer. Eur J Biochem 221:677–685.

Kaethner RJ, Stuermer CA (1992) Dynamics of terminal arbor formation and target approach of retinotectal axons in living zebrafish embryos: a time-lapse study of single axons. J Neurosci 12:3257–3271.

Kaisho Y, Shintani A, Ono Y, Kato K, Igarashi K (1991) Regional expression of the nerve growth factor gene family in rat brain during development. Biochem Biophys Res Commun 174:379–385.

Kaneko M, Stellwagen D, Malenka RC, Stryker MP (2008) Tumor necrosis factor-alpha mediates one component of competitive, experience-dependent plasticity in developing visual cortex. Neuron 58:673–680.

Karlsson M, Hallböök F (1998) Kainic acid, tetrodotoxin and light modulate expression of brain-derived neurotrophic factor in developing avian retinal ganglion cells and their tectal target. Neuroscience 83:137–150.

Karpova NN, Rantamäki T, Di Lieto A, Lindemann L, Hoener MC, Castrén E (2010) Darkness reduces BDNF expression in the visual cortex and induces repressive chromatin remodeling at the BDNF gene in both hippocampus and visual cortex. Cell Mol Neurobiol 30:1117–1123.

Kase H, Iwahashi K, Nakanishi S, Matsuda Y, Yamada K, Takahashi M, Murakata C, Sato A, Kaneko M (1987) K-252 compounds, novel and potent inhibitors of protein kinase C and cyclic nucleotide-dependent protein kinases. Biochem Biophys Res Commun 142:436–440.

Katoh-Semba R, Takeuchi IK, Semba R, Kato K (1997) Distribution of brain-derived neurotrophic factor in rats and its changes with development in the brain. J Neurochem 69:34–42.

Keating MJ, Grant S, Dawes EA, Nanchahal K (1986) Visual deprivation and the maturation of the retinotectal projection in Xenopus laevis. J Embryol Exp Morphol 91:101–115.

Kelleher RJ 3rd, Govindarajan A, Jung H-Y, Kang H, Tonegawa S (2004) Translational control by MAPK signaling in long-term synaptic plasticity and memory. Cell 116:467–479.

Kenchappa RS, Zampieri N, Chao MV, Barker PA, Teng HK, Hempstead BL, Carter BD (2006) Ligand-dependent cleavage of the P75 neurotrophin receptor is necessary for NRIF nuclear translocation and apoptosis in sympathetic neurons. Neuron 50:219–232.

Kerschensteiner D (2016) Glutamatergic Retinal Waves. Front Neural Circuits 10:38.

Khursigara G, Orlinick JR, Chao MV (1999) Association of the p75 neurotrophin receptor with TRAF6. J Biol Chem 274:2597–2600.

Kidane AH, Heinrich G, Dirks RPH, de Ruyck BA, Lubsen NH, Roubos EW, Jenks BG (2009) Differential neuroendocrine expression of multiple brain-derived neurotrophic factor transcripts. Endocrinology 150:1361–1368.

Kita EM, Scott EK, Goodhill GJ (2015) Topographic wiring of the retinotectal connection in zebrafish. Dev Neurobiol 75:542–556.

Klee CB, Draetta GF, Hubbard MJ (1988) Calcineurin. Adv Enzymol Relat Areas Mol Biol 61:149–200.

Kohara K, Kitamura A, Morishima M, Tsumoto T (2001) Activity-dependent transfer of brain-derived neurotrophic factor to postsynaptic neurons. Science 291:2419–2423.

Kojima M, Takei N, Numakawa T, Ishikawa Y, Suzuki S, Matsumoto T, Katoh-Semba R, Nawa H, Hatanaka H (2001) Biological characterization and optical imaging of brain-derived neurotrophic factor-green fluorescent protein suggest an activity-dependent local release of brain-derived neurotrophic factor in neurites of cultured hippocampal neurons. J Neurosci Res 64:1–10.

Kononenko NL, Claßen GA, Kuijpers M, Puchkov D, Maritzen T, Tempes A, Malik AR, Skalecka A, Bera S, Jaworski J, Haucke V (2017) Retrograde transport of TrkB-

containing autophagosomes via the adaptor AP-2 mediates neuronal complexity and prevents neurodegeneration. Nat Commun 8:14819.

Kornau HC, Schenker LT, Kennedy MB, Seeburg PH (1995) Domain interaction between NMDA receptor subunits and the postsynaptic density protein PSD-95. Science 269:1737–1740.

Korte M, Carroll P, Wolf E, Brem G, Thoenen H, Bonhoeffer T (1995) Hippocampal long-term potentiation is impaired in mice lacking brain-derived neurotrophic factor. Proc Natl Acad Sci U S A 92:8856–8860.

Korte M, Griesbeck O, Gravel C, Carroll P, Staiger V, Thoenen H, Bonhoeffer T (1996) Virus-mediated gene transfer into hippocampal CA1 region restores long-term potentiation in brain-derived neurotrophic factor mutant mice. Proc Natl Acad Sci U S A 93:12547–12552.

Koshimizu H, Kiyosue K, Hara T, Hazama S, Suzuki S, Uegaki K, Nagappan G, Zaitsev E, Hirokawa T, Tatsu Y, Ogura A, Lu B, Kojima M (2009) Multiple functions of precursor BDNF to CNS neurons: negative regulation of neurite growth, spine formation and cell survival. Mol Brain 2:27.

Kovalchuk Y, Hanse E, Kafitz KW, Konnerth A (2002) Postsynaptic Induction of BDNF-Mediated Long-Term Potentiation. Science 295:1729–1734.

Kubo F, Hablitzel B, Dal Maschio M, Driever W, Baier H, Arrenberg AB (2014) Functional architecture of an optic flow-responsive area that drives horizontal eye movements in zebrafish. Neuron 81:1344–1359.

Kuczewski N, Porcher C, Ferrand N, Fiorentino H, Pellegrino C, Kolarow R, Lessmann V, Medina I, Gaiarsa J-L (2008) Backpropagating action potentials trigger dendritic release of BDNF during spontaneous network activity. J Neurosci 28:7013–7023.

Lachner M, Jenuwein T (2002) The many faces of histone lysine methylation. Curr Opin Cell Biol 14:286–298.

Lamballe F, Klein R, Barbacid M (1991) trkC, a new member of the trk family of tyrosine protein kinases, is a receptor for neurotrophin-3. Cell 66:967–979.

Land PW, Lund RD (1979) Development of the rat's uncrossed retinotectal pathway and its relation to plasticity studies. Science 205:698–700.

Lan JY, Skeberdis VA, Jover T, Grooms SY, Lin Y, Araneda RC, Zheng X, Bennett MV, Zukin RS (2001) Protein kinase C modulates NMDA receptor trafficking and gating. Nat Neurosci 4:382–390.

Large TH, Weskamp G, Helder JC, Radeke MJ, Misko TP, Shooter EM, Reichardt LF (1989) Structure and developmental expression of the nerve growth factor receptor in the chicken central nervous system. Neuron 2:1123–1134.

Lau AG, Irier HA, Gu J, Tian D, Ku L, Liu G, Xia M, Fritsch B, Zheng JQ, Dingledine R, Xu B, Lu B, Feng Y (2010) Distinct 3'UTRs differentially regulate activity-dependent translation of brain-derived neurotrophic factor (BDNF). Proc Natl Acad Sci U S A 107:15945–15950.

Lee R, Kermani P, Teng KK, Hempstead BL (2001) Regulation of cell survival by secreted proneurotrophins. Science 294:1945–1948.

Leibrock J, Lottspeich F, Hohn A, Hofer M, Hengerer B, Masiakowski P, Thoenen H, Barde YA (1989) Molecular cloning and expression of brain-derived neurotrophic factor. Nature 341:149–152.

Lessmann V, Brigadski T (2009) Mechanisms, locations, and kinetics of synaptic BDNF secretion: an update. Neurosci Res 65:11–22.

Levi-Montalcini R (1965) TISSUE AND NERVE GROWTH PROMOTING FACTORS. BIOLOGICAL ASPECTS OF SPECIFIC GROWTH PROMOTING FACTORS. Proc R Soc Med 58:357–360.

Levi-Montalcini R, Booker B (1960) DESTRUCTION OF THE SYMPATHETIC GANGLIA IN MAMMALS BY AN ANTISERUM TO A NERVE-GROWTH PROTEIN. Proc Natl Acad Sci U S A 46:384–391.

Levi-Montalcini R, Cohen S (1956) IN VITRO AND IN VIVO EFFECTS OF A NERVE GROWTH-STIMULATING AGENT ISOLATED FROM SNAKE VENOM. Proc Natl Acad Sci U S A 42:695–699.

Levine RL, Jacobson M (1975) Discontinuous mapping of retina onto tectum innervated by both eyes. Brain Res 98:172–176.

Lewin GR, Barde YA (1996) Physiology of the neurotrophins. Annu Rev Neurosci 19:289–317.

Liepinsh E, Ilag LL, Otting G, Ibáñez CF (1997) NMR structure of the death domain of the p75 neurotrophin receptor. EMBO J 16:4999–5005.

Linden DC, Guillery RW, Cucchiaro J (1981) The dorsal lateral geniculate nucleus of the normal ferret and its postnatal development. J Comp Neurol 203:189–211.

Lindskog M, Li L, Groth RD, Poburko D, Thiagarajan TC, Han X, Tsien RW (2010) Postsynaptic GluA1 enables acute retrograde enhancement of presynaptic function to coordinate adaptation to synaptic inactivity. Proc Natl Acad Sci U S A 107:21806–21811.

Lipsky RH, Xu K, Zhu D, Kelly C, Terhakopian A, Novelli A, Marini AM (2001) Nuclear factor kappaB is a critical determinant in N-methyl-D-aspartate receptor-mediated neuroprotection. J Neurochem 78:254–264.

Li Y, Jia Y-C, Cui K, Li N, Zheng Z-Y, Wang Y-Z, Yuan X-B (2005) Essential role of TRPC channels in the guidance of nerve growth cones by brain-derived neurotrophic factor. Nature 434:894–898.

Lom B, Cogen J, Sanchez AL, Vu T, Cohen-Cory S (2002) Local and target-derived brain-derived neurotrophic factor exert opposing effects on the dendritic arborization of retinal ganglion cells in vivo. J Neurosci 22:7639–7649.

Lom B, Cohen-Cory S (1999) Brain-derived neurotrophic factor differentially regulates retinal ganglion cell dendritic and axonal arborization in vivo. J Neurosci 19:9928–9938.

Lou H, Kim S-K, Zaitsev E, Snell CR, Lu B, Loh YP (2005) Sorting and activity-dependent secretion of BDNF require interaction of a specific motif with the sorting receptor carboxypeptidase e. Neuron 45:245–255.

Luberg K, Wong J, Weickert CS, Timmusk T (2010) Human TrkB gene: novel alternative transcripts, protein isoforms and expression pattern in the prefrontal cerebral cortex during postnatal development. J Neurochem 113:952–964.

Lubin FD, Roth TL, Sweatt JD (2008) Epigenetic regulation of BDNF gene transcription in the consolidation of fear memory. J Neurosci 28:10576–10586.

Ma B, Savas JN, Chao MV, Tanese N (2012) Quantitative analysis of BDNF/TrkB protein and mRNA in cortical and striatal neurons using α-tubulin as a normalization factor. Cytometry A 81:704–717.

Maffei L, Galli-Resta L (1990) Correlation in the discharges of neighboring rat retinal ganglion cells during prenatal life. Proc Natl Acad Sci U S A 87:2861–2864.

Maisonpierre PC, Belluscio L, Friedman B, Alderson RF, Wiegand SJ, Furth ME, Lindsay RM, Yancopoulos GD (1990a) NT-3, BDNF, and NGF in the developing rat nervous system: parallel as well as reciprocal patterns of expression. Neuron 5:501–509.

Maisonpierre PC, Belluscio L, Squinto S, Ip NY, Furth ME, Lindsay RM, Yancopoulos GD (1990b) Neurotrophin-3: a neurotrophic factor related to NGF and BDNF. Science 247:1446–1451.

Mann F, Ray S, Harris W, Holt C (2002) Topographic mapping in dorsoventral axis of the Xenopus retinotectal system depends on signaling through ephrin-B ligands. Neuron 35:461–473.

Marcinkiewicz M, Savaria D, Marcinkiewicz J (1998) The pro-protein convertase PC1 is induced in the transected sciatic nerve and is present in cultured Schwann cells: comparison with PC5, furin and PC7, implication in pro-BDNF processing. Brain Res Mol Brain Res 59:229–246.

Marcus RC, Gale NW, Morrison ME, Mason CA, Yancopoulos GD (1996) Eph family receptors and their ligands distribute in opposing gradients in the developing mouse retina. Dev Biol 180:786–789.

Marshak S, Nikolakopoulou AM, Dirks R, Martens GJ, Cohen-Cory S (2007) Cell-autonomous TrkB signaling in presynaptic retinal ganglion cells mediates axon arbor growth and synapse maturation during the establishment of retinotectal synaptic connectivity. J Neurosci 27:2444–2456.

Martinowich K, Hattori D, Wu H, Fouse S, He F, Hu Y, Fan G, Sun YE (2003) DNA methylation-related chromatin remodeling in activity-dependent BDNF gene regulation. Science 302:890–893.

Mathew SJ, Haubert D, Krönke M, Leptin M (2009) Looking beyond death: a morphogenetic role for the TNF signalling pathway. J Cell Sci 122:1939–1946.

Matsuda N, Lu H, Fukata Y, Noritake J, Gao H, Mukherjee S, Nemoto T, Fukata M, Poo M-M (2009) Differential activity-dependent secretion of brain-derived neurotrophic factor from axon and dendrite. J Neurosci 29:14185–14198.

Maynard KR, Hobbs JW, Sukumar M, Kardian AS, Jimenez DV, Schloesser RJ, Martinowich K (2017) Bdnf mRNA splice variants differentially impact CA1 and CA3 dendrite complexity and spine morphology in the hippocampus. Brain Struct Funct 222:3295–3307.

McDonald NQ, Hendrickson WA (1993) A structural superfamily of growth factors containing a cystine knot motif. Cell 73:421–424.

McDonald NQ, Lapatto R, Murray-Rust J, Gunning J, Wlodawer A, Blundell TL (1991) New protein fold revealed by a 2.3-A resolution crystal structure of nerve growth factor. Nature 354:411–414.

McLaughlin T, Hindges R, Yates PA, O'Leary DDM (2003a) Bifunctional action of ephrin-B1 as a repellent and attractant to control bidirectional branch extension in dorsal-ventral retinotopic mapping. Development 130:2407–2418.

McLaughlin T, Torborg CL, Feller MB, O'Leary DDM (2003b) Retinotopic map refinement requires spontaneous retinal waves during a brief critical period of development. Neuron 40:1147–1160.

McLoon SC, Lund RD (1982) Transient retinofugal pathways in the developing chick. Exp Brain Res 45:277–284.

Meabon JS, De Laat R, Ieguchi K, Wiley JC, Hudson MP, Bothwell M (2015) LINGO-1 protein interacts with the p75 neurotrophin receptor in intracellular membrane compartments. J Biol Chem 290:9511–9520.

Meissner A, Mikkelsen TS, Gu H, Wernig M, Hanna J, Sivachenko A, Zhang X,

Bernstein BE, Nusbaum C, Jaffe DB, Gnirke A, Jaenisch R, Lander ES (2008) Genome-scale DNA methylation maps of pluripotent and differentiated cells. Nature 454:766–770.

Meister M, Wong RO, Baylor DA, Shatz CJ (1991) Synchronous bursts of action potentials in ganglion cells of the developing mammalian retina. Science 252:939–943.

Mellios N, Huang H-S, Grigorenko A, Rogaev E, Akbarian S (2008) A set of differentially expressed miRNAs, including miR-30a-5p, act as post-transcriptional inhibitors of BDNF in prefrontal cortex. Hum Mol Genet 17:3030–3042.

Metsis M, Timmusk T, Arenas E, Persson H (1993) Differential usage of multiple brain-derived neurotrophic factor promoters in the rat brain following neuronal activation. Proc Natl Acad Sci U S A 90:8802–8806.

Meyer MP, Smith SJ (2006) Evidence from in vivo imaging that synaptogenesis guides the growth and branching of axonal arbors by two distinct mechanisms. J Neurosci 26:3604–3614.

Meyer RL (1983) Tetrodotoxin inhibits the formation of refined retinotopography in goldfish. Brain Res 282:293–298.

Meyer RL, Wolcott LL (1987) Compression and expansion without impulse activity in the retinotectal projection of goldfish. J Neurobiol 18:549–567.

Middlemas DS, Lindberg RA, Hunter T (1991) trkB, a neural receptor protein-tyrosine kinase: evidence for a full-length and two truncated receptors. Mol Cell Biol 11:143–153.

Minichiello L, Calella AM, Medina DL, Bonhoeffer T, Klein R, Korte M (2002) Mechanism of TrkB-mediated hippocampal long-term potentiation. Neuron 36:121–137.

Mi S, Lee X, Shao Z, Thill G, Ji B, Relton J, Levesque M, Allaire N, Perrin S, Sands B, Crowell T, Cate RL, McCoy JM, Pepinsky RB (2004) LINGO-1 is a component of the Nogo-66 receptor/p75 signaling complex. Nat Neurosci 7:221–228.

Miyazaki S (1988) Inositol 1,4,5-trisphosphate-induced calcium release and guanine nucleotide-binding protein-mediated periodic calcium rises in golden hamster eggs. J Cell Biol 106:345–353.

Mizui T, Ishikawa Y, Kumanogoh H, Lume M, Matsumoto T, Hara T, Yamawaki S, Takahashi M, Shiosaka S, Itami C, Uegaki K, Saarma M, Kojima M (2015) BDNF pro-peptide actions facilitate hippocampal LTD and are altered by the common BDNF polymorphism Val66Met. Proc Natl Acad Sci U S A 112:E3067–E3074.

Mok S-A, Lund K, Lapointe P, Campenot RB (2013) A HaloTag® method for assessing

the retrograde axonal transport of the p75 neurotrophin receptor and other proteins in compartmented cultures of rat sympathetic neurons. J Neurosci Methods 214:91–104.

Monschau B, Kremoser C, Ohta K, Tanaka H, Kaneko T, Yamada T, Handwerker C, Hornberger MR, Löschinger J, Pasquale EB, Siever DA, Verderame MF, Müller BK, Bonhoeffer F, Drescher U (1997) Shared and distinct functions of RAGS and ELF-1 in guiding retinal axons. EMBO J 16:1258–1267.

Moore H-PH, Carnell L, Chavez RA, Chen Y-T, Hwang A, Miller SG, Yoon Y-A, Yu H (1993) Regulated and Constitutive Secretion Studied In Vitro: Control by GTPases at Multiple Levels. In: GTPases in Biology I (Dickey BF, Birnbaumer L, eds), pp 507–528. Berlin, Heidelberg: Springer Berlin Heidelberg.

Mowla SJ, Farhadi HF, Pareek S, Atwal JK, Morris SJ, Seidah NG, Murphy RA (2001) Biosynthesis and post-translational processing of the precursor to brain-derived neurotrophic factor. J Biol Chem 276:12660–12666.

Mowla SJ, Pareek S, Farhadi HF, Petrecca K, Fawcett JP, Seidah NG, Morris SJ, Sossin WS, Murphy RA (1999) Differential sorting of nerve growth factor and brain-derived neurotrophic factor in hippocampal neurons. J Neurosci 19:2069–2080.

Mrsic-Flogel TD, Hofer SB, Creutzfeldt C, Cloëz-Tayarani I, Changeux J-P, Bonhoeffer T, Hübener M (2005) Altered map of visual space in the superior colliculus of mice lacking early retinal waves. J Neurosci 25:6921–6928.

Munz M, Gobert D, Schohl A, Poquérusse J, Podgorski K, Spratt P, Ruthazer ES (2014) Rapid Hebbian axonal remodeling mediated by visual stimulation. Science 344:904–909.

Murray SS, Bartlett PF, Cheema SS (1999) Differential loss of spinal sensory but not motor neurons in the p75NTR knockout mouse. Neurosci Lett 267:45–48.

Mu Y, Poo M-M (2006) Spike timing-dependent LTP/LTD mediates visual experience-dependent plasticity in a developing retinotectal system. Neuron 50:115–125.

Myers SM, Ross GM, Dostaler SM, Anderson MN, Weaver DF, Riopelle RJ (1994) Putative cytoplasmic amphiphilic domains in the nerve growth factor/tumour necrosis factor receptor superfamily. Biochim Biophys Acta 1196:21–28.

Nakamura H, O'Leary DD (1989) Inaccuracies in initial growth and arborization of chick retinotectal axons followed by course corrections and axon remodeling to develop topographic order. J Neurosci 9:3776–3795.

Nevin LM, Taylor MR, Baier H (2008) Hardwiring of fine synaptic layers in the zebrafish visual pathway. Neural Dev 3:36.

Niculescu D, Michaelsen-Preusse K, Güner Ü, van Dorland R, Wierenga CJ, Lohmann C (2018) A BDNF-Mediated Push-Pull Plasticity Mechanism for Synaptic Clustering. Cell Rep 24:2063–2074.

Niell CM, Meyer MP, Smith SJ (2004) In vivo imaging of synapse formation on a growing dendritic arbor. Nat Neurosci 7:254–260.

Nieuwkoop PD, Faber J eds. (1994) Normal table of Xenopus laevis (Daudin): a systematical and chronological survey of the development from the fertilized egg till the end of metamorphosis. New York: Garland Pub.

Nilsson AS, Fainzilber M, Falck P, Ibáñez CF (1998) Neurotrophin-7: a novel member of the neurotrophin family from the zebrafish. FEBS Lett 424:285–290.

Noble MEM, Endicott JA, Johnson LN (2004) Protein kinase inhibitors: insights into drug design from structure. Science 303:1800–1805.

Nowak L, Bregestovski P, Ascher P, Herbet A, Prochiantz A (1984) Magnesium gates glutamate-activated channels in mouse central neurones. Nature 307:462–465.

Nykjaer A, Lee R, Teng KK, Jansen P, Madsen P, Nielsen MS, Jacobsen C, Kliemannel M, Schwarz E, Willnow TE, Hempstead BL, Petersen CM (2004) Sortilin is essential for proNGF-induced neuronal cell death. Nature 427:843–848.

Obermeier A, Bradshaw RA, Seedorf K, Choidas A, Schlessinger J, Ullrich A (1994) Neuronal differentiation signals are controlled by nerve growth factor receptor/Trk binding sites for SHC and PLC gamma. EMBO J 13:1585–1590.

Oe S, Miki H, Nishimura W, Noda Y (2016) Mechanism of the Dendritic Translation and Localization of Brain-derived Neurotrophic Factor. Cell Struct Funct 41:23–31.

Oe S, Yoneda Y (2010) Cytoplasmic polyadenylation element-like sequences are involved in dendritic targeting of BDNF mRNA in hippocampal neurons. FEBS Lett 584:3424–3430.

Ohira K, Kumanogoh H, Sahara Y, Homma KJ, Hirai H, Nakamura S, Hayashi M (2005) A truncated tropomyosin-related kinase B receptor, T1, regulates glial cell morphology via Rho GDP dissociation inhibitor 1. J Neurosci 25:1343–1353.

Olson MD, Meyer RL (1991) The effect of TTX-activity blockade and total darkness on the formation of retinotopy in the goldfish retinotectal projection. J Comp Neurol 303:412–423.

Orefice LL, Shih C-C, Xu H, Waterhouse EG, Xu B (2016) Control of spine maturation and pruning through proBDNF synthesized and released in dendrites. Mol Cell Neurosci 71:66–79.

Orefice LL, Waterhouse EG, Partridge JG, Lalchandani RR, Vicini S, Xu B (2013)

Distinct roles for somatically and dendritically synthesized brain-derived neurotrophic factor in morphogenesis of dendritic spines. J Neurosci 33:11618–11632.

O'Rourke NA, Fraser SE (1990) Dynamic changes in optic fiber terminal arbors lead to retinotopic map formation: an in vivo confocal microscopic study. Neuron 5:159–171.

Palm K, Belluardo N, Metsis M, Timmusk T (1998) Neuronal expression of zinc finger transcription factor REST/NRSF/XBR gene. J Neurosci 18:1280–1296.

Palomer E, Carretero J, Benvegnù S, Dotti CG, Martin MG (2016) Neuronal activity controls Bdnf expression via Polycomb de-repression and CREB/CBP/JMJD3 activation in mature neurons. Nat Commun 7:11081.

Pang PT, Teng HK, Zaitsev E, Woo NT, Sakata K, Zhen S, Teng KK, Yung W-H, Hempstead BL, Lu B (2004) Cleavage of proBDNF by tPA/plasmin is essential for long-term hippocampal plasticity. Science 306:487–491.

Park H, Poo M-M (2013) Neurotrophin regulation of neural circuit development and function. Nat Rev Neurosci 14:7–23.

Pattabiraman PP, Tropea D, Chiaruttini C, Tongiorgi E, Cattaneo A, Domenici L (2005) Neuronal activity regulates the developmental expression and subcellular localization of cortical BDNF mRNA isoforms in vivo. Mol Cell Neurosci 28:556–570.

Patterson SL, Abel T, Deuel TA, Martin KC, Rose JC, Kandel ER (1996) Recombinant BDNF rescues deficits in basal synaptic transmission and hippocampal LTP in BDNF knockout mice. Neuron 16:1137–1145.

Petros TJ, Rebsam A, Mason CA (2008) Retinal axon growth at the optic chiasm: to cross or not to cross. Annu Rev Neurosci 31:295–315.

Phenotypes associated with Ngfr/Ngfr. Alliance of Genome Resources. Available at: http://www.informatics.jax.org/diseasePortal/genoCluster/view/5099.

Plas DT, Lopez JE, Crair MC (2005) Pretarget sorting of retinocollicular axons in the mouse. J Comp Neurol 491:305–319.

Pratt KG, Aizenman CD (2007) Homeostatic regulation of intrinsic excitability and synaptic transmission in a developing visual circuit. J Neurosci 27:8268–8277.

Pratt KG, Hiramoto M, Cline HT (2016) An Evolutionarily Conserved Mechanism for Activity-Dependent Visual Circuit Development. Front Neural Circuits 10:79.

Proenca CC, Song M, Lee FS (2016) Differential effects of BDNF and neurotrophin 4 (NT4) on endocytic sorting of TrkB receptors. J Neurochem 138:397–406.

Pruunsild P, Kazantseva A, Aid T, Palm K, Timmusk T (2007) Dissecting the human BDNF locus: bidirectional transcription, complex splicing, and multiple promoters. Genomics 90:397–406.

Pruunsild P, Sepp M, Orav E, Koppel I, Timmusk T (2011) Identification of cis-elements and transcription factors regulating neuronal activity-dependent transcription of human BDNF gene. J Neurosci 31:3295–3308.

Radeke MJ, Misko TP, Hsu C, Herzenberg LA, Shooter EM (1987) Gene transfer and molecular cloning of the rat nerve growth factor receptor. Nature 325:593–597.

Radziejewski C, Robinson RC, DiStefano PS, Taylor JW (1992) Dimeric structure and conformational stability of brain-derived neurotrophic factor and neurotrophin-3. Biochemistry 31:4431–4436.

Rajan I, Witte S, Cline HT (1999) NMDA receptor activity stabilizes presynaptic retinotectal axons and postsynaptic optic tectal cell dendrites in vivo. J Neurobiol 38:357–368.

Ramakers GM, Pasinelli P, Hens JJ, Gispen WH, De Graan PN (1997) Protein kinase C in synaptic plasticity: changes in the in situ phosphorylation state of identified pre- and postsynaptic substrates. Prog Neuropsychopharmacol Biol Psychiatry 21:455–486.

Raper JA, Grunewald EB (1990) Temporal retinal growth cones collapse on contact with nasal retinal axons. Exp Neurol 109:70–74.

Rashid T, Upton AL, Blentic A, Ciossek T, Knöll B, Thompson ID, Drescher U (2005) Opposing gradients of ephrin-As and EphA7 in the superior colliculus are essential for topographic mapping in the mammalian visual system. Neuron 47:57–69.

Reber M, Burrola P, Lemke G (2004) A relative signalling model for the formation of a topographic neural map. Nature 431:847–853.

Reh TA, Constantine-Paton M (1985) Eye-specific segregation requires neural activity in three-eyed Rana pipiens. J Neurosci 5:1132–1143.

Reichardt LF (2006) Neurotrophin-regulated signalling pathways. Philos Trans R Soc Lond B Biol Sci 361:1545–1564.

Robinson RC, Radziejewski C, Spraggon G, Greenwald J, Kostura MR, Burtnick LD, Stuart DI, Choe S, Jones EY (1999) The structures of the neurotrophin 4 homodimer and the brain-derived neurotrophic factor/neurotrophin 4 heterodimer reveal a common Trk-binding site. Protein Sci 8:2589–2597.

Robinson RC, Radziejewski C, Stuart DI, Jones EY (1995) Structure of the brain-derived neurotrophic factor/neurotrophin 3 heterodimer. Biochemistry 34:4139–4146.

Rodriguez-Tébar A, Barde YA (1988) Binding characteristics of brain-derived neurotrophic factor to its receptors on neurons from the chick embryo. J Neurosci 8:3337–3342.

Rodríguez-Tébar A, Dechant G, Götz R, Barde YA (1992) Binding of neurotrophin-3 to its neuronal receptors and interactions with nerve growth factor and brain-derived neurotrophic factor. EMBO J 11:917–922.

Roh T-Y, Ngau WC, Cui K, Landsman D, Zhao K (2004) High-resolution genome-wide mapping of histone modifications. Nat Biotechnol 22:1013–1016.

Rösch H, Schweigreiter R, Bonhoeffer T, Barde Y-A, Korte M (2005) The neurotrophin receptor p75NTR modulates long-term depression and regulates the expression of AMPA receptor subunits in the hippocampus. Proc Natl Acad Sci U S A 102:7362–7367.

Ross AH, Grob P, Bothwell M, Elder DE, Ernst CS, Marano N, Ghrist BF, Slemp CC, Herlyn M, Atkinson B (1984) Characterization of nerve growth factor receptor in neural crest tumors using monoclonal antibodies. Proc Natl Acad Sci U S A 81:6681–6685.

Rossi FM, Pizzorusso T, Porciatti V, Marubio LM, Maffei L, Changeux JP (2001) Requirement of the nicotinic acetylcholine receptor beta 2 subunit for the anatomical and functional development of the visual system. Proc Natl Acad Sci U S A 98:6453–6458.

Roth TL, Lubin FD, Funk AJ, Sweatt JD (2009) Lasting epigenetic influence of early-life adversity on the BDNF gene. Biol Psychiatry 65:760–769.

Roth TL, Matt S, Chen K, Blaze J (2014) Bdnf DNA methylation modifications in the hippocampus and amygdala of male and female rats exposed to different caregiving environments outside the homecage. Dev Psychobiol 56:1755–1763.

Rouillé Y, Duguay SJ, Lund K, Furuta M, Gong Q, Lipkind G, Oliva AA Jr, Chan SJ, Steiner DF (1995) Proteolytic processing mechanisms in the biosynthesis of neuroendocrine peptides: the subtilisin-like proprotein convertases. Front Neuroendocrinol 16:322–361.

Roux PP, Barker PA (2002) Neurotrophin signaling through the p75 neurotrophin receptor. Prog Neurobiol 67:203–233.

Roux PP, Colicos MA, Barker PA, Kennedy TE (1999) p75 neurotrophin receptor expression is induced in apoptotic neurons after seizure. J Neurosci 19:6887–6896.

Ruiz CR, Shi J, Meffert MK (2014) Transcript specificity in BDNF-regulated protein synthesis. Neuropharmacology 76 Pt C:657–663.

Ruthazer ES, Akerman CJ, Cline HT (2003) Control of axon branch dynamics by

correlated activity in vivo. Science 301:66–70.

Ruthazer ES, Li J, Cline HT (2006) Stabilization of axon branch dynamics by synaptic maturation. J Neurosci 26:3594–3603.

Sakaguchi DS, Murphey RK (1985) Map formation in the developing Xenopus retinotectal system: an examination of ganglion cell terminal arborizations. J Neurosci 5:3228–3245.

Sakata K, Woo NH, Martinowich K, Greene JS, Schloesser RJ, Shen L, Lu B (2009) Critical role of promoter IV-driven BDNF transcription in GABAergic transmission and synaptic plasticity in the prefrontal cortex. Proc Natl Acad Sci U S A 106:5942–5947.

Sanchez AL, Matthews BJ, Meynard MM, Hu B, Javed S, Cohen Cory S (2006) BDNF increases synapse density in dendrites of developing tectal neurons in vivo. Development 133:2477–2486.

Sarret P, Krzywkowski P, Segal L, Nielsen MS, Petersen CM, Mazella J, Stroh T, Beaudet A (2003) Distribution of NTS3 receptor/sortilin mRNA and protein in the rat central nervous system. J Comp Neurol 461:483–505.

Schiller PH (1972) The role of the monkey superior colliculus in eye movement and vision. Invest Ophthalmol 11:451–460.

Schmidt J, Coen T (1995) Changes in retinal arbors in compressed projections to half tecta in goldfish. J Neurobiol 28:409–418.

Schmidt JT, Buzzard M (1990) Activity-driven sharpening of the regenerating retinotectal projection: effects of blocking or synchronizing activity on the morphology of individual regenerating arbors. J Neurobiol 21:900–917.

Schmidt JT, Buzzard M (1993) Activity-driven sharpening of the retinotectal projection in goldfish: development under stroboscopic illumination prevents sharpening. J Neurobiol 24:384–399.

Schmidt JT, Buzzard M, Borress R, Dhillon S (2000) MK801 increases retinotectal arbor size in developing zebrafish without affecting kinetics of branch elimination and addition. J Neurobiol 42:303–314.

Schmidt JT, Easter SS (1978) Independent biaxial reorganization of the retinotectal projection: a reassessment. Exp Brain Res 31:155–162.

Schmidt JT, Edwards DL (1983) Activity sharpens the map during the regeneration of the retinotectal projection in goldfish. Brain Res 269:29–39.

Schmidt JT, Eisele LE (1985) Stroboscopic illumination and dark rearing block the sharpening of the regenerated retinotectal map in goldfish. Neuroscience 14:535–

546.

Schneider R, Schweiger M (1991) A novel modular mosaic of cell adhesion motifs in the extracellular domains of the neurogenic trk and trkB tyrosine kinase receptors. Oncogene 6:1807–1811.

Schwartz N, Schohl A, Ruthazer ES (2011) Activity-dependent transcription of BDNF enhances visual acuity during development. Neuron 70:455–467.

Sehgal RNM, Lovette IJ (2003) Molecular evolution of three avian neurotrophin genes: implications for proregion functional constraints. J Mol Evol 57:335–342.

Semmelhack JL, Donovan JC, Thiele TR, Kuehn E, Laurell E, Baier H (2014) A dedicated visual pathway for prey detection in larval zebrafish. Elife 3:e04878.

Session AM et al. (2016) Genome evolution in the allotetraploid frog Xenopus laevis. Nature 538:336–343.

Sharma SC (1973) Anomalous retinal projection after removal of contralateral optic tectum in adult goldfish. Exp Neurol 41:661–669.

Shimada A, Mason CA, Morrison ME (1998) TrkB signaling modulates spine density and morphology independent of dendrite structure in cultured neonatal Purkinje cells. J Neurosci 18:8559–8570.

Silingardi D, Scali M, Belluomini G, Pizzorusso T (2010) Epigenetic treatments of adult rats promote recovery from visual acuity deficits induced by long-term monocular deprivation. Eur J Neurosci 31:2185–2192.

Simon DK, Prusky GT, O'Leary DD, Constantine-Paton M (1992) N-methyl-D-aspartate receptor antagonists disrupt the formation of a mammalian neural map. Proc Natl Acad Sci U S A 89:10593–10597.

Slack SE, Pezet S, McMahon SB, Thompson SWN, Malcangio M (2004) Brain-derived neurotrophic factor induces NMDA receptor subunit one phosphorylation via ERK and PKC in the rat spinal cord. Eur J Neurosci 20:1769–1778.

Smear MC, Tao HW, Staub W, Orger MB, Gosse NJ, Liu Y, Takahashi K, Poo M-M, Baier H (2007) Vesicular glutamate transport at a central synapse limits the acuity of visual perception in zebrafish. Neuron 53:65–77.

Solek C, Farooqi NAI, Brake N, Ruthazer ES (2017) Microglia-mediated effects of inflammation on visual system development in the zebrafish. In, pp 78. Canadian Neuroscience Meeting.

Sossin WS (2006) Tracing the evolution and function of the Trk superfamily of receptor tyrosine kinases. Brain Behav Evol 68:145–156.

Sperry RW (1943) Effect of 180 degree rotation of the retinal field on visuomotor coordination. J Exp Zool 92:263–279.

Sperry RW (1963) CHEMOAFFINITY IN THE ORDERLY GROWTH OF NERVE FIBER PATTERNS AND CONNECTIONS. Proc Natl Acad Sci U S A 50:703–710.

Springer AD, Cohen SM (1981) Optic fiber segregation in goldfish with two eyes innervating one tectal lobe. Brain Res 225:23–36.

Stent GS (1973) A physiological mechanism for Hebb's postulate of learning. Proc Natl Acad Sci U S A 70:997–1001.

Stewart AA, Ingebritsen TS, Manalan A, Klee CB, Cohen P (1982) Discovery of A Ca 2+ -and calmodulin-dependent protein phosphatase. FEBS Lett 137:80–84.

Strohmaier C, Carter BD, Urfer R, Barde YA, Dechant G (1996) A splice variant of the neurotrophin receptor trkB with increased specificity for brain-derived neurotrophic factor. EMBO J 15:3332–3337.

Stuermer CA, Rohrer B, Münz H (1990) Development of the retinotectal projection in zebrafish embryos under TTX-induced neural-impulse blockade. J Neurosci 10:3615–3626.

Suetterlin P, Drescher U (2014) Target-independent ephrina/EphA-mediated axon-axon repulsion as a novel element in retinocollicular mapping. Neuron 84:740–752.

Sui W-H, Huang S-H, Wang J, Chen Q, Liu T, Chen Z-Y (2015) Myosin Va mediates BDNF-induced postendocytic recycling of full-length TrkB and its translocation into dendritic spines. J Cell Sci 128:1108–1122.

Sun Y, Lim Y, Li F, Liu S, Lu J-J, Haberberger R, Zhong J-H, Zhou X-F (2012) ProBDNF collapses neurite outgrowth of primary neurons by activating RhoA. PLoS One 7:e35883.

Tabuchi A, Sakaya H, Kisukeda T, Fushiki H, Tsuda M (2002) Involvement of an upstream stimulatory factor as well as cAMP-responsive element-binding protein in the activation of brain-derived neurotrophic factor gene promoter I. J Biol Chem 277:35920–35931.

Tadesse T, Cheng Q, Xu M, Baro DJ, Young LJ, Pallas SL (2013) Regulation of ephrin-A expression in compressed retinocollicular maps. Dev Neurobiol 73:274–296.

Taha S, Stryker MP (2002) Rapid ocular dominance plasticity requires cortical but not geniculate protein synthesis. Neuron 34:425–436.

Tao X, West AE, Chen WG, Corfas G, Greenberg ME (2002) A calcium-responsive transcription factor, CaRF, that regulates neuronal activity-dependent expression of BDNF. Neuron 33:383–395.

Teng HK, Teng KK, Lee R, Wright S, Tevar S, Almeida RD, Kermani P, Torkin R, Chen Z-Y, Lee FS, Kraemer RT, Nykjaer A, Hempstead BL (2005) ProBDNF induces neuronal apoptosis via activation of a receptor complex of p75NTR and sortilin. J Neurosci 25:5455–5463.

Tian F, Marini AM, Lipsky RH (2010) NMDA receptor activation induces differential epigenetic modification of Bdnf promoters in hippocampal neurons. Amino Acids 38:1067–1074.

Timmusk T, Palm K, Lendahl U, Metsis M (1999) Brain-derived neurotrophic factor expression in vivo is under the control of neuron-restrictive silencer element. J Biol Chem 274:1078–1084.

Tongiorgi E, Righi M, Cattaneo A (1997) Activity-dependent dendritic targeting of BDNF and TrkB mRNAs in hippocampal neurons. J Neurosci 17:9492–9505.

Torborg CL, Hansen KA, Feller MB (2005) High frequency, synchronized bursting drives eye-specific segregation of retinogeniculate projections. Nat Neurosci 8:72–78.

Tremblay M, Fugère V, Tsui J, Schohl A, Tavakoli A, Travençolo BAN, Costa L da F, Ruthazer ES (2009) Regulation of radial glial motility by visual experience. J Neurosci 29:14066–14076.

Tsankova NM, Kumar A, Nestler EJ (2004) Histone modifications at gene promoter regions in rat hippocampus after acute and chronic electroconvulsive seizures. J Neurosci 24:5603–5610.

Tsui J, Schwartz N, Ruthazer ES (2010) A developmental sensitive period for spike timing-dependent plasticity in the retinotectal projection. Front Synaptic Neurosci 2:13.

Turrigiano GG, Nelson SB (2004) Homeostatic plasticity in the developing nervous system. Nat Rev Neurosci 5:97–107.

Ultsch MH, Wiesmann C, Simmons LC, Henrich J, Yang M, Reilly D, Bass SH, de Vos AM (1999) Crystal structures of the neurotrophin-binding domain of TrkA, TrkB and TrkC. J Mol Biol 290:149–159.

Urfer R, Tsoulfas P, Soppet D, Escandon E, Parada LF, Presta LG (1994) The binding epitopes of neurotrophin-3 to its receptors trkC and gp75 and the design of a multifunctional human neurotrophin. EMBO J 13:5896–5909.

Vaegter CB, Jansen P, Fjorback AW, Glerup S, Skeldal S, Kjolby M, Richner M, Erdmann B, Nyengaard JR, Tessarollo L, Lewin GR, Willnow TE, Chao MV, Nykjaer A (2011) Sortilin associates with Trk receptors to enhance anterograde transport and neurotrophin signaling. Nat Neurosci 14:54–61.

Valdés-Sánchez T, Kirstein M, Pérez-Villalba A, Vega JA, Fariñas I (2010) BDNF is

essentially required for the early postnatal survival of nociceptors. Dev Biol 339:465–476.

Valdez G, Philippidou P, Rosenbaum J, Akmentin W, Shao Y, Halegoua S (2007) Trk-signaling endosomes are generated by Rac-dependent macroendocytosis. Proc Natl Acad Sci U S A 104:12270–12275.

Van Horn MR, Strasser A, Miraucourt LS, Pollegioni L, Ruthazer ES (2017) The Gliotransmitter d-Serine Promotes Synapse Maturation and Axonal Stabilization In Vivo. J Neurosci 37:6277–6288.

Vashishta A, Habas A, Pruunsild P, Zheng J-J, Timmusk T, Hetman M (2009) Nuclear factor of activated T-cells isoform c4 (NFATc4/NFAT3) as a mediator of antiapoptotic transcription in NMDA receptor-stimulated cortical neurons. J Neurosci 29:15331–15340.

Vaughn JE, Barber RP, Sims TJ (1988) Dendritic development and preferential growth into synaptogenic fields: A quantitative study of Golgi-impregnated spinal motor neurons. Synapse 2:69–78.

Verpelli C, Piccoli G, Zibetti C, Zanchi A, Gardoni F, Huang K, Brambilla D, Di Luca M, Battaglioli E, Sala C (2010) Synaptic activity controls dendritic spine morphology by modulating eEF2-dependent BDNF synthesis. J Neurosci 30:5830–5842.

Vignoli B, Battistini G, Melani R, Blum R, Santi S, Berardi N, Canossa M (2016) Peri-Synaptic Glia Recycles Brain-Derived Neurotrophic Factor for LTP Stabilization and Memory Retention. Neuron 92:873–887.

Vilar M, Charalampopoulos I, Kenchappa RS, Simi A, Karaca E, Reversi A, Choi S, Bothwell M, Mingarro I, Friedman WJ, Schiavo G, Bastiaens PIH, Verveer PJ, Carter BD, Ibáñez CF (2009) Activation of the p75 neurotrophin receptor through conformational rearrangement of disulphide-linked receptor dimers. Neuron 62:72–83.

Vislay-Meltzer RL, Kampff AR, Engert F (2006) Spatiotemporal specificity of neuronal activity directs the modification of receptive fields in the developing retinotectal system. Neuron 50:101–114.

von Bartheld CS, Williams R, Lefcort F, Clary DO, Reichardt LF, Bothwell M (1996) Retrograde transport of neurotrophins from the eye to the brain in chick embryos: roles of the p75NTR and trkB receptors. J Neurosci 16:2995–3008.

von Schack D, Casademunt E, Schweigreiter R, Meyer M, Bibel M, Dechant G (2001) Complete ablation of the neurotrophin receptor p75NTR causes defects both in the nervous and the vascular system. Nat Neurosci 4:977–978.

Walter J, Henke-Fahle S, Bonhoeffer F (1987) Avoidance of posterior tectal membranes by temporal retinal axons. Development 101:909–913.

Wang B-Y, Zhong Y, Zhao Z, Miao Y (2014) Epigenetic suppression of hippocampal BDNF mediates the memory deficiency induced by amyloid fibrils. Pharmacol Biochem Behav 126:83–89.

Wang KC, Koprivica V, Kim JA, Sivasankaran R, Guo Y, Neve RL, He Z (2002a) Oligodendrocyte-myelin glycoprotein is a Nogo receptor ligand that inhibits neurite outgrowth. Nature 417:941–944.

Wang X, Bauer JH, Li Y, Shao Z, Zetoune FS, Cattaneo E, Vincenz C (2001) Characterization of a p75(NTR) apoptotic signaling pathway using a novel cellular model. J Biol Chem 276:33812–33820.

Wang X, Chun S-J, Treloar H, Vartanian T, Greer CA, Strittmatter SM (2002b) Localization of Nogo-A and Nogo-66 receptor proteins at sites of axon-myelin and synaptic contact. J Neurosci 22:5505–5515.

Wehrman T, He X, Raab B, Dukipatti A, Blau H, Garcia KC (2007) Structural and mechanistic insights into nerve growth factor interactions with the TrkA and p75 receptors. Neuron 53:25–38.

West AE, Pruunsild P, Timmusk T (2014) Neurotrophins: Transcription and Translation. In: Neurotrophic Factors (Lewin GR, Carter BD, eds), pp 67–100. Berlin, Heidelberg: Springer Berlin Heidelberg.

Wilson KHS (2009) The genome sequence of the protostome Daphnia pulex encodes respective orthologues of a neurotrophin, a Trk and a p75NTR: evolution of neurotrophin signaling components and related proteins in the bilateria. BMC Evol Biol 9:243.

Winnubst J, Cheyne JE, Niculescu D, Lohmann C (2015) Spontaneous Activity Drives Local Synaptic Plasticity In Vivo. Neuron 87:399–410.

Wong RO, Meister M, Shatz CJ (1993) Transient period of correlated bursting activity during development of the mammalian retina. Neuron 11:923–938.

Wong Y-H, Lee C-M, Xie W, Cui B, Poo M-M (2015) Activity-dependent BDNF release via endocytic pathways is regulated by synaptotagmin-6 and complexin. Proc Natl Acad Sci U S A 112:E4475–E4484.

Woo NH, Teng HK, Siao C-J, Chiaruttini C, Pang PT, Milner TA, Hempstead BL, Lu B (2005) Activation of p75NTR by proBDNF facilitates hippocampal long-term depression. Nat Neurosci 8:1069–1077.

Wu G, Malinow R, Cline HT (1996) Maturation of a central glutamatergic synapse. Science 274:972–976.

Xenopus ntrk2. Xenopus ntrk2, Xenbase Available at: http://www.xenbase.org/gene/geneExpressionChart.do?method=draw&geneId=922

931&geneSymbol=ntrk2 [Accessed August 3, 2018b].

Xiong Z-G, Raouf R, Lu W-Y, Wang L-Y, Orser BA, Dudek EM, Browning MD, MacDonald JF (1998) Regulation of N-Methyl-d-Aspartate Receptor Function by Constitutively Active Protein Kinase C. Mol Pharmacol 54:1055–1063.

Xu B, Zang K, Ruff NL, Zhang YA, McConnell SK, Stryker MP, Reichardt LF (2000) Cortical degeneration in the absence of neurotrophin signaling: dendritic retraction and neuronal loss after removal of the receptor TrkB. Neuron 26:233–245.

Xu H-P, Burbridge TJ, Chen M-G, Ge X, Zhang Y, Zhou ZJ, Crair MC (2015) Spatial pattern of spontaneous retinal waves instructs retinotopic map refinement more than activity frequency. Dev Neurobiol 75:621–640.

Xu H-P, Furman M, Mineur YS, Chen H, King SL, Zenisek D, Zhou ZJ, Butts DA, Tian N, Picciotto MR, Crair MC (2011a) An instructive role for patterned spontaneous retinal activity in mouse visual map development. Neuron 70:1115–1127.

Xu H, Khakhalin AS, Nurmikko AV, Aizenman CD (2011b) Visual experience-dependent maturation of correlated neuronal activity patterns in a developing visual system. J Neurosci 31:8025–8036.

Xu H-T, Pan F, Yang G, Gan W-B (2007) Choice of cranial window type for in vivo imaging affects dendritic spine turnover in the cortex. Nat Neurosci 10:549–551.

Yacoubian TA, Lo DC (2000) Truncated and full-length TrkB receptors regulate distinct modes of dendritic growth. Nat Neurosci 3:342–349.

Yamashita T, Tucker KL, Barde YA (1999) Neurotrophin binding to the p75 receptor modulates Rho activity and axonal outgrowth. Neuron 24:585–593.

Yang J, Harte-Hargrove LC, Siao C-J, Marinic T, Clarke R, Ma Q, Jing D, Lafrancois JJ, Bath KG, Mark W, Ballon D, Lee FS, Scharfman HE, Hempstead BL (2014) proBDNF negatively regulates neuronal remodeling, synaptic transmission, and synaptic plasticity in hippocampus. Cell Rep 7:796–806.

Yang J, Siao C-J, Nagappan G, Marinic T, Jing D, McGrath K, Chen Z-Y, Mark W, Tessarollo L, Lee FS, Lu B, Hempstead BL (2009) Neuronal release of proBDNF. Nat Neurosci 12:113–115.

Yano H, Ninan I, Zhang H, Milner TA, Arancio O, Chao MV (2006) BDNF-mediated neurotransmission relies upon a myosin VI motor complex. Nat Neurosci 9:1009.

Yates, P. A., Holub, A. D., McLaughlin, T., Sejnowski, T. J., and O'Leary, D. D. M. (2004) Computational modeling of retinotopic map development to define contributions of EphA-ephrinA gradients, axon-axon interactions and patterned activity. J Neurobiol 59:95–113.

Yeiser EC, Rutkoski NJ, Naito A, Inoue J-I, Carter BD (2004) Neurotrophin signaling through the p75 receptor is deficient in traf6-/- mice. J Neurosci 24:10521–10529.

Ying S-W, Futter M, Rosenblum K, Webber MJ, Hunt SP, Bliss TVP, Bramham CR (2002) Brain-derived neurotrophic factor induces long-term potentiation in intact adult hippocampus: requirement for ERK activation coupled to CREB and upregulation of Arc synthesis. J Neurosci 22:1532–1540.

Yoon MG (1976) Progress of topographic regulation of the visual projection in the halved optic tectum of adult goldfish. J Physiol 257:621–643.

Yoshii A, Constantine-Paton M (2007) BDNF induces transport of PSD-95 to dendrites through PI3K-AKT signaling after NMDA receptor activation. Nat Neurosci 10:702–711.

Yoshii A, Constantine-Paton M (2010) Postsynaptic BDNF-TrkB signaling in synapse maturation, plasticity, and disease. Dev Neurobiol 70:304–322.

Yoshii A, Constantine-Paton M (2014) Postsynaptic localization of PSD-95 is regulated by all three pathways downstream of TrkB signaling. Front Synaptic Neurosci 6:172.

Zagrebelsky M, Holz A, Dechant G, Barde Y-A, Bonhoeffer T, Korte M (2005) The p75 neurotrophin receptor negatively modulates dendrite complexity and spine density in hippocampal neurons. J Neurosci 25:9989–9999.

Zagrebelsky M, Korte M (2014) Form follows function: BDNF and its involvement in sculpting the function and structure of synapses. Neuropharmacology 76 Pt C:628–638.

Zakharenko SS, Patterson SL, Dragatsis I, Zeitlin SO, Siegelbaum SA, Kandel ER, Morozov A (2003) Presynaptic BDNF required for a presynaptic but not postsynaptic component of LTP at hippocampal CA1-CA3 synapses. Neuron 39:975–990.

Zhang J, Ackman JB, Xu H-P, Crair MC (2011) Visual map development depends on the temporal pattern of binocular activity in mice. Nat Neurosci 15:298–307.

Zhang LI, Tao HW, Holt CE, Harris WA, Poo M (1998) A critical window for cooperation and competition among developing retinotectal synapses. Nature 395:37–44.

Zheng J, Shen W-H, Lu T-J, Zhou Y, Chen Q, Wang Z, Xiang T, Zhu Y-C, Zhang C, Duan S, Xiong Z-Q (2008) Clathrin-dependent endocytosis is required for TrkB-dependent Akt-mediated neuronal protection and dendritic growth. J Biol Chem 283:13280–13288.

Zheng Z, Ambigapathy G, Keifer J (2017) MeCP2 regulates Tet1-catalyzed demethylation, CTCF binding, and learning-dependent alternative splicing of the

BDNF gene in Turtle. Elife 6: e25384.

Zhou XF, Rush RA (1996) Endogenous brain-derived neurotrophic factor is anterogradely transported in primary sensory neurons. Neuroscience 74:945–953.

Zhou X, Xiao H, Wang H (2011) Developmental changes of TrkB signaling in response to exogenous brain-derived neurotrophic factor in primary cortical neurons. J Neurochem 119:1205–1216.

Zhu B, Pennack JA, McQuilton P, Forero MG, Mizuguchi K, Sutcliffe B, Gu C-J, Fenton JC, Hidalgo A (2008) Drosophila neurotrophins reveal a common mechanism for nervous system formation. PLoS Biol 6:e284.

Zou DJ, Cline HT (1996) Expression of constitutively active CaMKII in target tissue modifies presynaptic axon arbor growth. Neuron 16:529–539.

Zupan AA, Osborne PA, Smith CE, Siegel NR, Leimgruber RM, Johnson EM Jr (1989) Identification, purification, and characterization of truncated forms of the human nerve growth factor receptor. J Biol Chem 264:11714–11720.